

FRACTURE MECHANICS

A Collection of Data

Collected and Edited by:

Dr. M. Perl

Griffith's^{*} Fracture Criterion

The Energy Balance Approach

Incipient fracture in ideally brittle materials occurs when the magnitude of the elastic energy supplied at the crack tip during an incremented increase in the crack length is equal to or greater than the magnitude of the elastic-surface energy required to create the new surface area of the crack.

*

A. A. Griffith, "The Phenomena of Rupture and Flow in Solids," Philosophical Transactions of the Royal Society of London, Series A, Vol. 221, 1921, pp. 163-198.

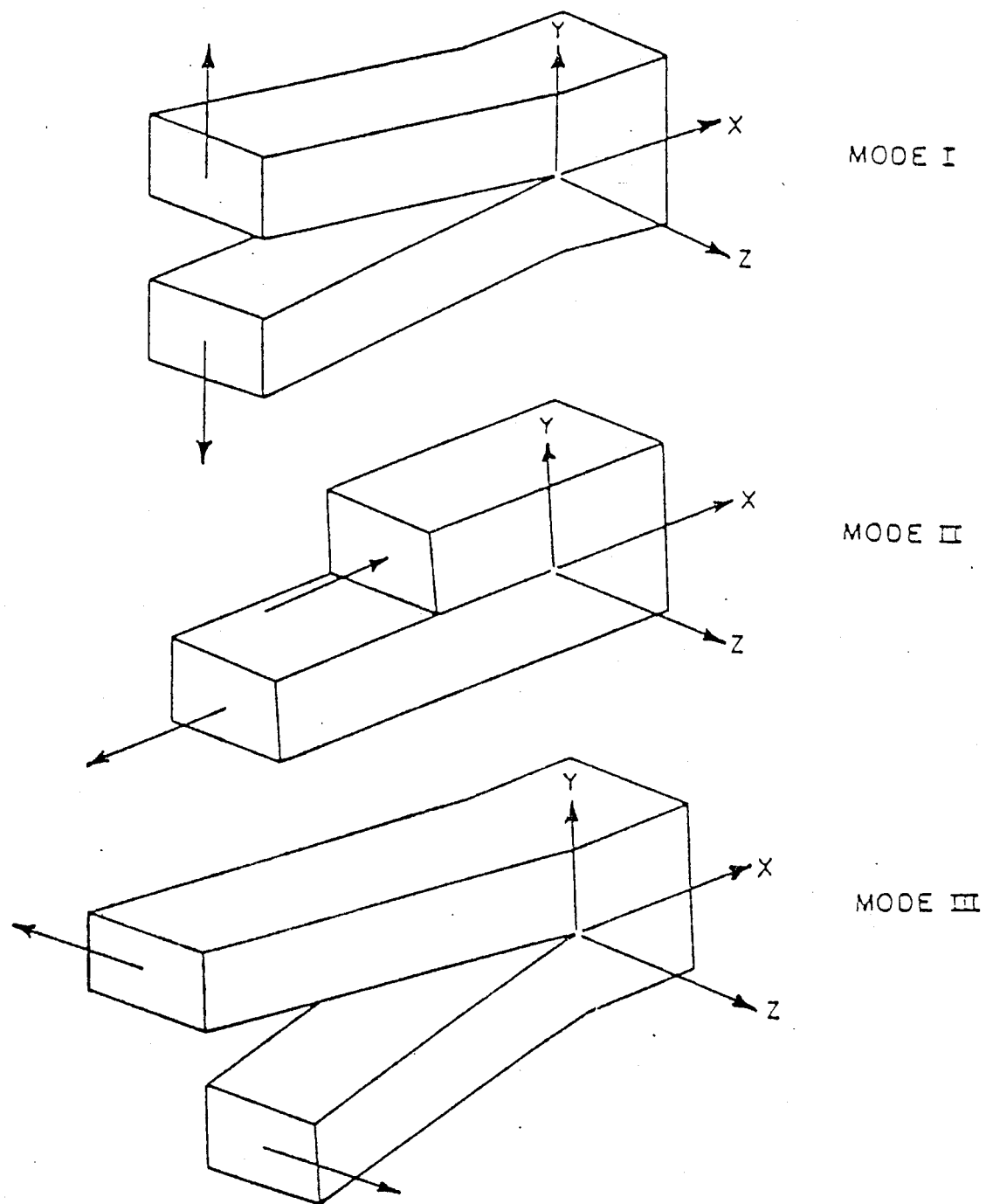


FIG. 2.1. The three basic modes of crack surface displacements

2.2.1. Modes de sollicitations

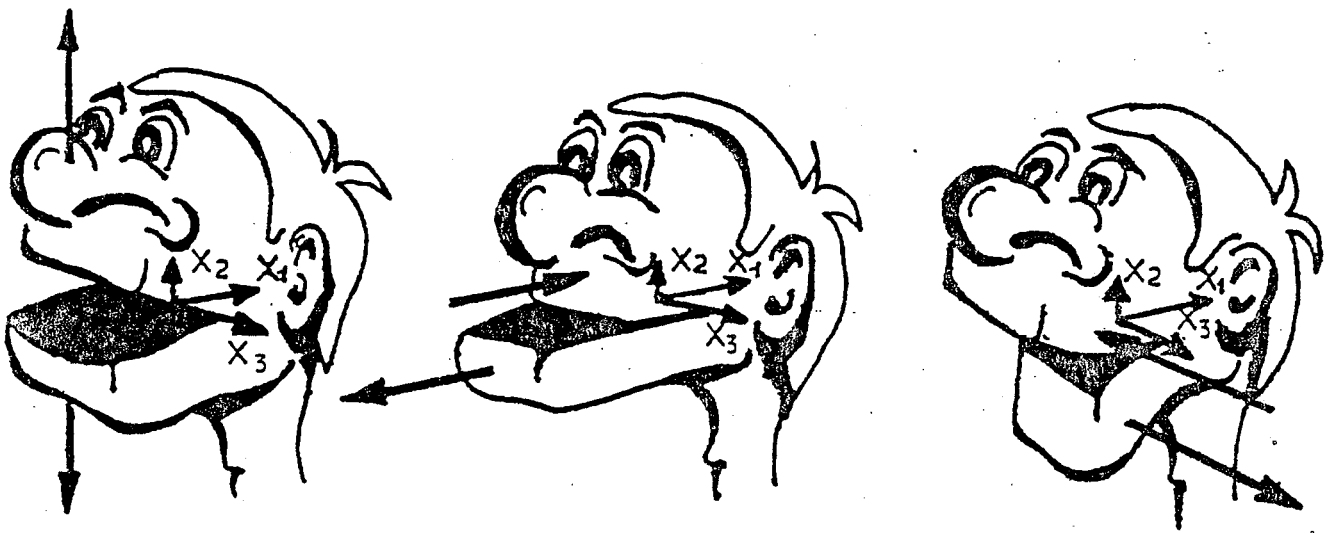


Fig. 2. Modes de sollicitations d'une fissure (dessins de Bill Bocquet).

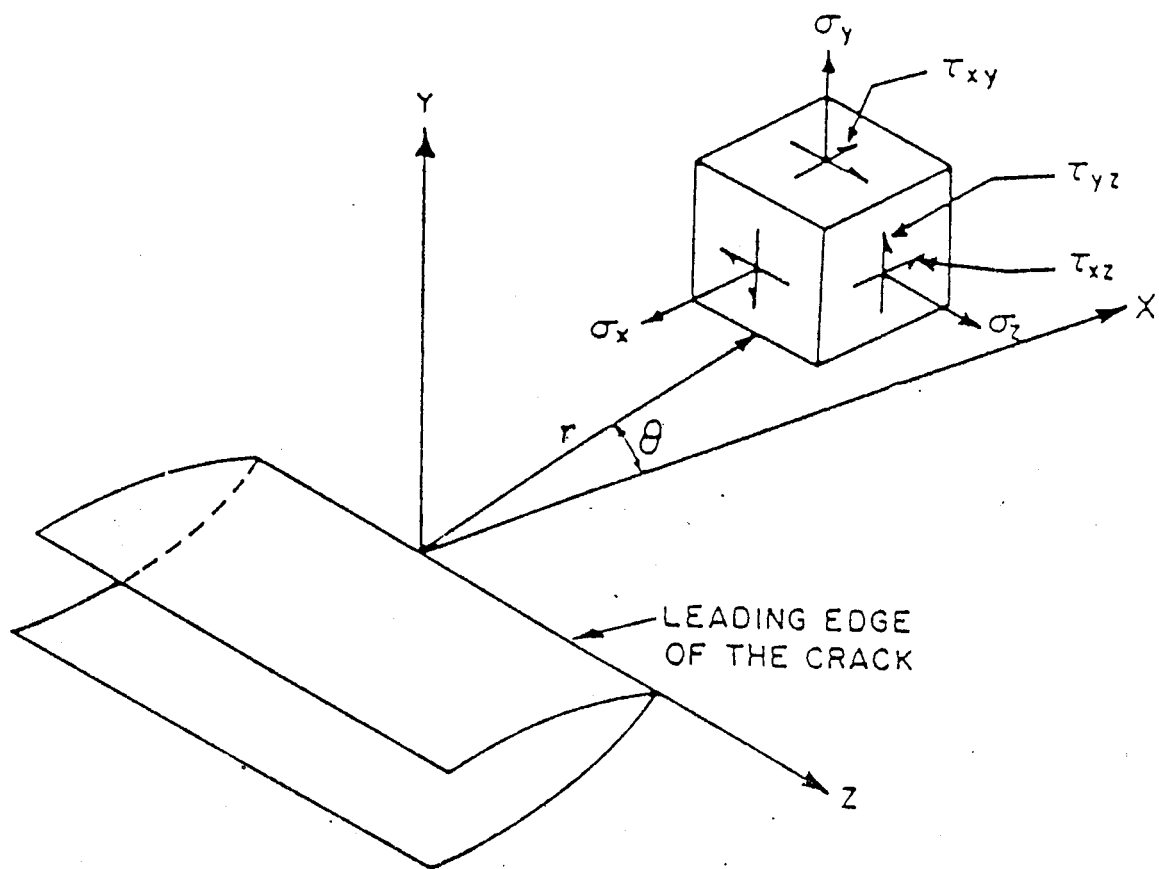


FIG. 2.2. Coordinate system and stress components ahead of a crack tip

Mode I:

$$\sigma_x = \frac{K_I}{(2\pi r)^{1/2}} \cos \frac{\theta}{2} \left[1 - \sin \frac{\theta}{2} \sin \frac{3\theta}{2} \right]$$

$$\sigma_y = \frac{K_I}{(2\pi r)^{1/2}} \cos \frac{\theta}{2} \left[1 + \sin \frac{\theta}{2} \sin \frac{3\theta}{2} \right]$$

$$\tau_{xy} = \frac{K_I}{(2\pi r)^{1/2}} \sin \frac{\theta}{2} \cos \frac{\theta}{2} \cos \frac{3\theta}{2}$$

$$\sigma_z = \nu(\sigma_x + \sigma_y), \quad \tau_{xz} = \tau_{yz} = 0$$

$$u = \frac{K_I}{G} \left[\frac{r}{2\pi} \right]^{1/2} \cos \frac{\theta}{2} \left[1 - 2\nu + \sin^2 \frac{\theta}{2} \right]$$

$$v = \frac{K_I}{G} \left[\frac{r}{2\pi} \right]^{1/2} \sin \frac{\theta}{2} \left[2 - 2\nu - \cos^2 \frac{\theta}{2} \right]$$

$$w = 0$$

Mode II:

$$\sigma_x = -\frac{K_{II}}{(2\pi r)^{1/2}} \sin \frac{\theta}{2} \left[2 + \cos \frac{\theta}{2} \cos \frac{3\theta}{2} \right]$$

$$\sigma_y = \frac{K_{II}}{(2\pi r)^{1/2}} \sin \frac{\theta}{2} \cos \frac{\theta}{2} \cos \frac{3\theta}{2}$$

$$\tau_{xy} = \frac{K_{II}}{(2\pi r)^{1/2}} \cos \frac{\theta}{2} \left[1 - \sin \frac{\theta}{2} \sin \frac{3\theta}{2} \right]$$

$$\sigma_z = \nu(\sigma_x + \sigma_y), \quad \tau_{xz} = \tau_{yz} = 0$$

$$u = \frac{K_{II}}{G} \left[\frac{r}{2\pi} \right]^{1/2} \sin \frac{\theta}{2} \left[2 - 2\nu + \cos^2 \frac{\theta}{2} \right]$$

$$v = \frac{K_{II}}{G} \left[\frac{r}{2\pi} \right]^{1/2} \cos \frac{\theta}{2} \left[-1 + 2\nu + \sin^2 \frac{\theta}{2} \right]$$

$$w = 0$$

Mode III:

$$\tau_{xz} = -\frac{K_{III}}{(2\pi r)^{1/2}} \sin \frac{\theta}{2}$$

$$\tau_{yz} = \frac{K_{III}}{(2\pi r)^{1/2}} \cos \frac{\theta}{2}$$

$$\sigma_x = \sigma_y = \sigma_z = \tau_{xy} = 0$$

$$w = \frac{K_{III}}{G} \left[\frac{2r}{\pi} \right]^{1/2} \sin \frac{\theta}{2}$$

$$u = v = 0$$

Irwin's^{**} Fracture Criterion

The Stress Approach

Onset of fracture occurs when the magnitude of the stress intensity factor prevailing at the crack tip reaches its critical value - the material toughness.

**

G.R. Irwin "Analysis of Stresses and Strains Near the End of a Crack Traversing a Plate," *Journal of Applied Mechanics*, Vol. 24, 1957, pp. 361-364.

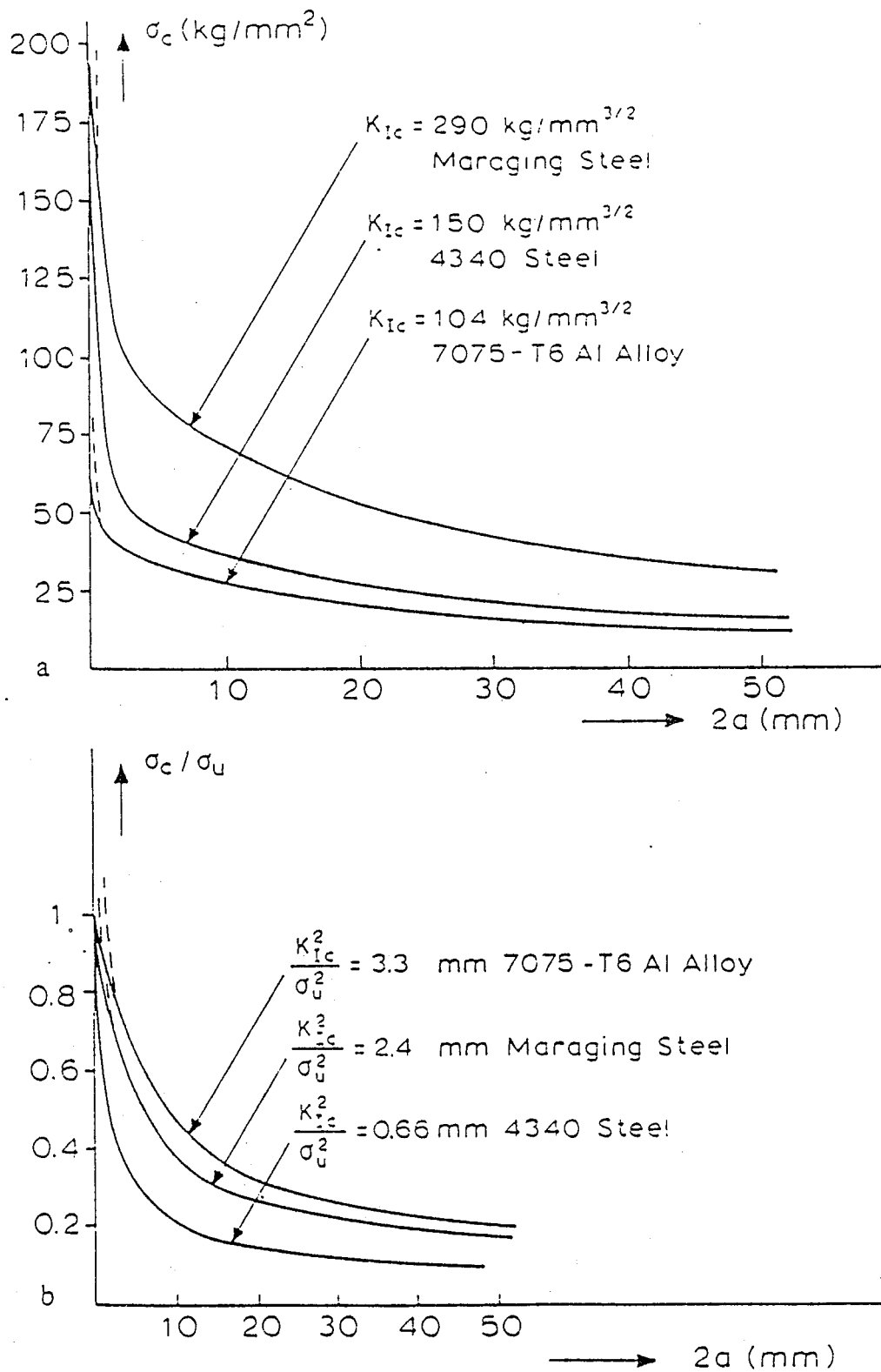


Figure 1.7. Crack toughness of three high strength materials
a. Residual strength as a function of crack size; b. Relative residual strength

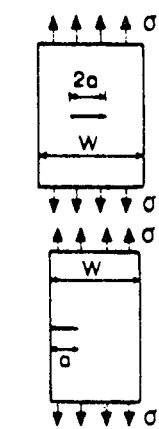
EXAMPLE # 2: MATERIAL SELECTION

Property Material	$\frac{\sigma_u}{\rho}$ [in]	σ_u [ksi]	K_{IC} [ksi $\sqrt{\text{in}}$]	$\eta_u = \frac{\sigma_u}{\sigma_w}$	$\eta_f = \frac{\sigma_f}{\sigma_w}$	$\frac{K_{IC}}{\sigma_u}$ [$\sqrt{\text{m}}$]
Steel	880	250	100	2	1.43	0.4
Al	870	85	30	2	1.25	0.35
Titanium	860	140	80	2	2.09	0.57

EXAMPLE # 4 MAXIMUM TOLERATED CRACK LENGTH

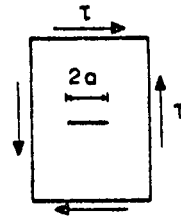
Property Material	σ_u [Kg/mm ²]	K_{IC} [Kg . mm ^{-3/2}]	Tolerated Crack 2a [mm]
7075-T6 Al alloy	57	104	8.46
Maraging 300 Steel	188	290	6.04
4340 Steel	185	150	1.67

TABLE 3.1
K for practical geometries



$$K_I = \sigma \sqrt{\pi a} \left(\sec \frac{\pi a}{W} \right)^{1/2}$$

$$K_{II} = \tau \sqrt{\pi a} \left(\text{small } \frac{a}{W} \right)$$

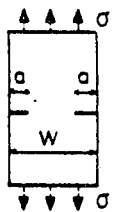


$$K_I = 1.12 \sigma \sqrt{\pi a} \left(\text{small } \frac{a}{W} \right)$$

or $K_I = Y \sigma \sqrt{a}$

with $Y = 1.99 - 0.41 \frac{a}{W} + 18.7 \left(\frac{a}{W} \right)^2 - 38.48 \left(\frac{a}{W} \right)^3 + 53.85 \left(\frac{a}{W} \right)^4$

$(1.99 = 1.12\sqrt{\pi})$

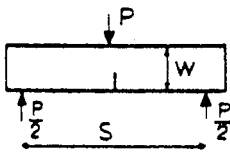


$$K_I = 1.12 \sigma \sqrt{\pi a} \left(\text{small } \frac{a}{W} \right)$$

or $K_I = Y \sigma \sqrt{a}$

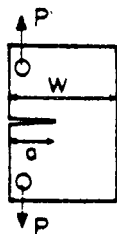
with $Y = 1.99 + 0.76 \frac{a}{W} - 8.48 \left(\frac{a}{W} \right)^2 + 27.36 \left(\frac{a}{W} \right)^3$

$(1.99 = 1.12\sqrt{\pi})$



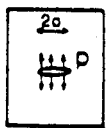
Thickness B

$$K_I = \frac{PS}{BW^{3/2}} \left[2.9 \left(\frac{a}{W} \right)^{1/2} - 4.6 \left(\frac{a}{W} \right)^{3/2} + 21.8 \left(\frac{a}{W} \right)^{5/2} - 37.6 \left(\frac{a}{W} \right)^{7/2} + 38.7 \left(\frac{a}{W} \right)^{9/2} \right]$$



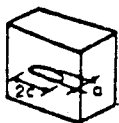
Thickness B

$$K_I = \frac{P}{BW^{1/2}} \left[29.6 \left(\frac{a}{W} \right)^{1/2} - 185.5 \left(\frac{a}{W} \right)^{3/2} + 655.7 \left(\frac{a}{W} \right)^{5/2} - 1017 \left(\frac{a}{W} \right)^{7/2} + 63.9 \left(\frac{a}{W} \right)^{9/2} \right]$$



p per unit thickness

$$K_I = p \sqrt{\pi a}$$



$$K_{I_{max}} = 1.12 \frac{\sigma}{\Phi} \sqrt{\pi a}$$

$$K_{I_{min}} = 1.12 \frac{\sigma}{\Phi} \sqrt{\pi a^2/c}$$

$$\Phi = \int_0^{\pi/2} \left[1 - \frac{c^2 - a^2}{c^2} \sin^2 \varphi \right] d\varphi$$

$$\Phi \approx \frac{3\pi}{8} + \frac{\pi}{8} \frac{a^2}{c^2}$$

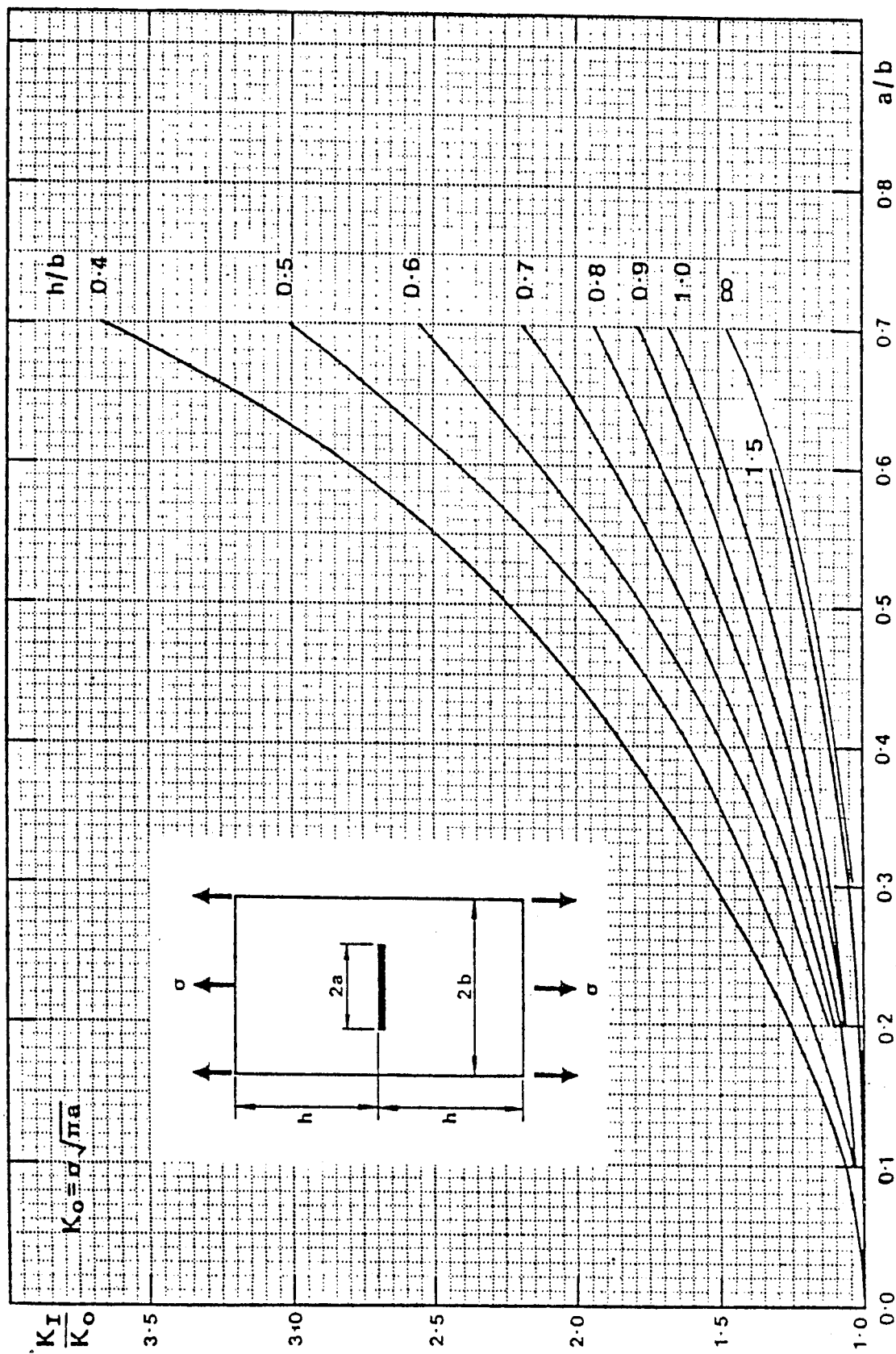


Fig.1 K_I for a central crack in a rectangular sheet subjected to a uniform uniaxial tensile stress

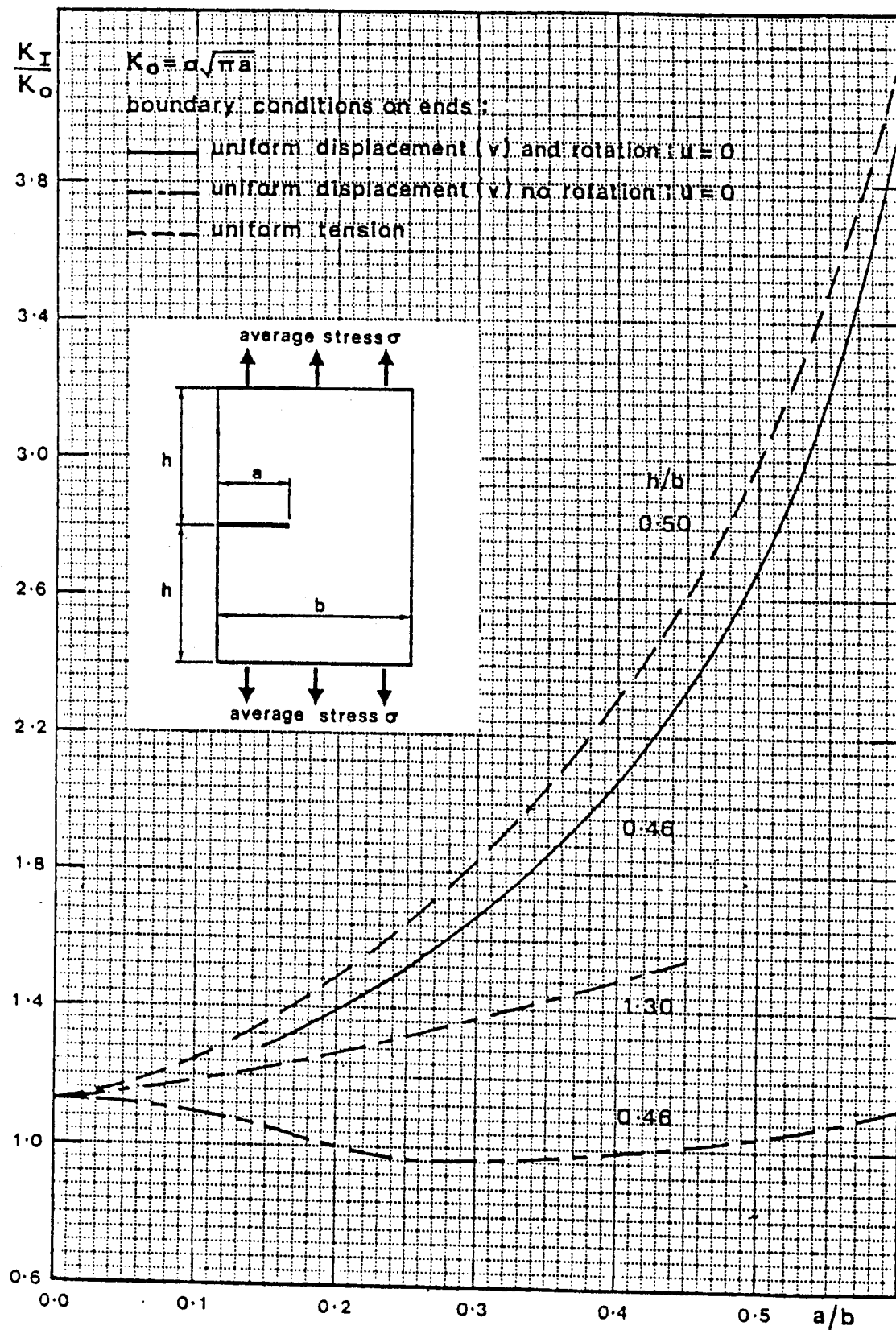


Fig.57 K_I for an edge crack in a rectangular sheet subjected to a uniform normal displacement

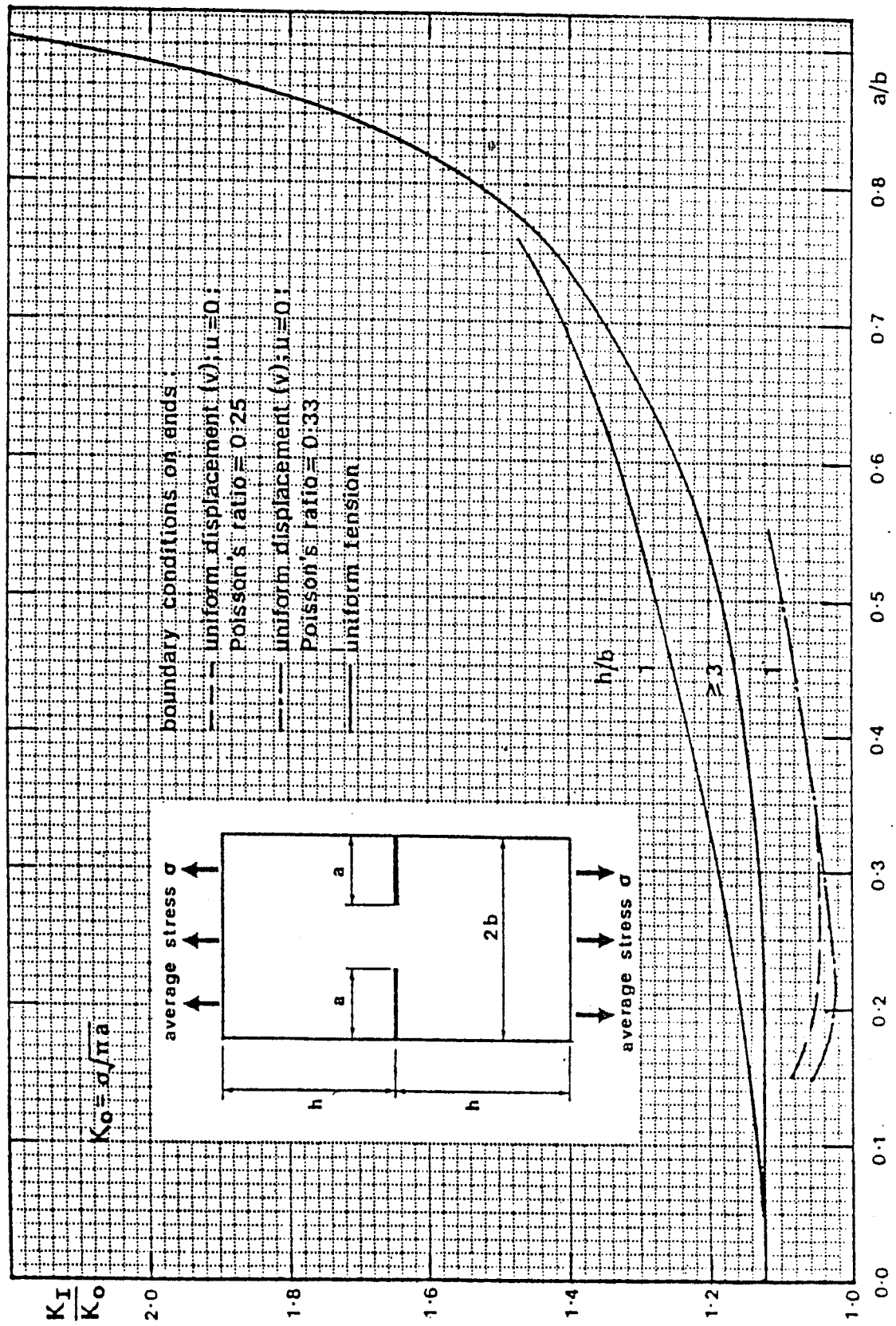


Fig.72 K_I for two edge cracks in a rectangular sheet subjected to a uniform uniaxial tensile stress or a uniform normal displacement

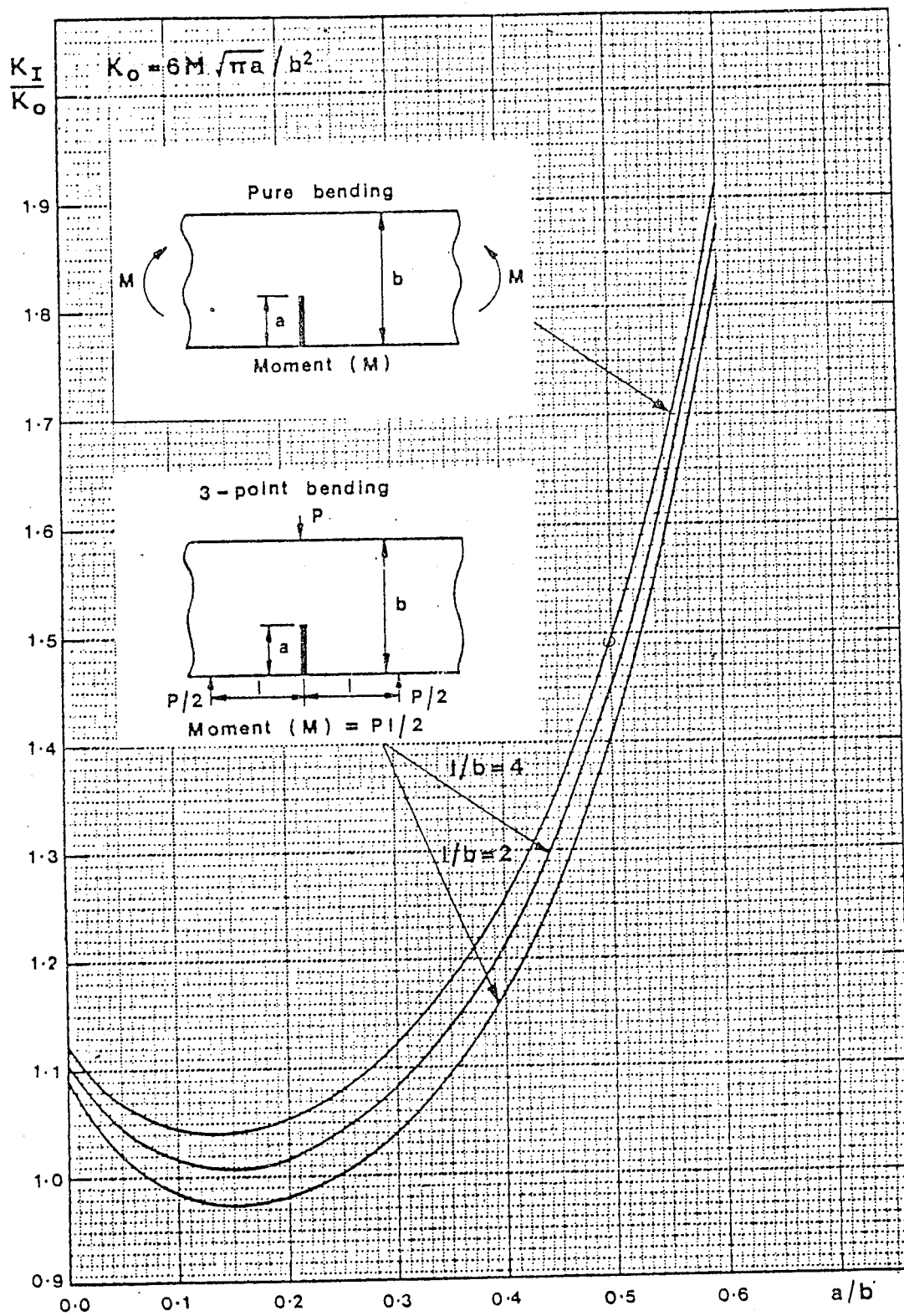


Fig.56 K_I for an edge crack in a finite width sheet subjected to pure bending or three point bending

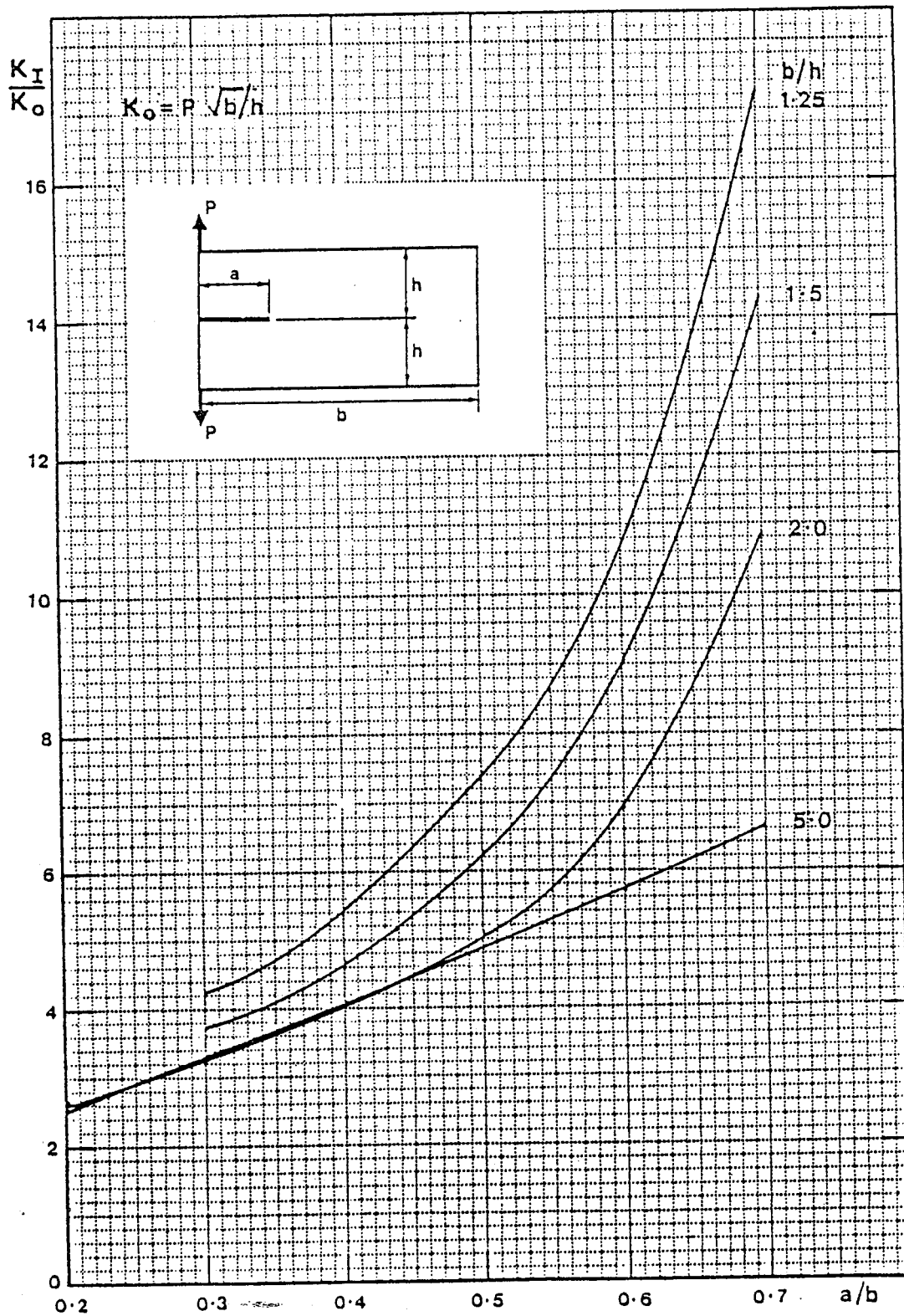


Fig.64 K_I for an edge crack in a rectangular sheet subjected to splitting forces

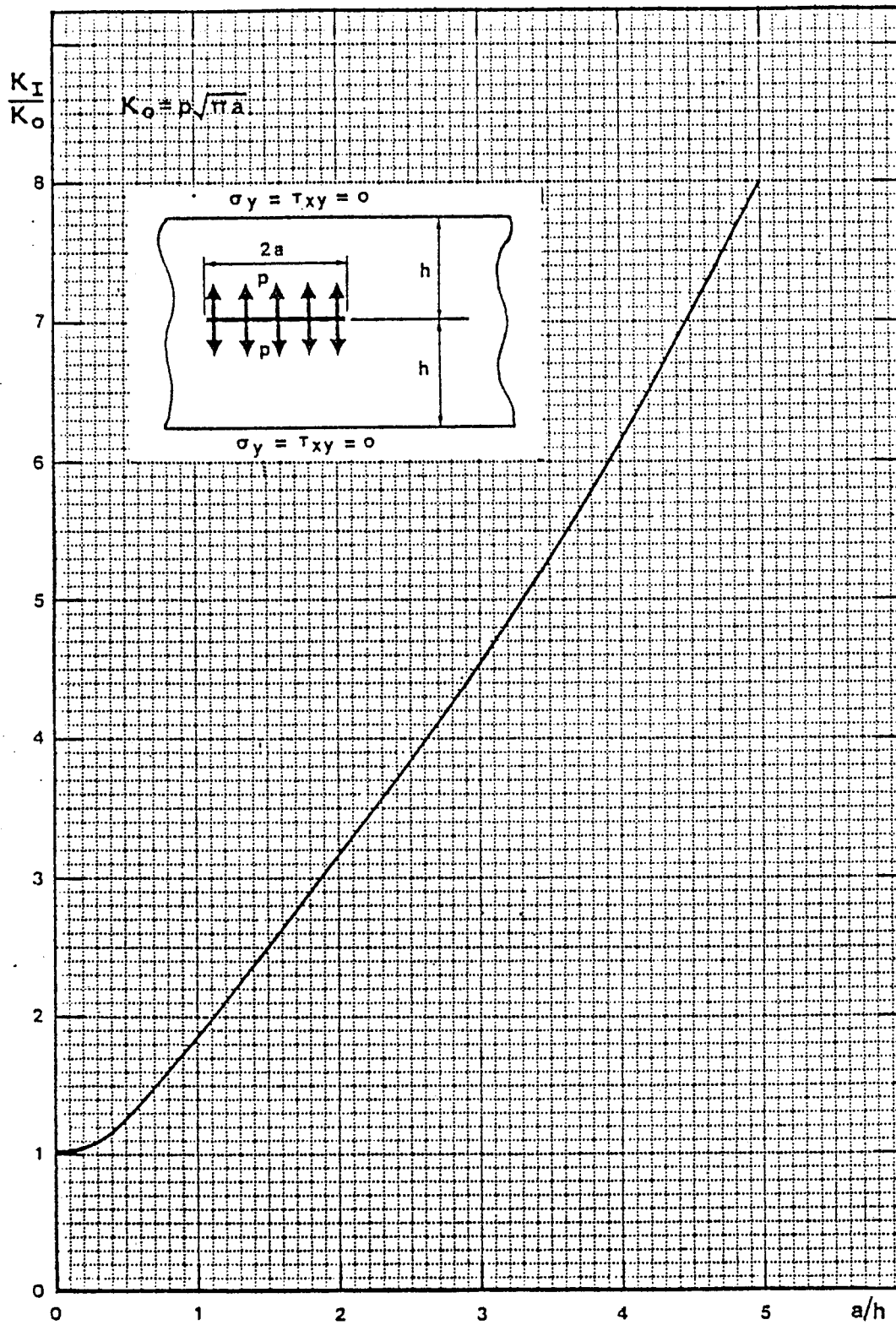


Fig. 7 K_I for a crack subjected to a uniform internal pressure in a finite height sheet

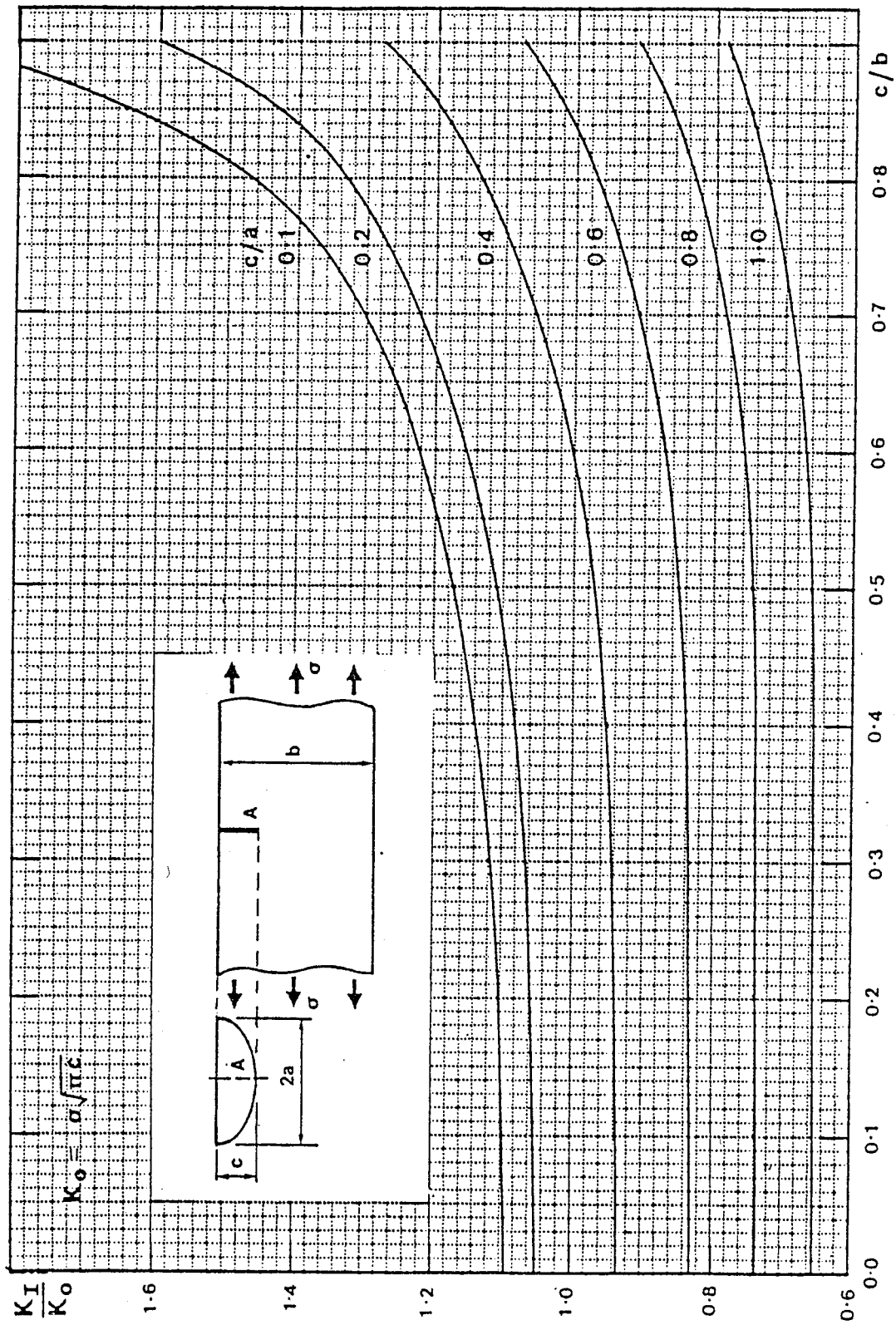


Fig. 186 K_I for point A on a semi-elliptical edge crack in a slab subjected to a uniform uniaxial tensile stress

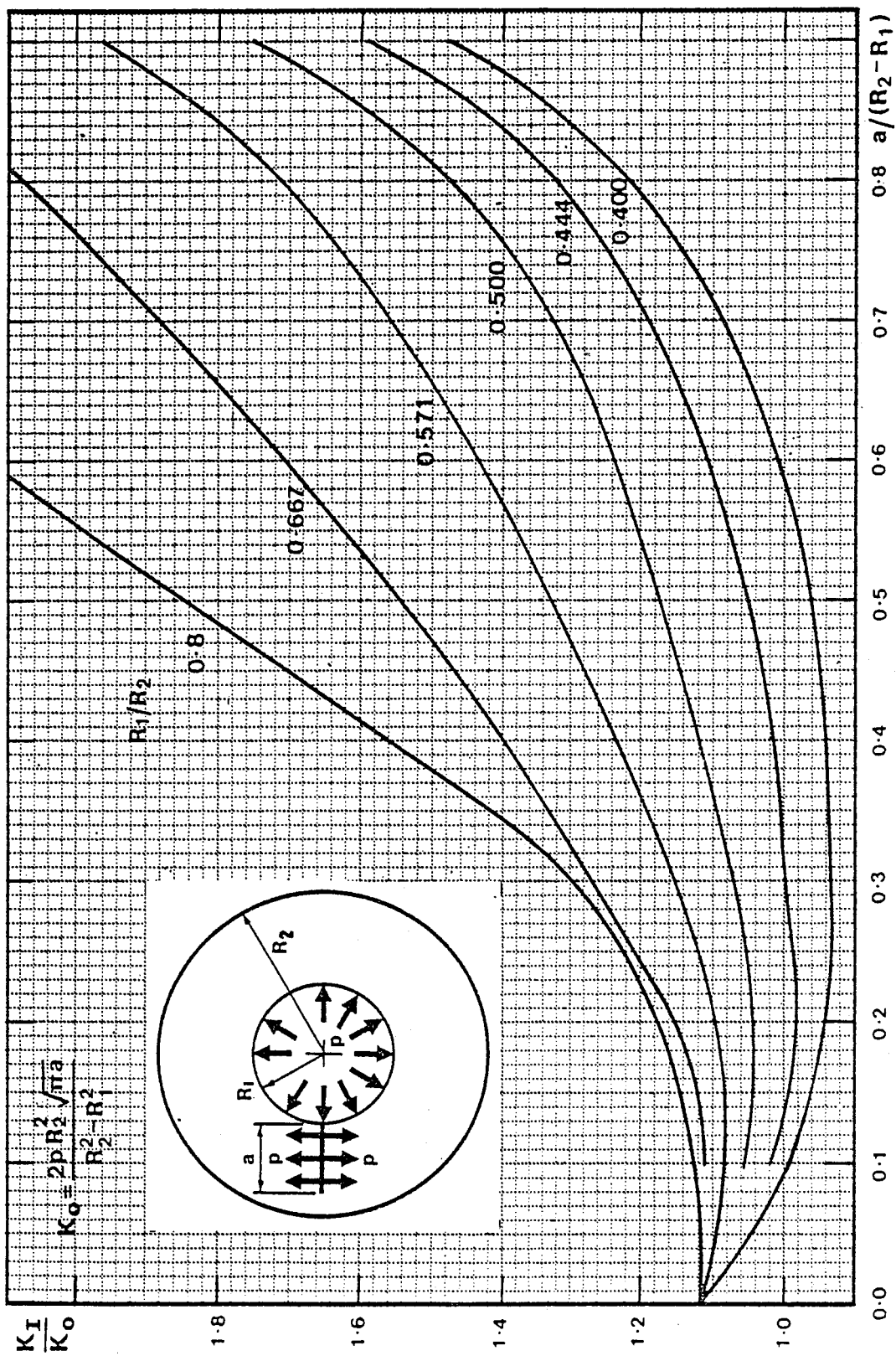
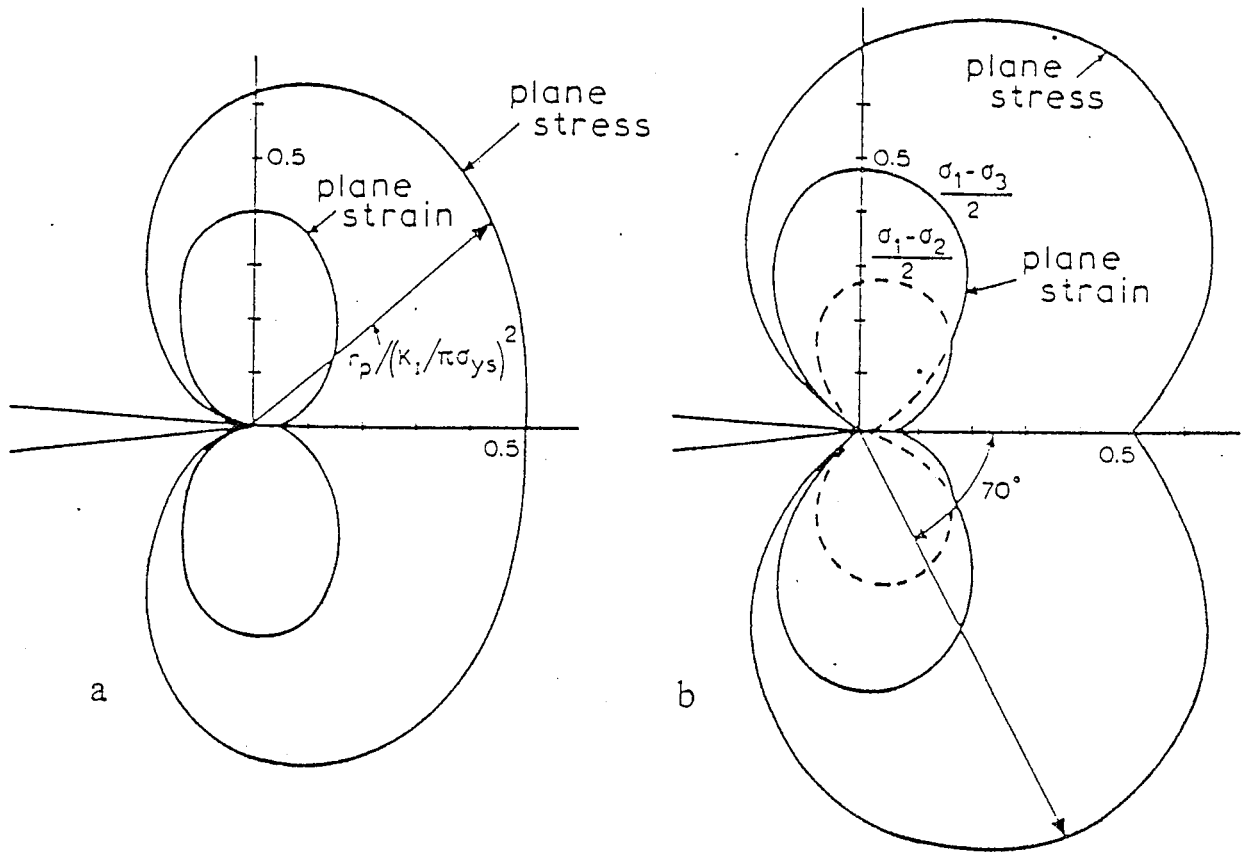


Fig.160 K_I for a pressurised internal radial edge crack in a tube subjected to a uniform internal pressure

crack tip plastic zone



Plastic zone shapes according to Von Mises and Tresca yield criteria
a. Von Mises criterion; b. Tresca criterion

Von Mises

$$\text{Plane strain: } r_p(\theta) = \frac{K^2}{4\pi\sigma_{ys}^2} \left[\frac{3}{2} \sin^2 \theta + (1-2\nu)^2 (1 + \cos \theta) \right]$$

$$\text{Plane stress: } r_p(\theta) = \frac{K^2}{4\pi\sigma_{ys}^2} \left[1 + \frac{3}{2} \sin^2 \theta + \cos \theta \right].$$

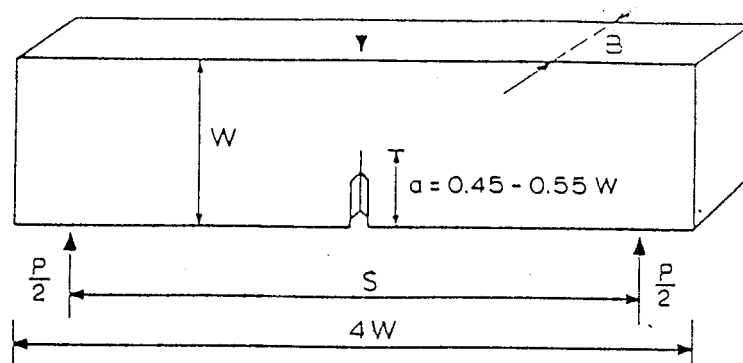
Tresca

$$\text{Plane stress: } r_p = \frac{K^2}{2\pi\sigma_{ys}^2} \left[\cos \frac{\theta}{2} \left(1 + \sin \frac{\theta}{2} \right) \right]^2$$

Plane strain: the larger of

$$r_p = \frac{K^2}{2\pi\sigma_{ys}^2} \cos^2 \frac{\theta}{2} \left[1 - 2\nu + \sin \frac{\theta}{2} \right]^2 \quad \text{and} \quad r_p = \frac{K^2}{2\pi\sigma_{ys}^2} \cos^2 \frac{\theta}{2}.$$

a



b

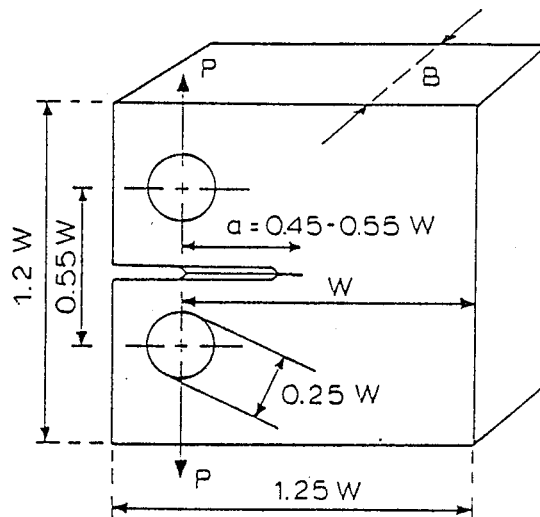


Figure 7.1. Standard specimens
a. Bend specimen; b. Compact tension specimen

bend specimen*

$$K = \frac{PS}{BW^{\frac{3}{2}}} \frac{3\left(\frac{a}{W}\right)^{\frac{3}{2}} \left[1.99 - \frac{a}{W} \left(1 - \frac{a}{W} \right) \left(2.15 - 3.93 \frac{a}{W} + 2.7 \frac{a^2}{W^2} \right) \right]}{2 \left(1 + 2 \frac{a}{W} \right) \left(1 - \frac{a}{W} \right)^{\frac{3}{2}}} \quad (7.3)$$

compact tension specimen**

$$K = \frac{P}{BW^{\frac{3}{2}}} \times \frac{\left(2 + \frac{a}{W} \right) \left[0.886 + 4.64 \frac{a}{W} - 13.32 \left(\frac{a}{W} \right)^2 + 14.72 \left(\frac{a}{W} \right)^3 - 5.6 \left(\frac{a}{W} \right)^4 \right]}{\left(1 - \frac{a}{W} \right)^{\frac{3}{2}}} \quad (7.4)$$

* Eq (7.3) is accurate within 0.5 per cent over the entire range of a/W .
Eq (7.4) is also accurate within 0.5 per cent, but only in the range $0.2 < a/W < 1$.

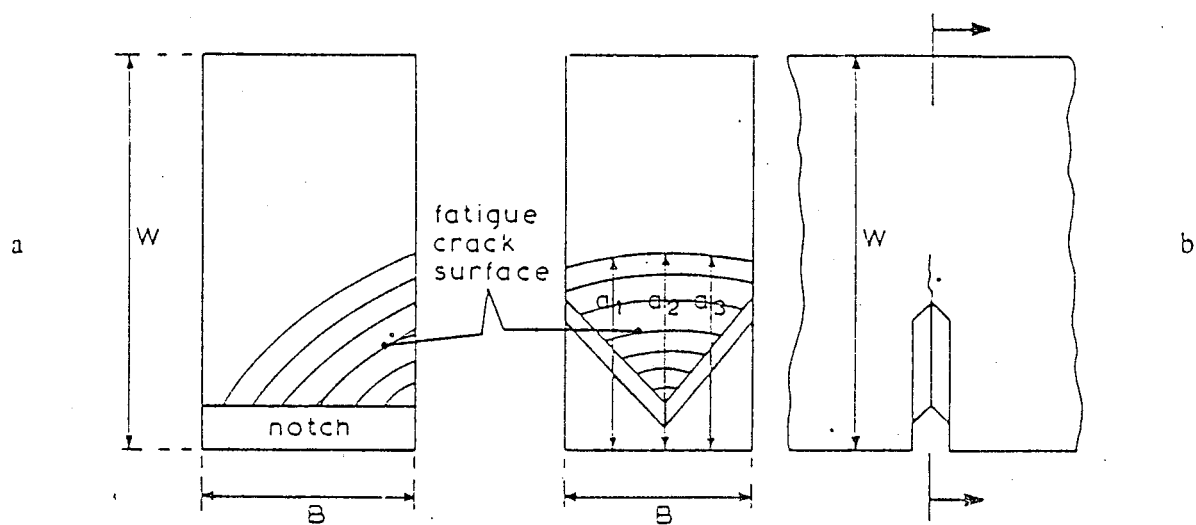


Figure 7.2. Starter notch
a. Normal edge notch; b. Chevron notch

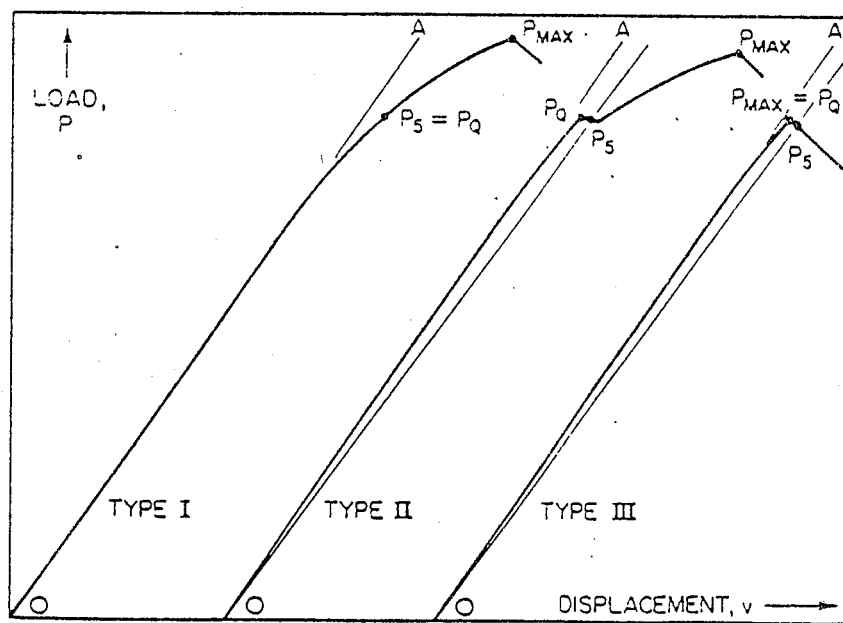


FIG. 3.21. Types of load displacement curves illustrating procedure for determination of K_{Ic} .

TABLE 7.1 Typical K_{Ic} data at room temperature

Material	Condition	σ_{ys}	K_{Ic}		Minimum required thickness B	
			kg/mm ²	ksi	mm	inches
<i>Steel</i>						
Maraging steel						
300	900 F 3 hrs	200	285	182	52	2.1 0.09
300	850 F 3 hrs	170	242	300	85	7.8 0.31
250	900 F 3 hrs	181	259	238	68	4.3 0.18
D 6 AC steel	heat treated	152	217	210	60	4.8 0.20
	heat treated	150	214	311	89	10.7 0.44
4340 steel	Forging	150	214	178-280	51-80	
	hardened	185	265	150	43	1.7 0.07
A 533 B	reactor steel	35	50	≈ 630	≈ 180	810 33
Carbon steel	low strength	24	35	> 700	> 200	2150 82
<i>Titanium</i>						
6Al-4V	($\alpha + \beta$) STA	112	160	122	35	3 0.12
13V-11Cr-3Al	STA	115	164	89	25	1.5 0.07
6Al-2Sn-4Zr-6Mo	($\alpha + \beta$) STA	120	171	85	24	1.3 0.05
6Al-6V-2Sn	($\alpha + \beta$) STA	110	157	120	34	3.0 0.12
4Al-4Mo-2Sn-0.5Si	($\alpha + \beta$) STA	96	137	224	64	13.6 0.55
<i>Aluminium</i>						
7075	T651	55	79	94	27	7.3 0.30
7079	T651	47	68	105	30	12.5 0.49
DTD 5024	Forged					
	Longitudinal	50	72	126	36	15.9 0.65
	Short transverse	49	70	53	15	3.0 0.12
2014	T4	46	65	90	26	9.6 0.40
2024	T3	40	57	110	31	19.0 0.75
Plexiglass				5.3	1.5	

Effect of Stress Concentration on Fatigue-Crack Initiation

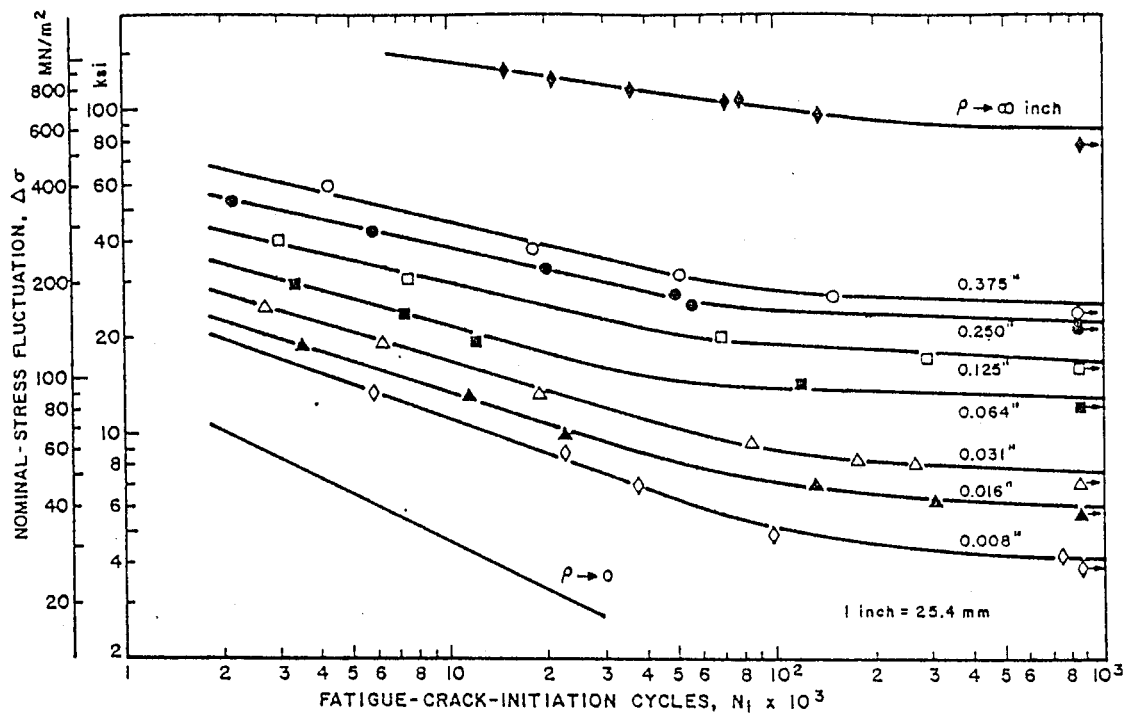


FIG. 7.6. Dependence of fatigue-crack initiation of HY-130 steel on nominal-stress fluctuations for various notch geometries.

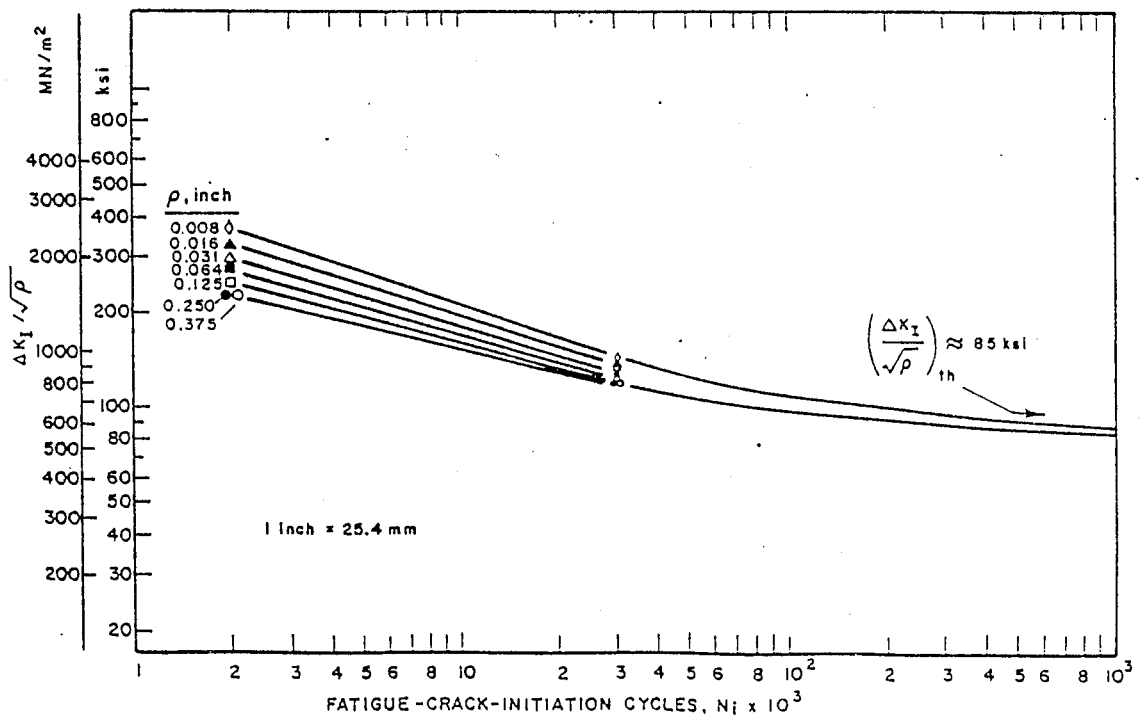


FIG. 7.7. Correlation of fatigue-crack-initiation life with the parameter $\Delta K_I / \sqrt{\rho}$ for HY-130 steel.

FATIGUE

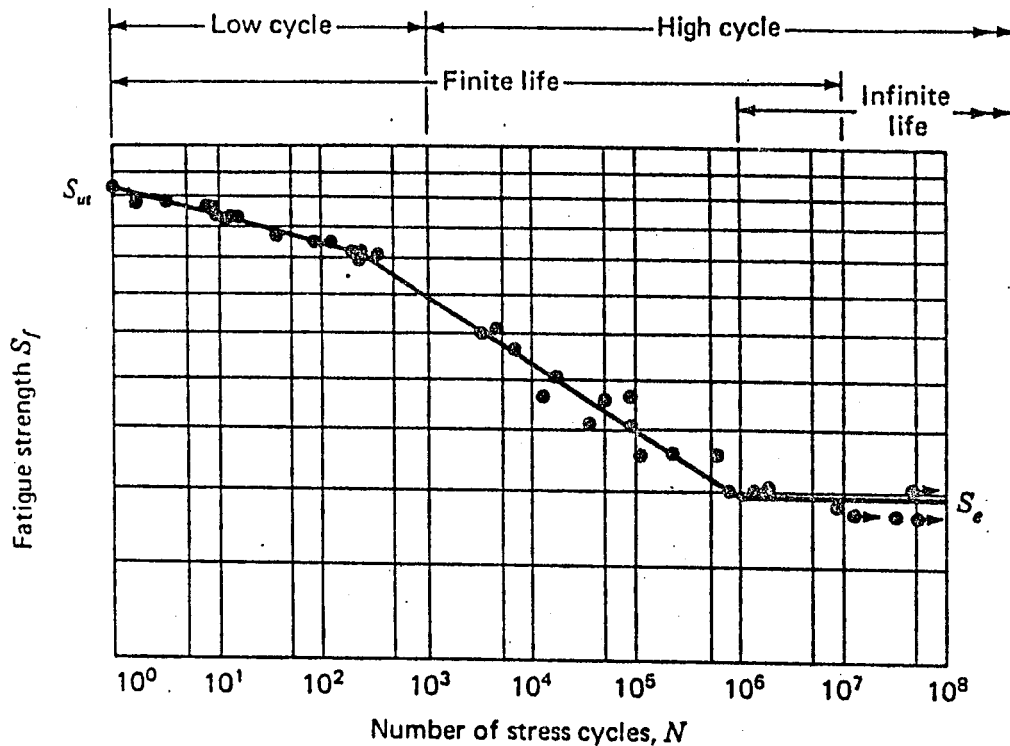


FIGURE 7-3 An S - N diagram plotted from the results of completely reversed axial fatigue tests. Material: chromium-molybdenum steel, normalized; $S_{ut} = 800$ MPa; maximum $S_{ut} = 860$ MPa; $S_e = 338$ MPa. (Data from NACA Technical Note 3866, December 1966.)

CUMULATIVE FATIGUE DAMAGE

Palmgren-Miner cycle-ratio summation theory*

$$\sum \frac{n_i}{N_i} = 1$$

* A. Palmgren «Die Lebensdauer von Kugellagern», *ZVDI*, vol. 68, 1924, pp. 339-341; M. A. Miner, "Cumulative Damage in Fatigue," *J. Appl. Mech.*, vol. 12, *Trans. ASME*, vol. 67, 1945, pp. A159-A164.

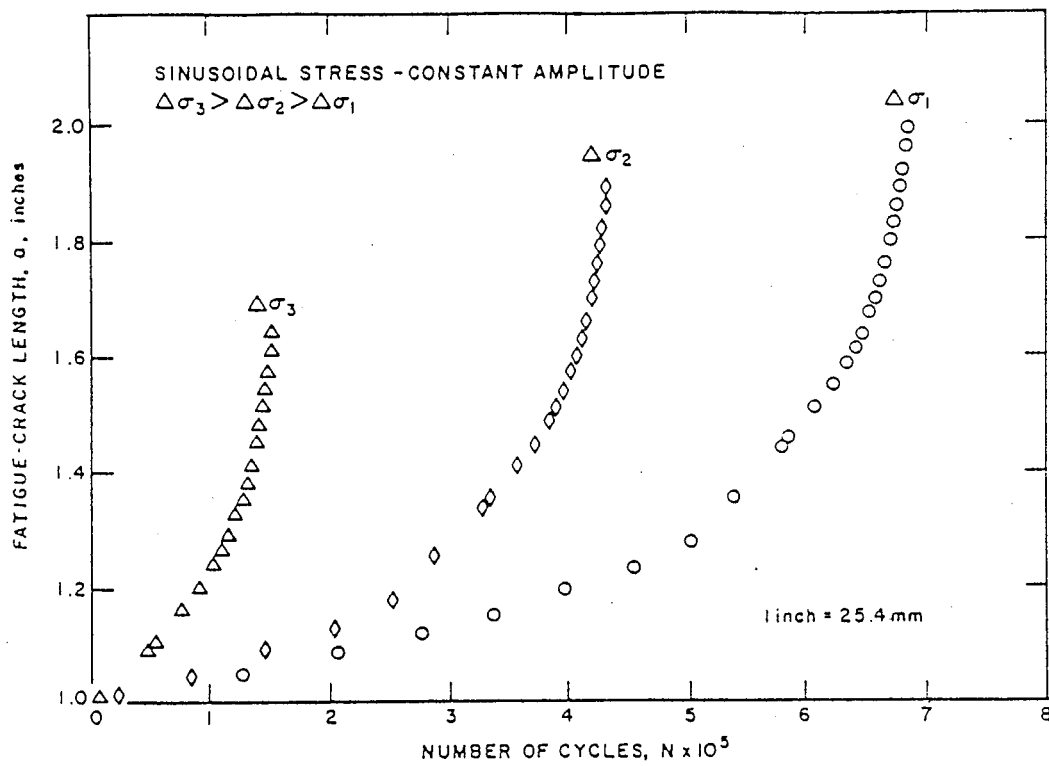


FIG. 8.2. Effect of cyclic-stress range on crack growth.

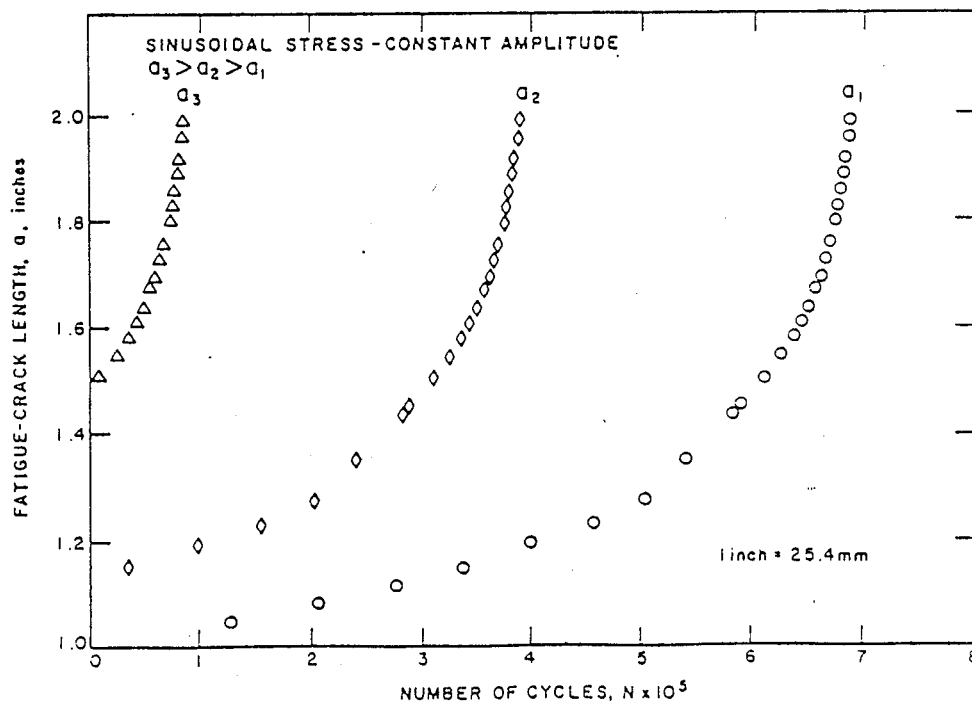


FIG. 8.3. Effect of initial crack length on crack growth.

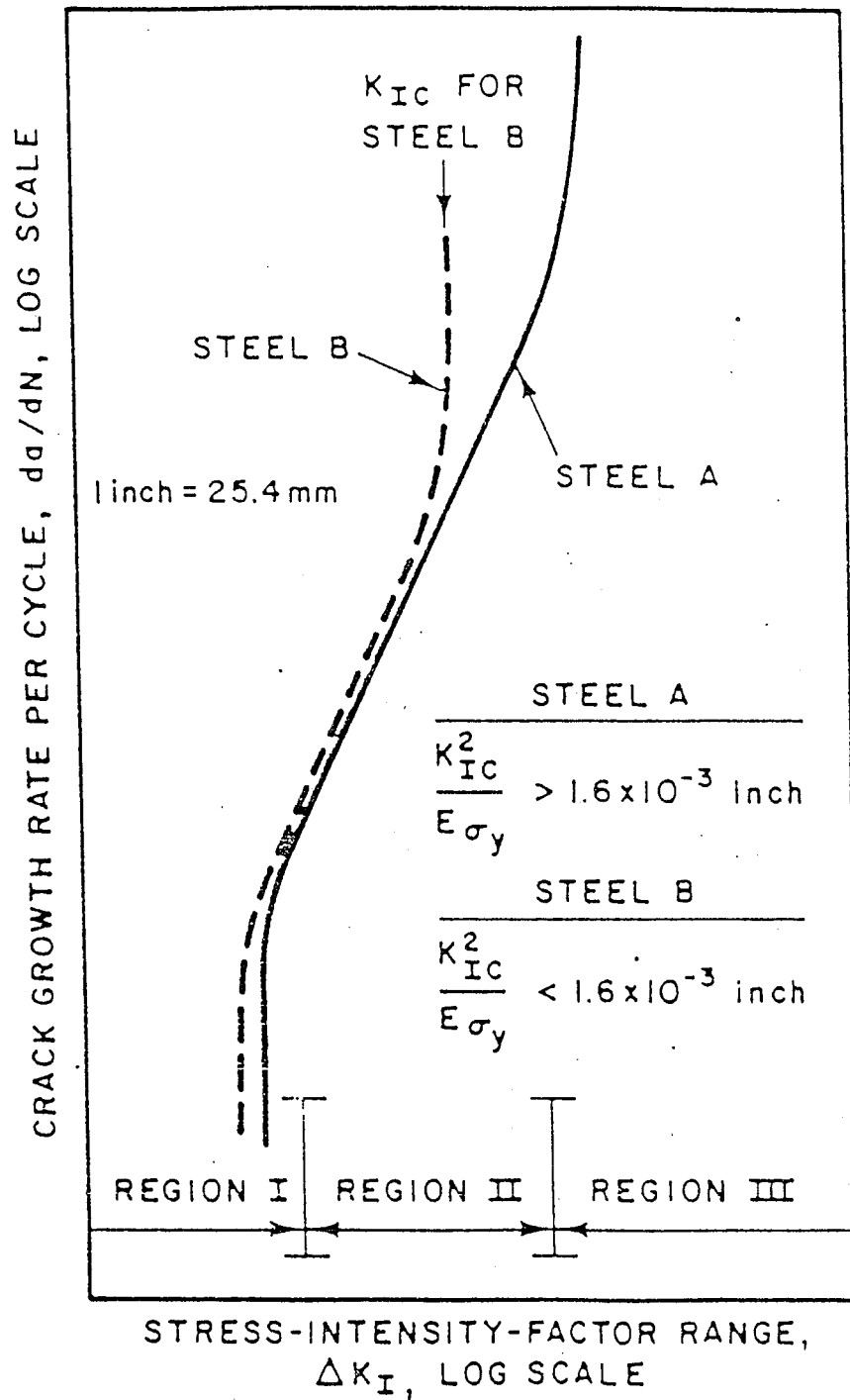


FIG. 8.4. Schematic representation of fatigue-crack growth in steel.

$$\delta_T = \frac{K_T^2}{E\sigma_{ys}} = 1.6 \times 10^{-3} \text{ in. } (0.04 \text{ mm})$$

K_T = stress-intensity-factor-range value corresponding to onset of
celeration in fatigue-crack-growth rates,
 E = Young's modulus,

Martensitic Steels

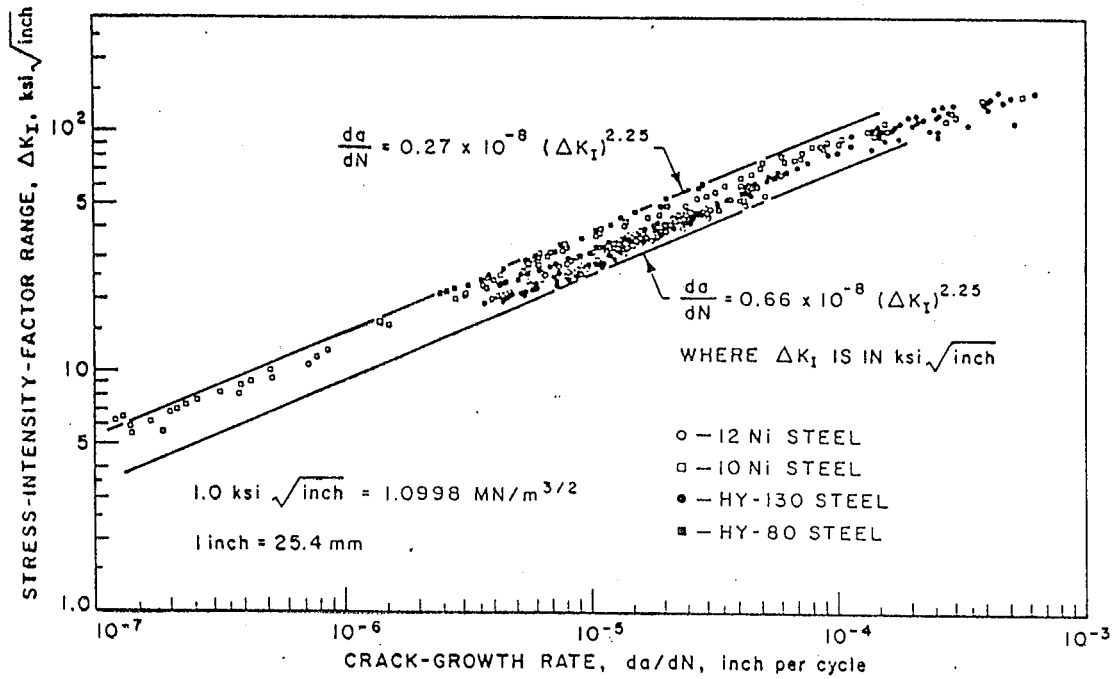


FIG. 8.5. Summary of fatigue-crack-propagation for martensitic steels.

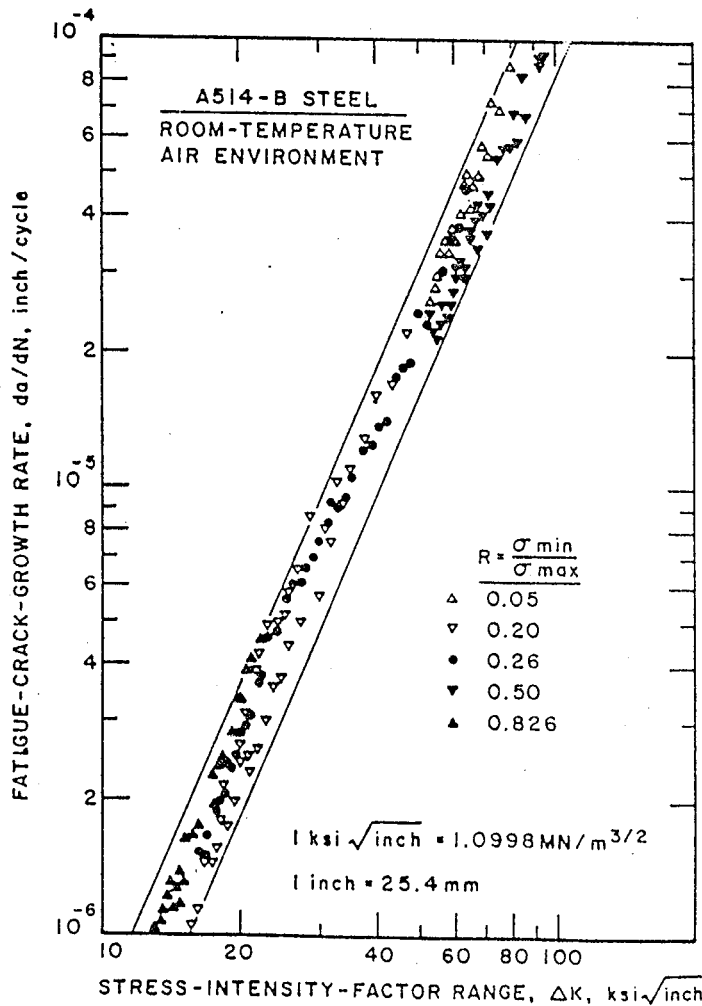


FIG. 8.6. Crack-growth rate as a function of stress-intensity range for A514-B steel.

Ferrite-Pearlite Steels

$$\frac{da}{dN} = 3.6 \times 10^{-10} (\Delta K_I)^{3.0}$$

where $a = \text{in.}$,
 $\Delta K_I = \text{ksi}\sqrt{\text{in.}}$

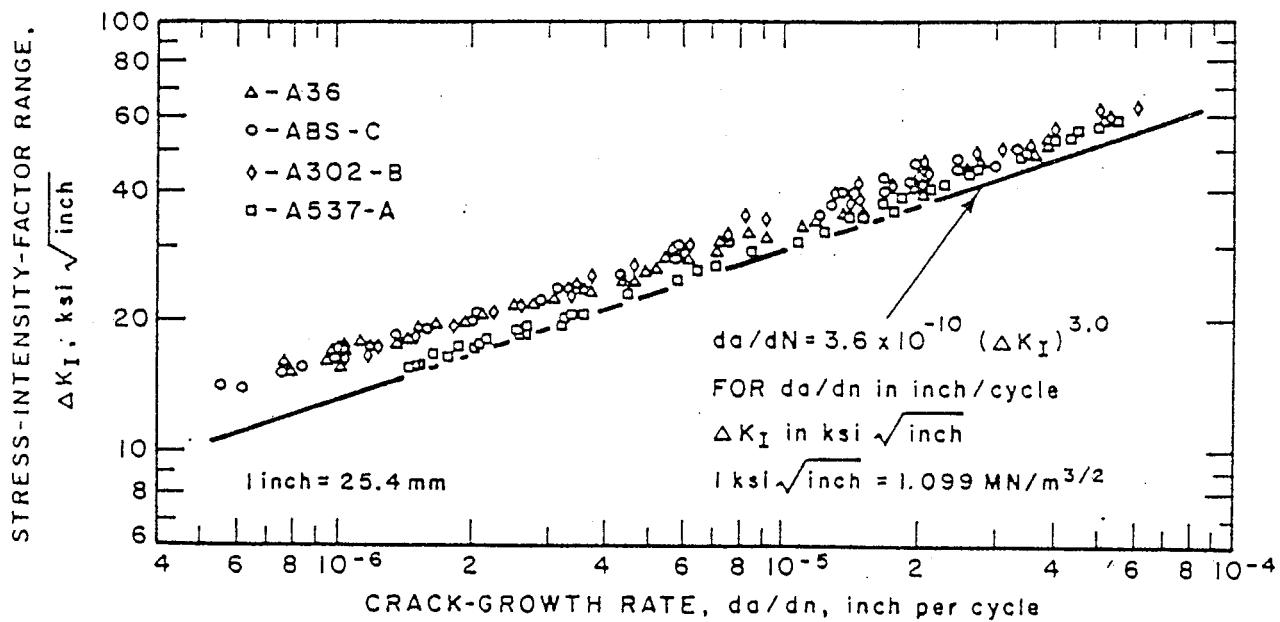


FIG. 8.8. Summary of fatigue-crack-growth data for ferrite-pearlite steels.

Austenitic Stainless Steels

$$\frac{da}{dN} = 3.0 \times 10^{-10} (\Delta K_I)^{3.25}$$

$a = \text{in.},$
 $K_I = \text{ksi}\sqrt{\text{in.}}$

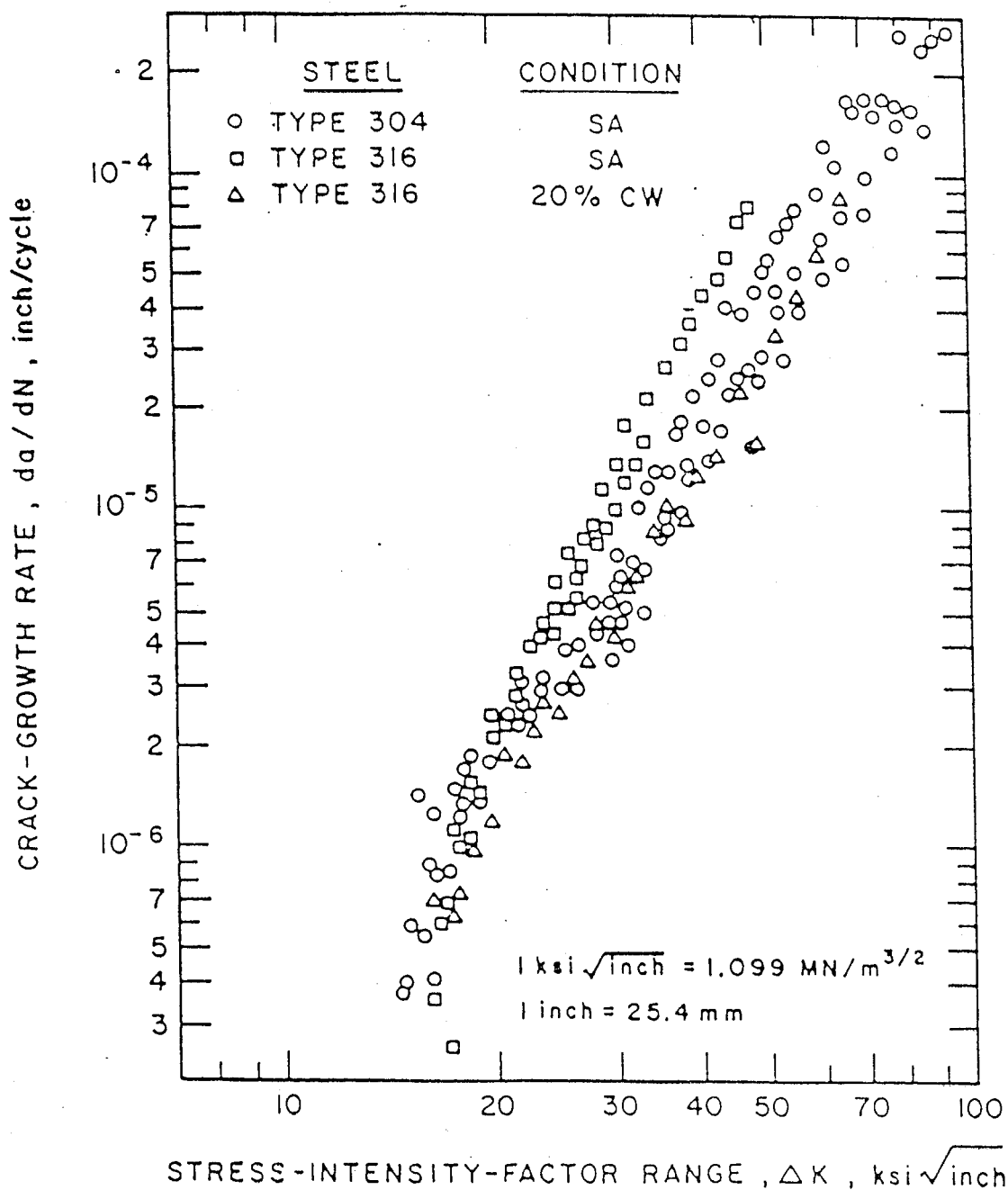


FIG. 8.9. Fatigue-crack-growth rate of solution-annealed type 304 and 316 stainless steels and 20 percent cold-worked type 316 stainless steel at 75°F.

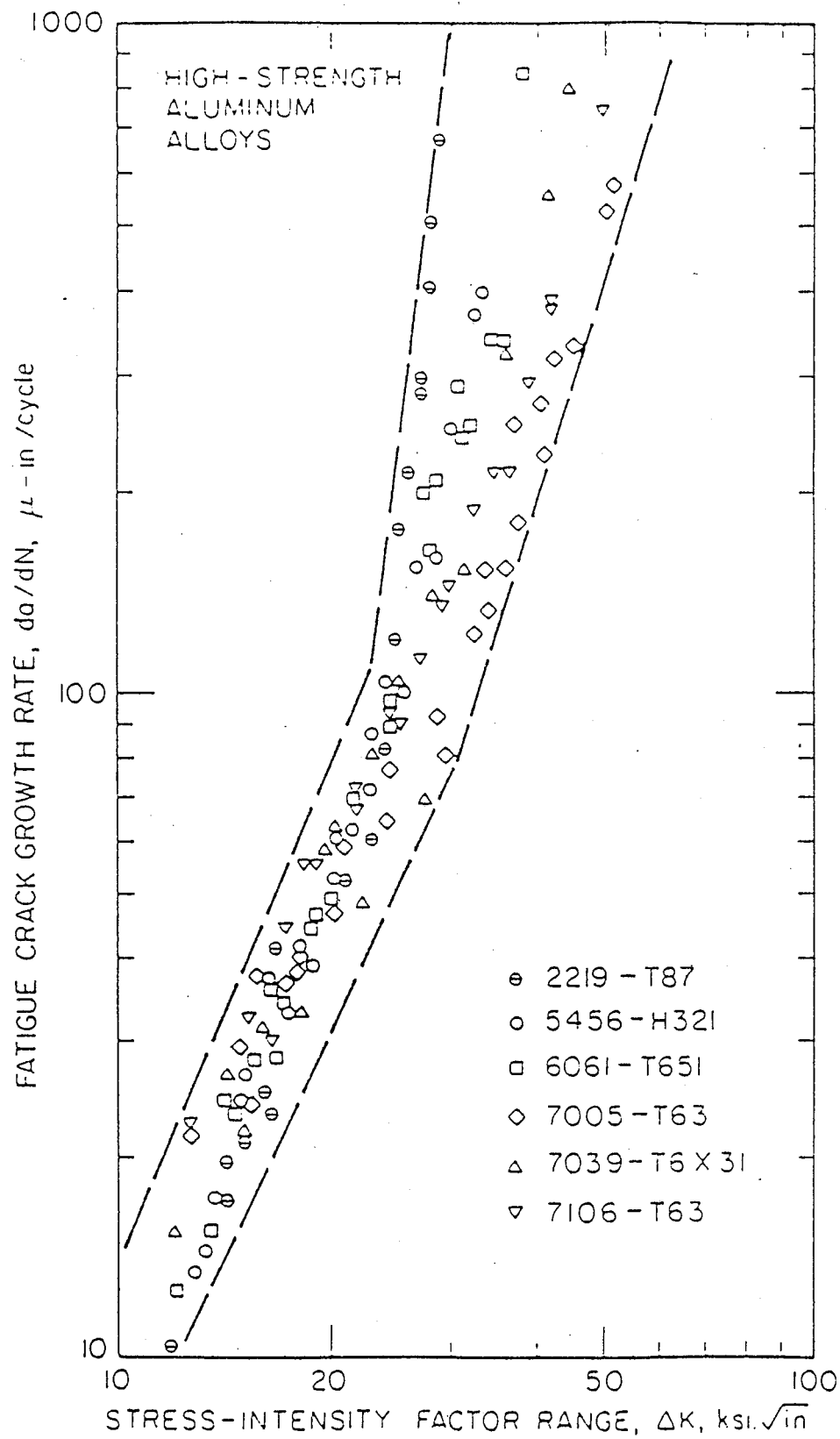


FIG. 8.13. Summary plot of da/dN versus ΔK for six aluminum alloys. The yield strengths of these alloys range from 34 to 55 ksi.

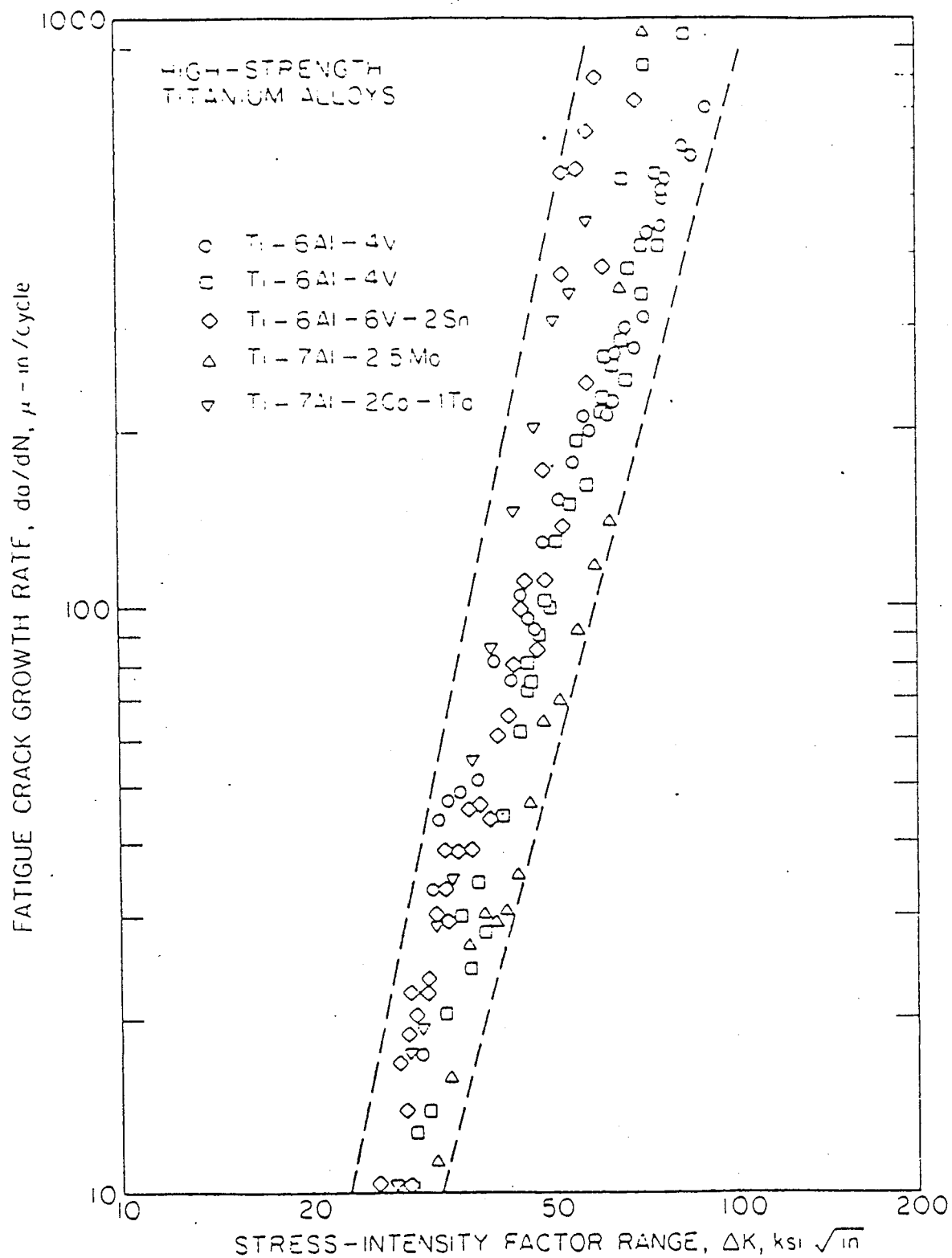


FIG. 8.14. Summary plot of da/dN versus ΔK data for five titanium alloys ranging in yield strength from 110 to 150 ksi.

STRESS-INTENSITY-FACTOR RANGE, ΔK_I , ksi $\sqrt{\text{inch}}$

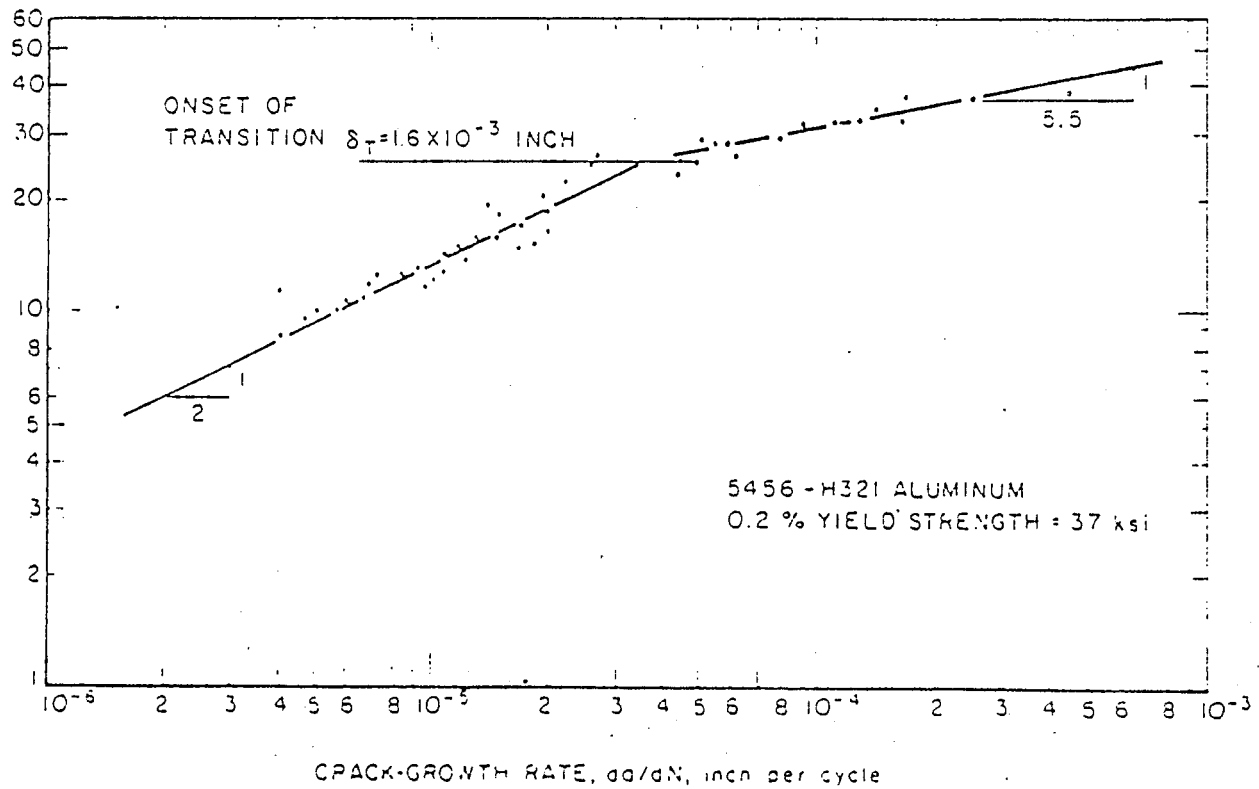


FIG. 8.15. Fatigue-crack-growth rate as a function of stress intensity for 5456-H321 aluminum.

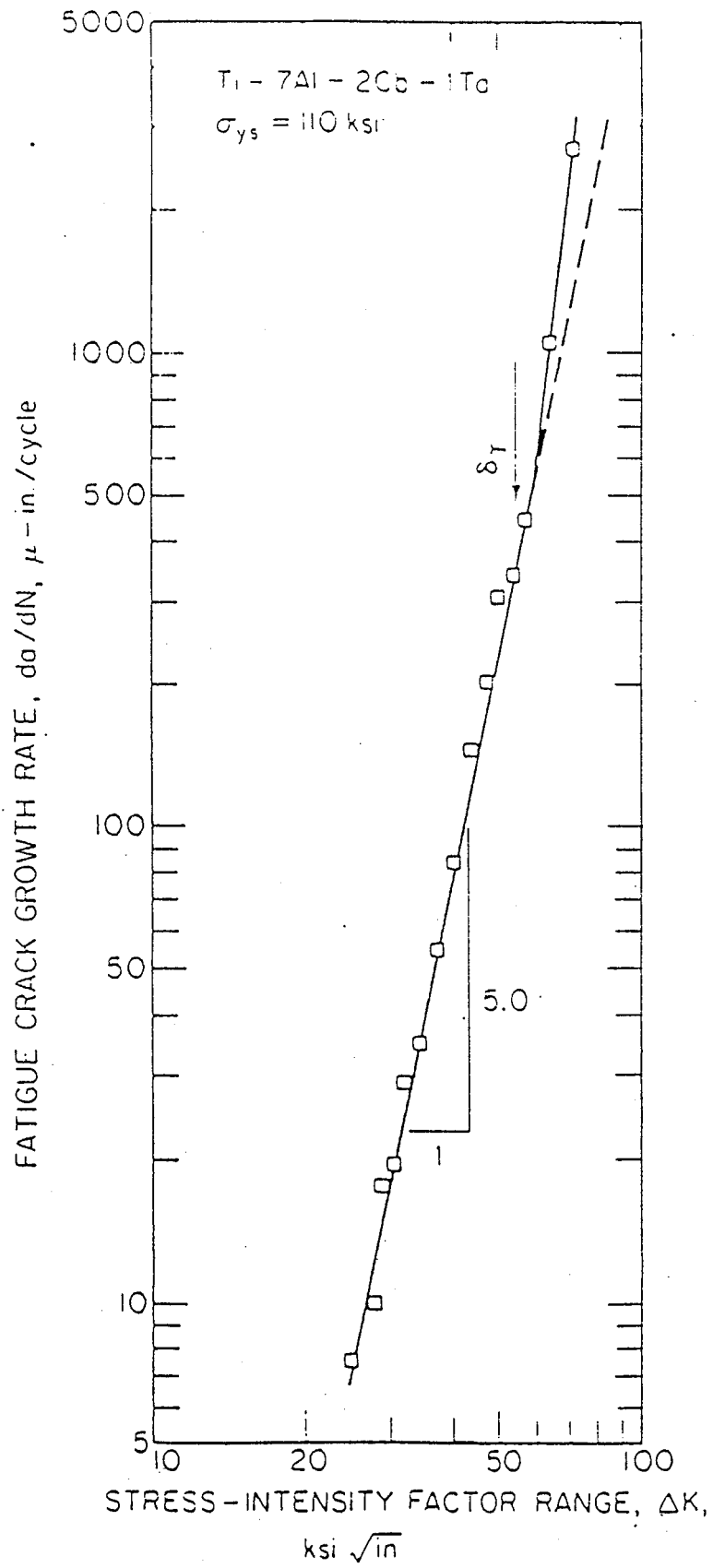


FIG. 8.16. Fatigue-crack-growth rate in a titanium alloy.

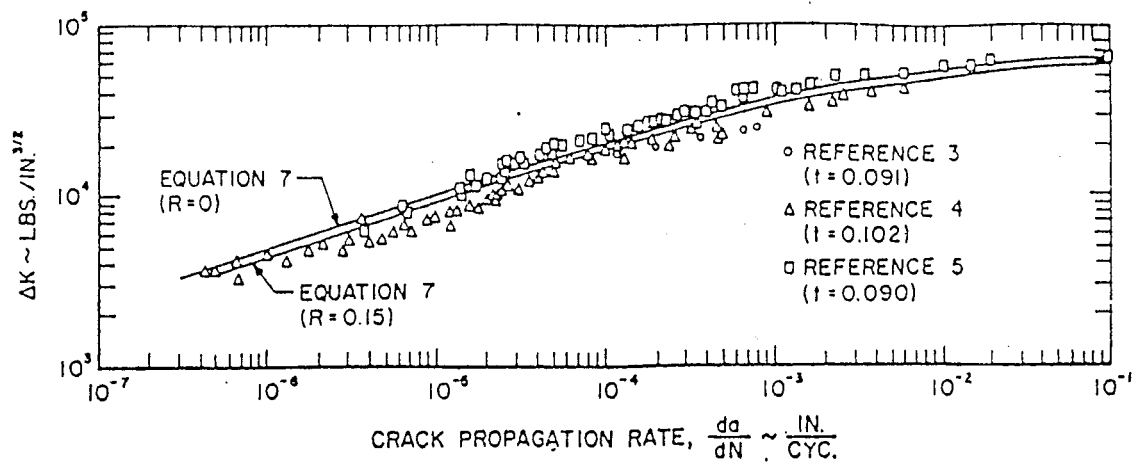


Fig. 1 Comparison of experimental and theoretical crack-propagation rates in 7075-T6 aluminum plate for $R = 0$ to $R = 0.15$

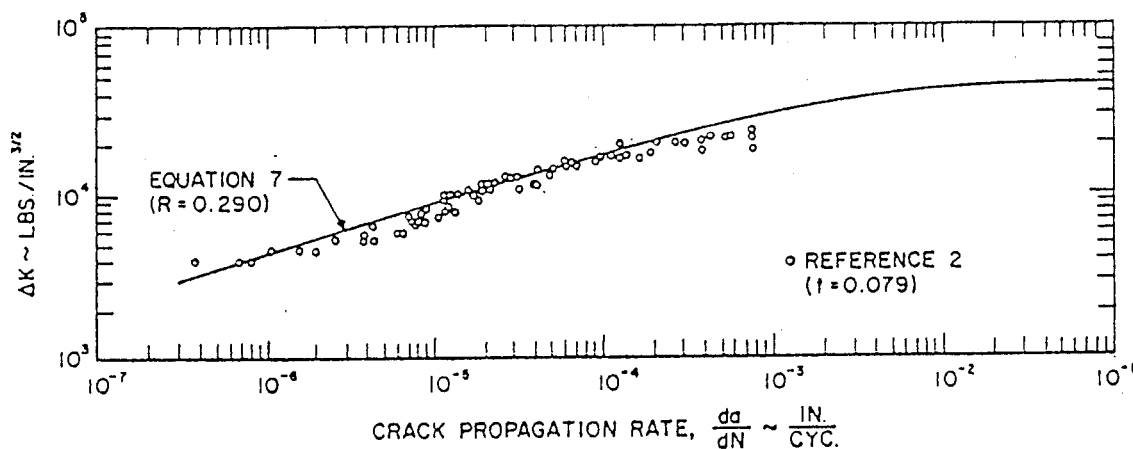


Fig. 2 Comparison of experimental and theoretical crack-propagation rates in 7075-T6 aluminum plate for $R = 0.285$ to $R = 0.297$

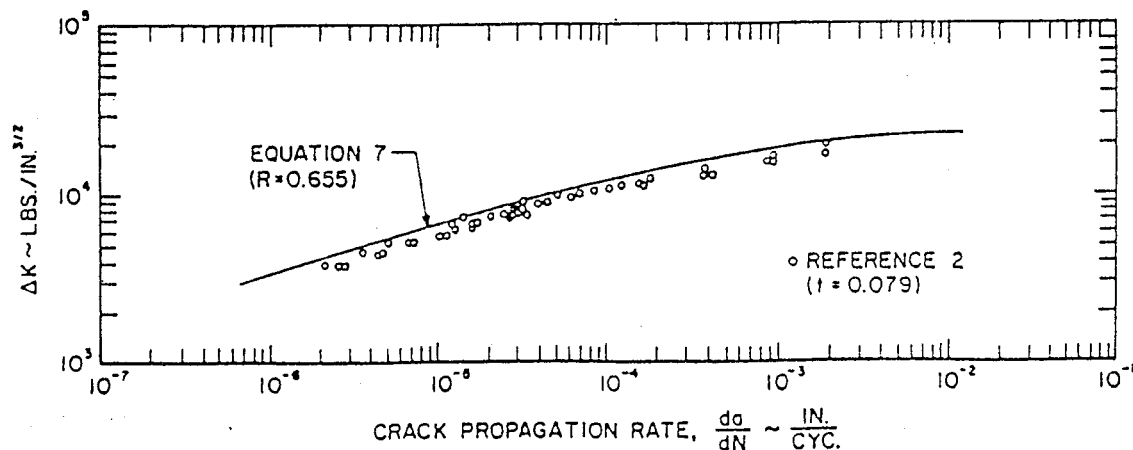


Fig. 3 Comparison of experimental and theoretical crack-propagation rates in 7075-T6 aluminum plate for $R = 0.655$

$$\frac{da}{dN} = \frac{C(\Delta K)^n}{(1-R)K_2 - \Delta K}$$

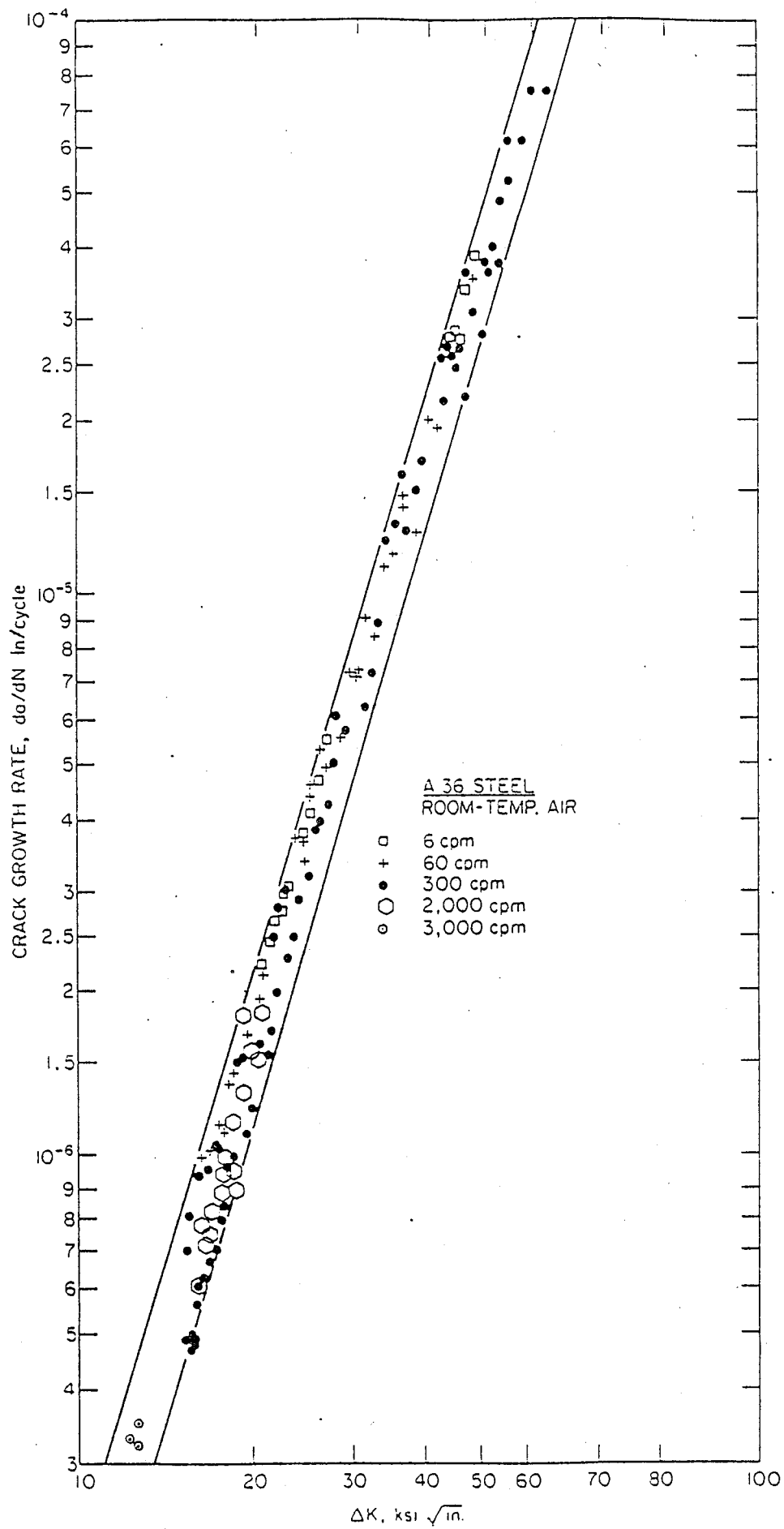


FIG. 8.19. Effect of cyclic frequency on crack growth rates in benign environment.

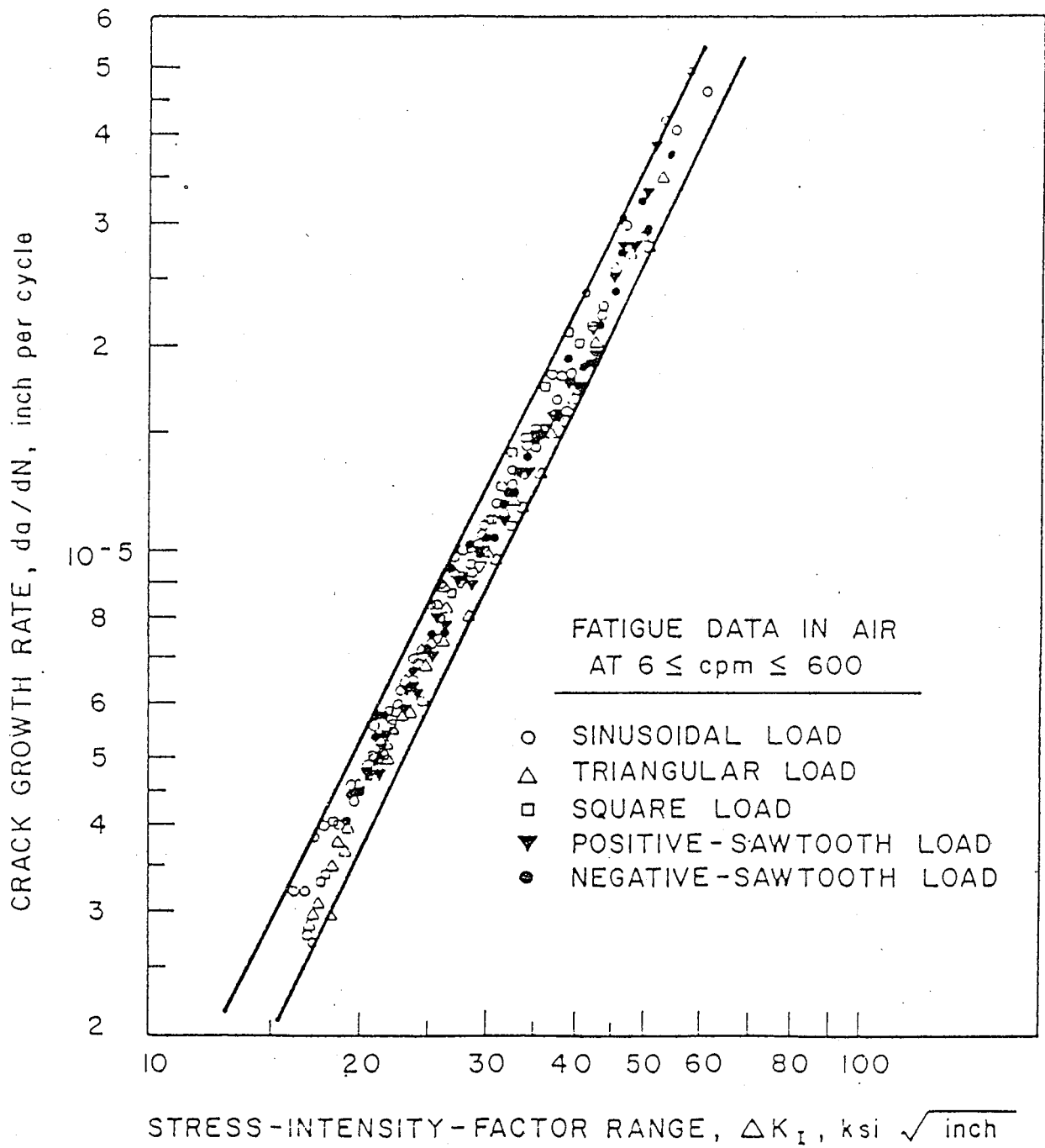


FIG. 8.20. Fatigue-crack-growth rates in 12Ni-5Cr-3Mo steel under various cyclic-stress fluctuations with different stress-time profiles.

FATIGUE - LIFE PREDICTION

The Basic Algorithm

- a) Determine the initial crack size a_o by measuring it, or by estimating it based on the NDT resolution.
- b) Determine the relation $K_I(a)$ for the given structure and loading conditions.
- c) Calculate K_T
- d) Determine the crack critical size a_{cr} based on K_{IC} or K_T .
- e) Determine experimentally or from handbook the appropriate fatigue-crack growth rate equation e.g.,:

$$\frac{da}{dN} = A_p (\Delta K_I)^{n_p}$$

- f) Determine ΔK_I from the prescribed loading
- g) Integrate from a_o to a_{cr}

$$N_f = \int_{a_o}^{a_{cr}} \frac{da}{A_p (\Delta K_I)^{n_p}}$$

Fatigue-Crack-Growth Calculations

$$\Delta N = \frac{\Delta a}{0.66 \times 10^{-8} [1.985(\Delta \sigma) \sqrt{a_{\text{avg}}}]^{2.25}} = \frac{\Delta a}{0.66 \times 10^8 [39.7 \sqrt{a_{\text{avg}}}]^{2.25}}$$

a_0 (in.)	a_f (in.)	a_{avg} (in.)	ΔK_I (ksi $\sqrt{\text{in.}}$)	ΔN (cycles)	ΣN (cycles)
0.3	0.4	0.35	23.5	12,477	12,477
0.4	0.5	0.45	26.7	9,404	21,881
0.5	0.6	0.55	29.4	7,504	29,385
0.6	0.7	0.65	32.0	6,218	35,603
0.7	0.8	0.75	34.4	5,293	40,896
0.8	0.9	0.85	36.6	4,598	45,494
0.9	1.0	0.95	38.7	4,057	49,551
1.0	1.1	1.05	40.7	3,625	53,176
1.1	1.2	1.15	42.6	3,273	56,419
1.2	1.3	1.25	44.4	2,980	54,429
1.3	1.4	1.35	46.1	2,732	62,161
1.4	1.5	1.45	47.8	2,521	64,682
1.5	1.6	1.55	49.4	2,339	67,021
1.6	1.7	1.65	51.0	2,180	69,201
1.7	1.8	1.75	52.5	2,041	71,242
1.8	1.9	1.85	54.0	1,917	73,159
1.9	2.0	1.95	55.4	1,807	74,966
2.0	2.1	2.05	56.8	1,708	76,674
2.1	2.2	2.15	58.2	1,619	78,293
2.2	2.3	2.25	59.6	1,538	79,831
2.3	2.4	2.35	60.9	1,464	81,295
2.4	2.5	2.45	62.1	1,396	82,691
2.5	2.6	2.55	63.4	1,336	84,027
2.6	2.7	2.65	64.6	1,280	85,307
2.7	2.8	2.75	65.8	1,227	86,534

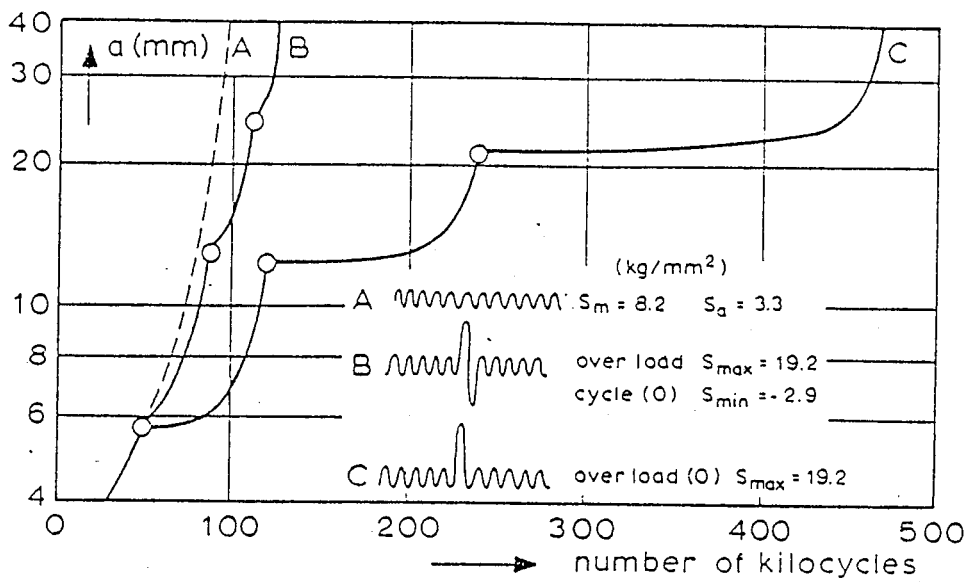


Figure 10.10. Retardation as a result of overloads [48] 2024-T3 Al-alloy

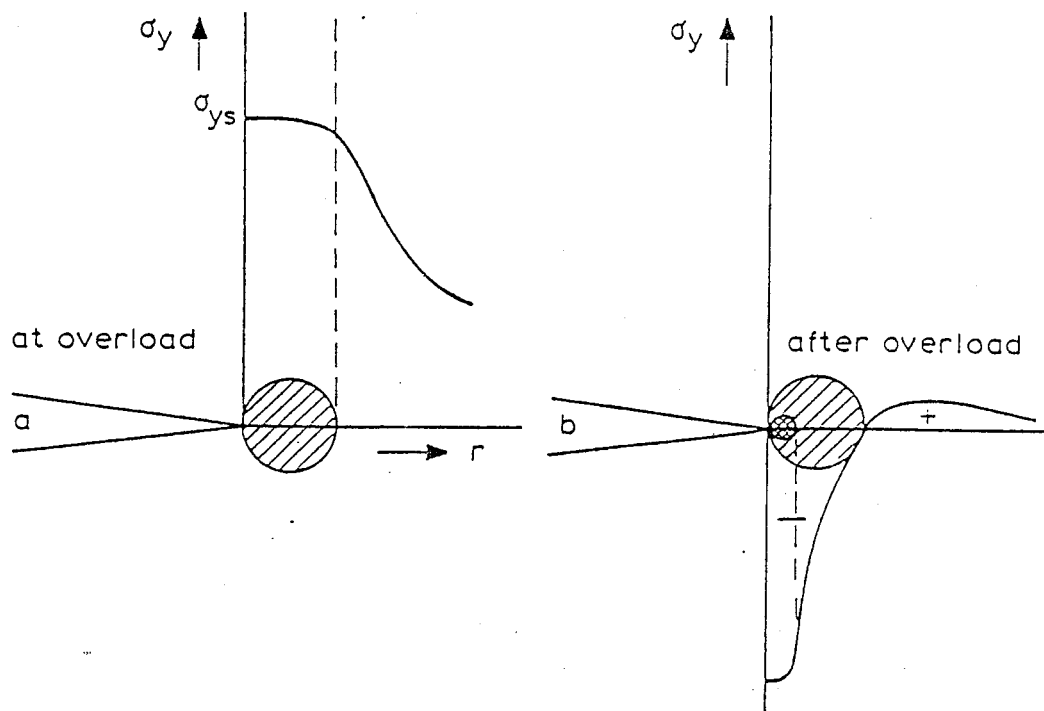


Figure 10.11. Residual compressive stresses at crack tip as a result of overload

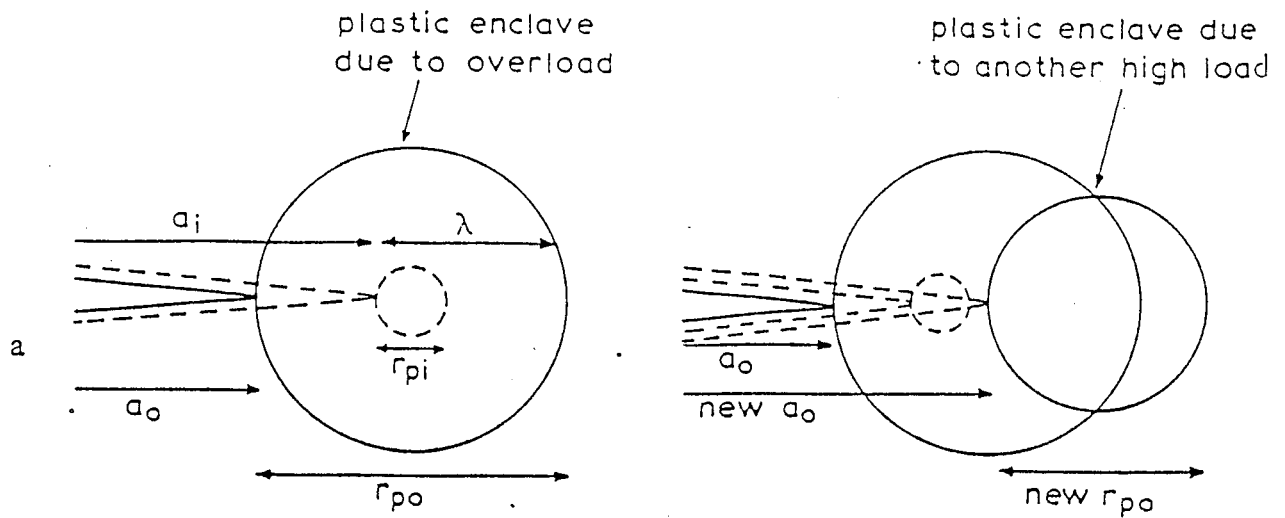


Figure 10.15. The model of Wheeler [61]
a. Situation after overload; b. Situation after second overload

$$\left(\frac{da}{dN}\right)_{\text{retarded}} = \phi \left(\frac{da}{dN}\right)_{\text{linear}} = \phi f(\Delta K)$$

$$\text{with } \phi = \left(\frac{r_{pi}}{a_o + r_{po} - a_i}\right)^m \text{ as long as } a_i + r_{pi} < a_o + r_{po}.$$

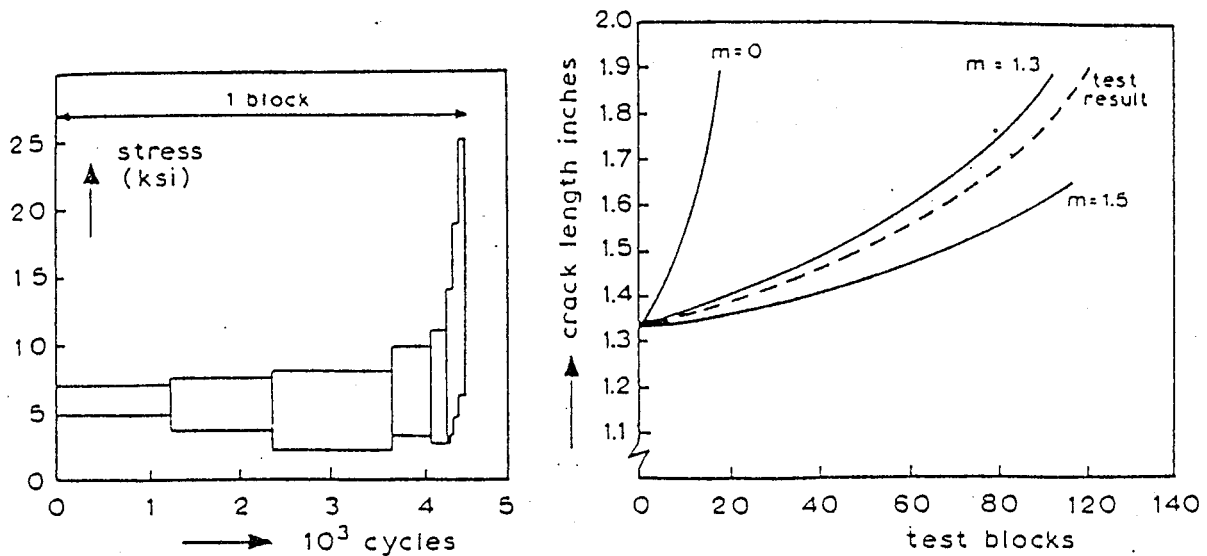


Figure 10.16. Prediction of crack growth made by Wheeler [61] (courtesy ASME)

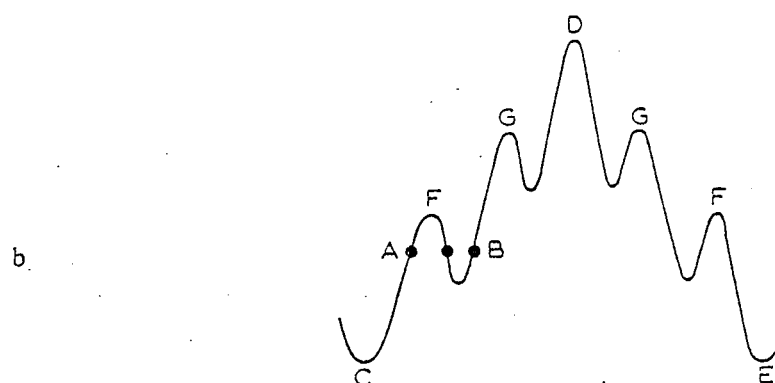
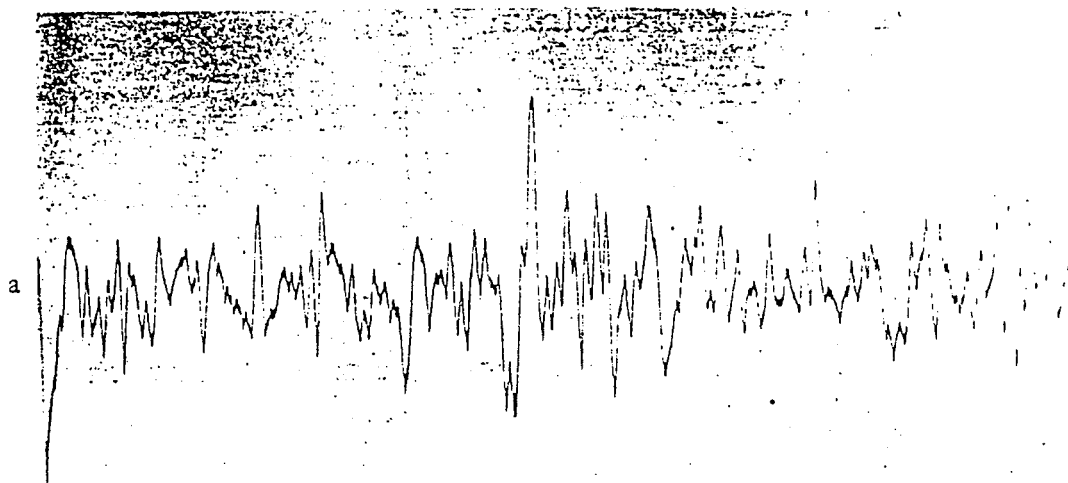


Figure 17.1. Analysis of load-time history

a. Measured load-time history of aircraft wing [2]; b. Two examples of counting procedures
 Alternatives: 4 cycles AB plus one cycle CDE or 2 peaks to F, 2 peaks to G, 1 peak to D

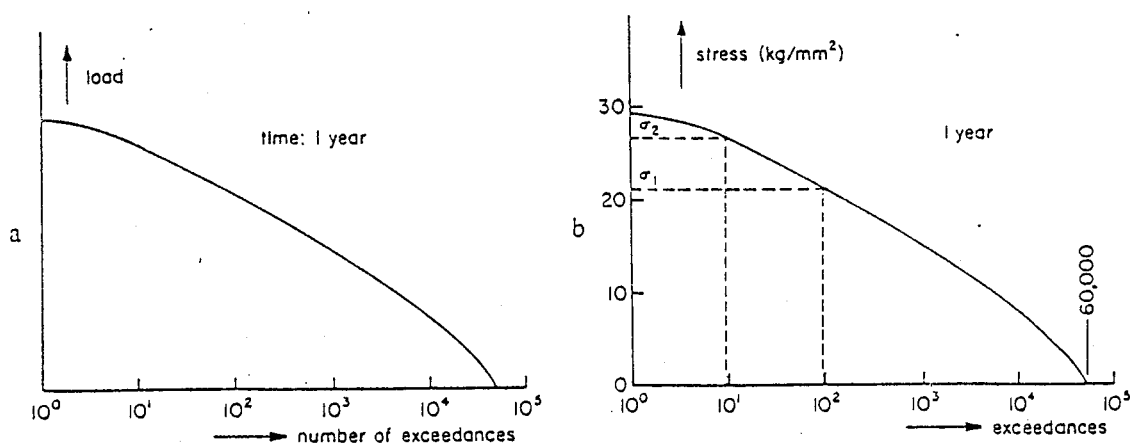


Figure 17.2. Assumed exceedance curve
 a. Load exceedances; b. Stress exceedances

Approximation of the stress spectrum

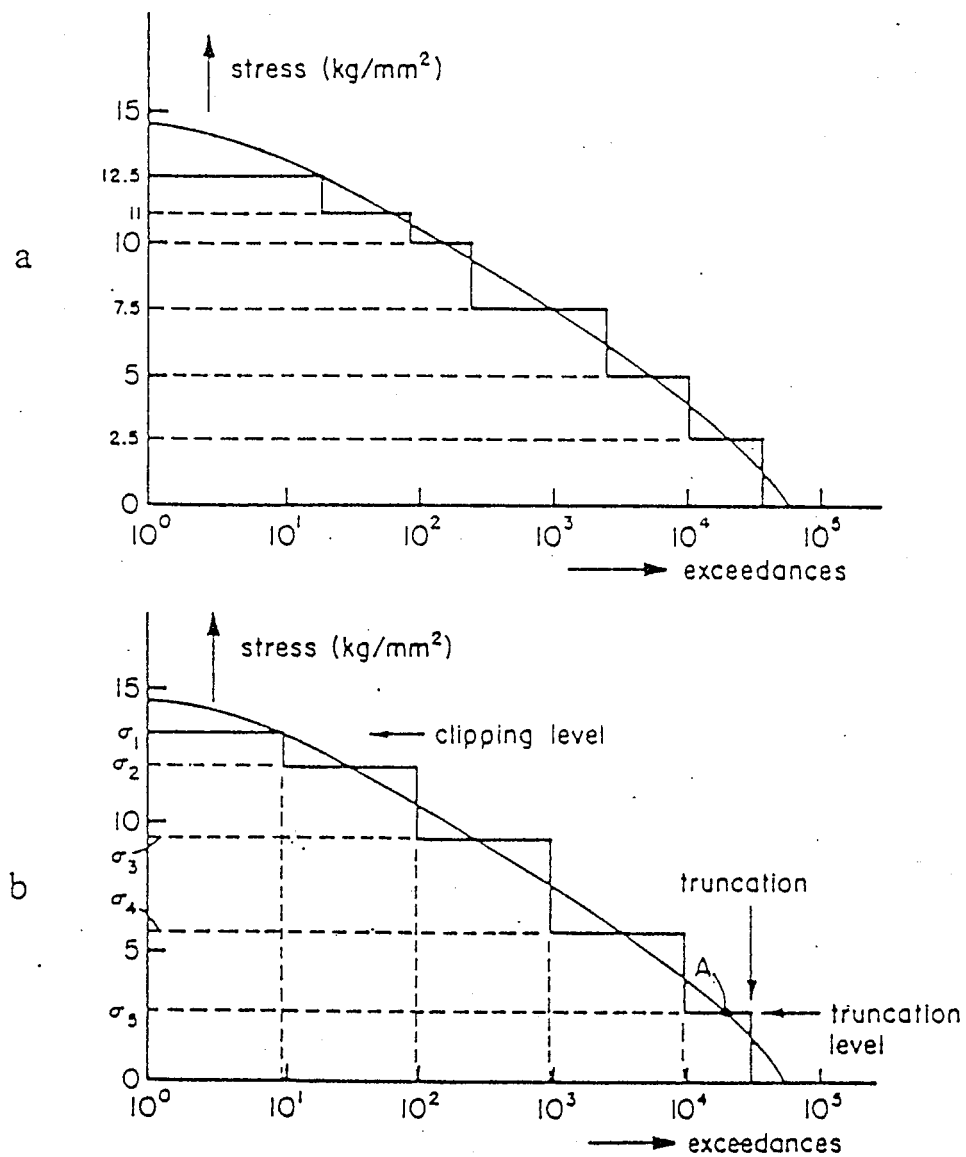


Figure 17.3. Stepwise approximation of exceedance curve
 a. Discrete stress levels; b. Discrete exceedances

TABLE 17.1
Establishment of loads block

Stress Level, kg/mm ²	Exceedances	Occurrences	Occurrences per day	Occurrences in one-tenth year
13.5	10	10	0.027	1
12	100	90	0.247	9
9	1,000	900	2.47	90
5.8	10,000	9,000	24.7	900
2.8	30,000	20,000	54.8	2000

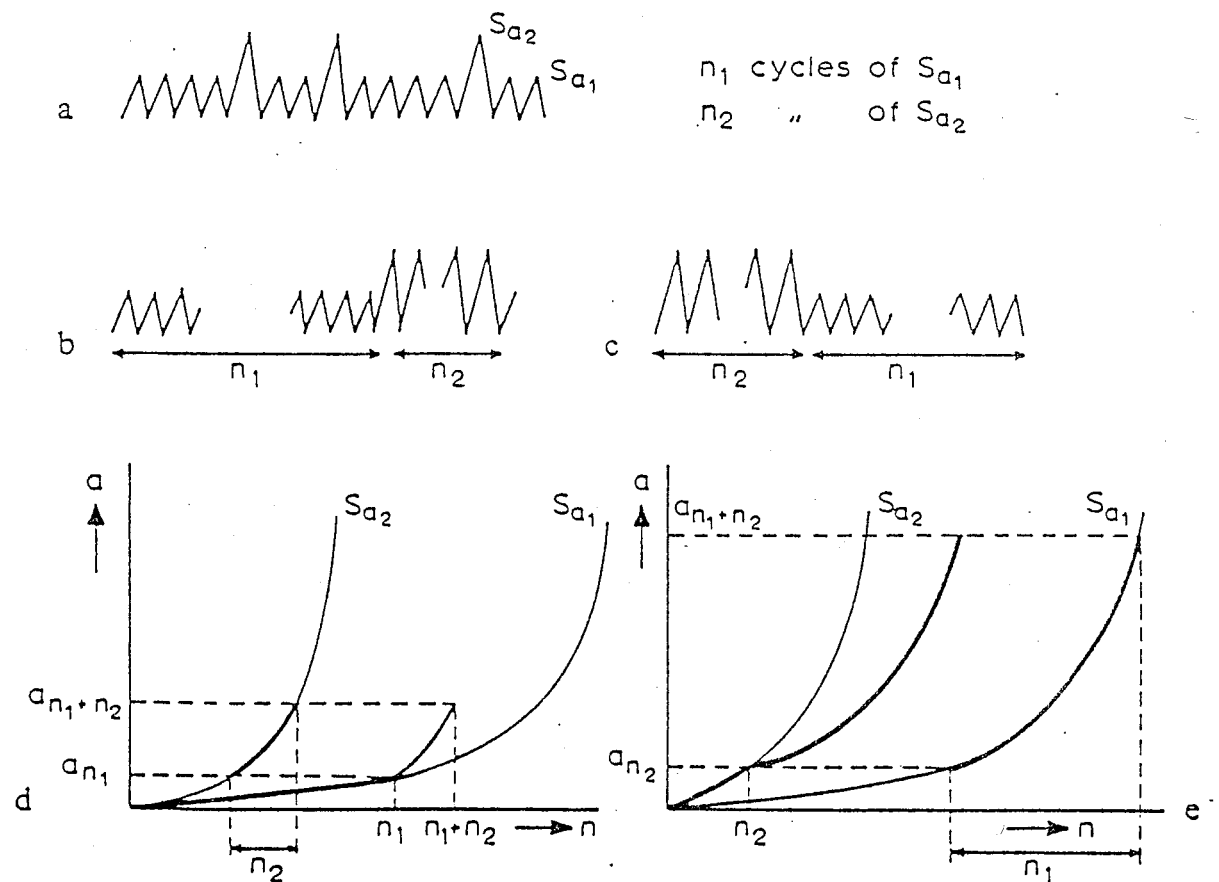


Figure 17.4. Effect of sequence on integration
a. Actual history; b. Simplification; c. Simplification; d. Result of b; e. Result of c

TABLE 17.2

Linear crack growth integration (no retardation)

First block						Second block			
Stress level, (kg/mm ²)	Cycles in block	Crack size, (mm)	ΔK, kg/mm ^{3/2}	da/dN, mm/cycles	Δa, (mm)	Crack size, (mm)	ΔK, (kg/mm ^{3/2})	da/dN mm/cycles	Δa, mm
13.5	1	5.0	53.5	2.45 × 10 ⁻³	× 1 = 0.00245	5.1471	54.29	2.60 × 10 ⁻³	0.0026
12	9	5.00245	47.57	1.54 × 10 ⁻³	× 9 = 0.01382	5.1497	48.27	1.63 × 10 ⁻³	0.0147
9	90	5.0163	35.73	4.89 × 10 ⁻⁴	× 90 = 0.0440	5.1644	36.25	5.18 × 10 ⁻⁴	0.0466
5.8	900	5.0603	23.13	8.58 × 10 ⁻⁵	× 900 = 0.0772	5.2110	23.47	9.10 × 10 ⁻⁵	0.0819
2.8	2000	5.1375	11.24	4.80 × 10 ⁻⁶	× 2000 = 0.0096	5.2929	11.41	5.10 × 10 ⁻⁶	0.0102
Alternative with fixed crack size per block									
13.5	1	5.0	53.5	2 × 10 ⁻³	0.002	5.14	54.2	2.6 × 10 ⁻³	0.0026
12	9	5.0	47.5	1.5 × 10 ⁻³	0.0105	5.14	48.2	1.6 × 10 ⁻³	0.0145
9	90	5.0	35.6	4.8 × 10 ⁻⁴	0.0435	5.14	36.2	5.1 × 10 ⁻⁴	0.0460
5.8	900	5.0	22.9	8.3 × 10 ⁻⁵	0.0748	5.14	23.3	8.9 × 10 ⁻⁵	0.0800
2.8	2000	5.0	11.1	4.5 × 10 ⁻⁶	0.009	5.14	11.2	4.8 × 10 ⁻⁶	0.0096
						+ Δa = 0.1527 New a = 5.28			

TABLE 17.3

Crack-growth integration with retardation

Stress level, kg/mm ²	Cycles in block	Crack size a, mm	ΔK , kg/mm ^{3/2}	da/dN linear, mm/cycle	r_p , mm	$a + r_p$, mm	$a + r_{p0}$, mm	$a + r_{p0} - a_i$, mm	$\phi = \left(\frac{r_p}{a + r_{p0} - a_i} \right)^m$	da/dN retarded, mm/cycle	Δa , mm	New a, mm
<i>First block</i>												
13.5	1	5.0	53.5	2.45×10^{-3}	0.061	5.061	5.061	0.061	1	2.45×10^{-3}	$\times 1 = 0.00245$	5.00245
12	9	5.00245	47.57	1.54×10^{-3}	0.048	5.051	5.061	0.059	0.76	1.17×10^{-3}	$\times 9 = 0.01053$	5.01298
9	90	5.01298	35.72	4.88×10^{-4}	0.027	5.040	5.061	0.048	0.47	2.29×10^{-4}	$\times 90 = 0.02061$	5.03359
5.8	900	5.03359	23.06	8.48×10^{-5}	0.011	5.044	5.061	0.027	0.31	2.68×10^{-5}	$\times 900 = 0.02366$	5.05725
2.8	2000	5.05725	11.16	4.65×10^{-6}	0.003	5.060	5.061	0.004	0.69	3.21×10^{-6}	$\times 312 = 0.001$	5.05825
2.8	1688	5.05825	11.16	4.65×10^{-6}	0.003	5.061	5.061	0.003	1	4.65×10^{-6}	$\times 1688 = 0.00785$	5.06610
<i>Second block</i>												
13.5	1	5.066	53.9	2.5×10^{-3}	0.062	5.128	5.128	0.062	1	2.5×10^{-3}	$\times 1 = 0.03$	5.069
12	9	5.069	47.9	1.6×10^{-3}	0.049	5.118	5.128	0.059	0.79	1.3×10^{-3}	$\times 9 = 0.012$	5.081
9	90	5.081	36.0	5.0×10^{-4}	0.028	5.109	5.128	0.047	0.51	2.6×10^{-4}	$\times 90 = 0.023$	5.104
5.8	900	5.104	23.2	8.7×10^{-5}	0.011	5.115	5.128	0.024	0.36	3.1×10^{-5}	$\times 774 = 0.024$	5.128
5.8	126	5.128	23.3	8.8×10^{-5}	0.012	5.140	5.140	0.012	1	8.8×10^{-5}	$\times 126 = 0.011$	5.139
2.8	2000	5.139	11.3	4.9×10^{-6}	0.003	5.142	5.142	0.003	1	4.9×10^{-6}	$\times 2000 = 0.010$	5.149

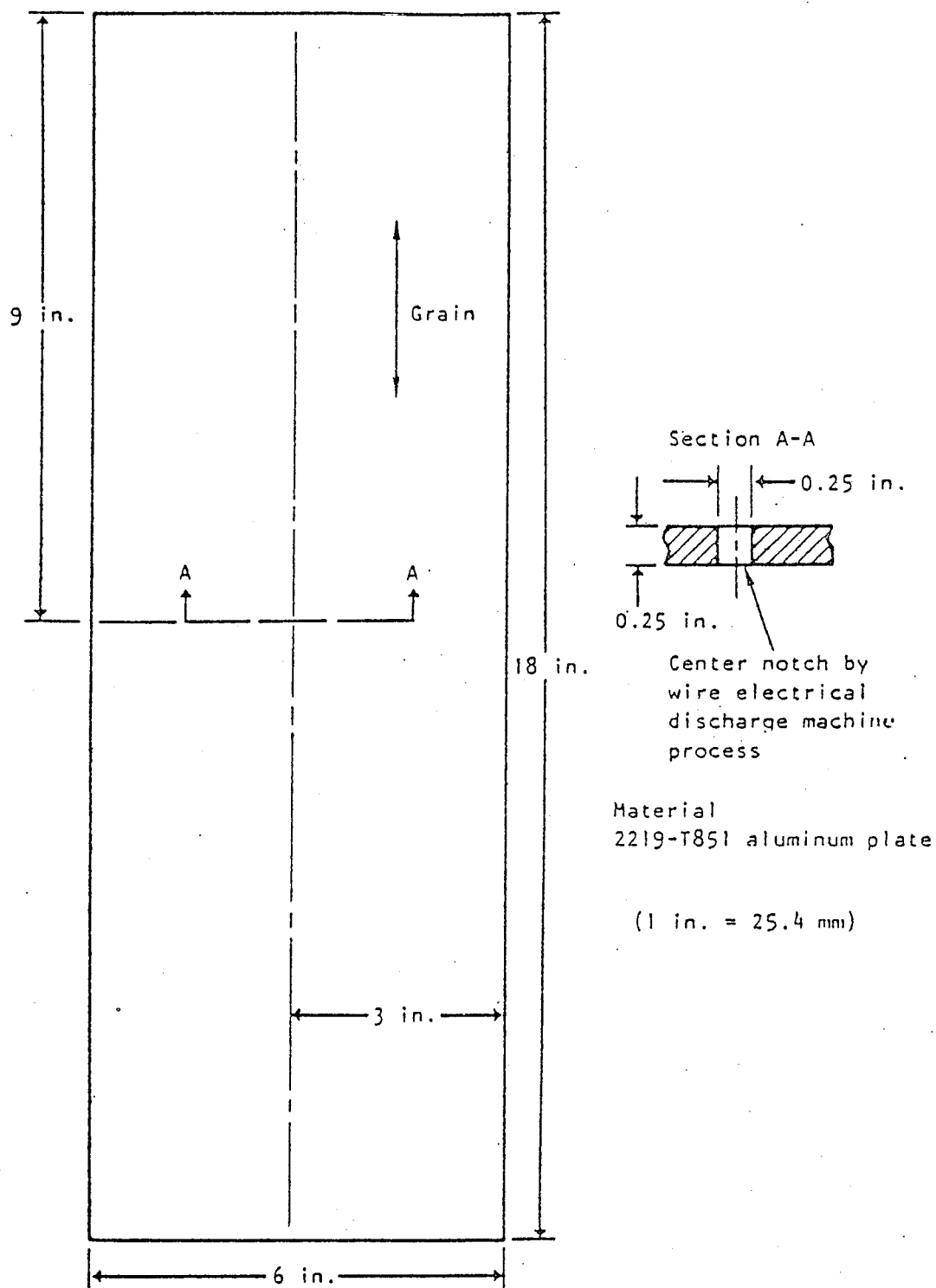


FIG. 2—Test specimen configuration.

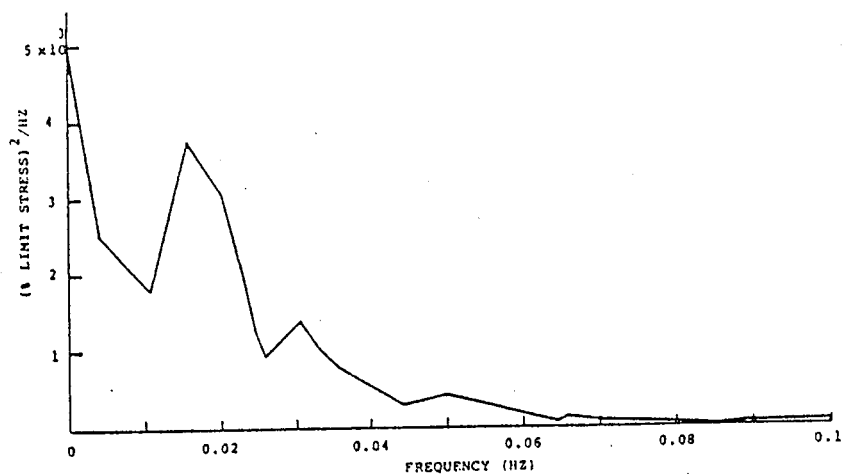


FIG. 4—Power spectral density for a Fighter A-A mission.

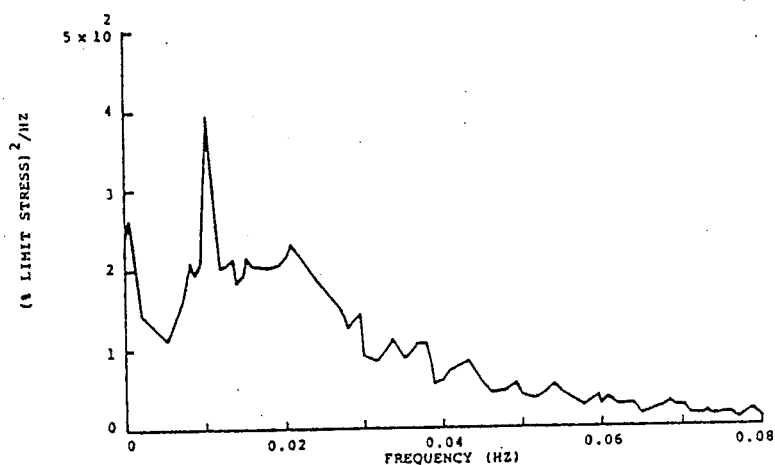


FIG. 5—Power spectral density for a Fighter A-G mission.

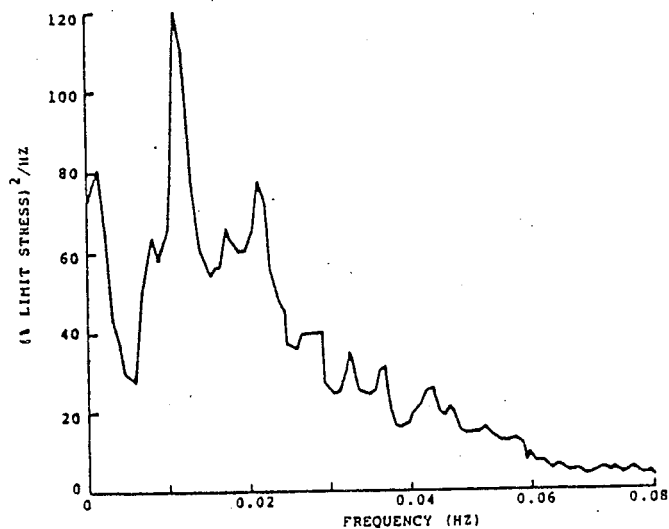


FIG. 6—Power spectral density for a Fighter I-N mission.

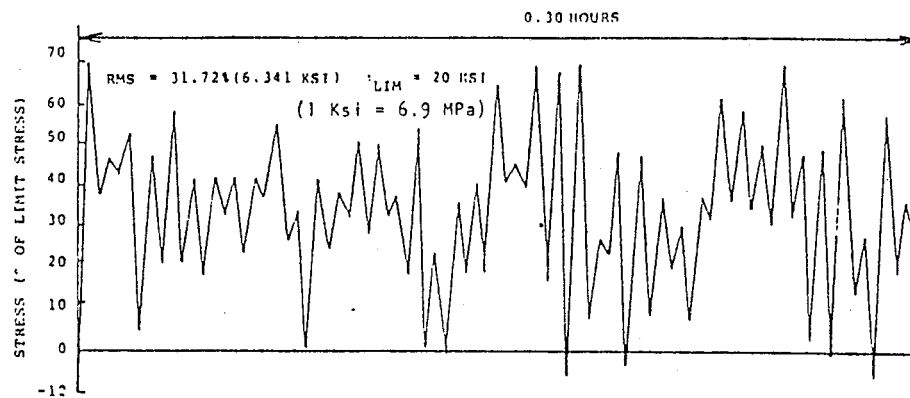


FIG. 7—Sample load history for a Fighter A-A mission.

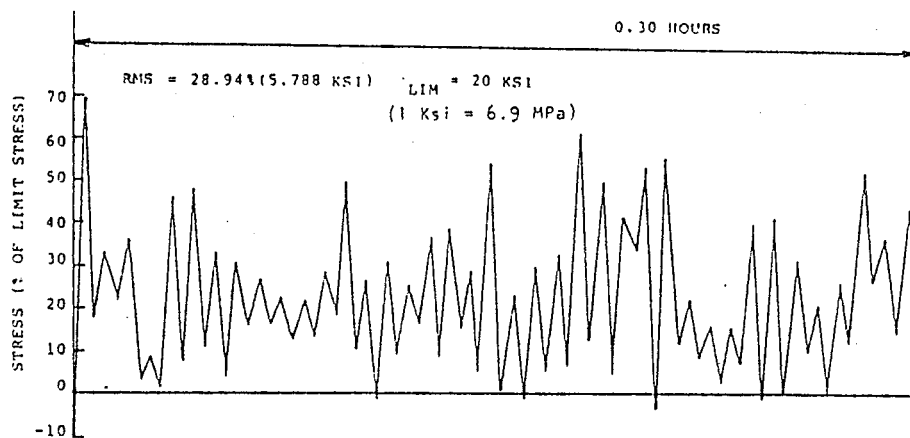


FIG. 8—Sample load history for a Fighter A-G mission.

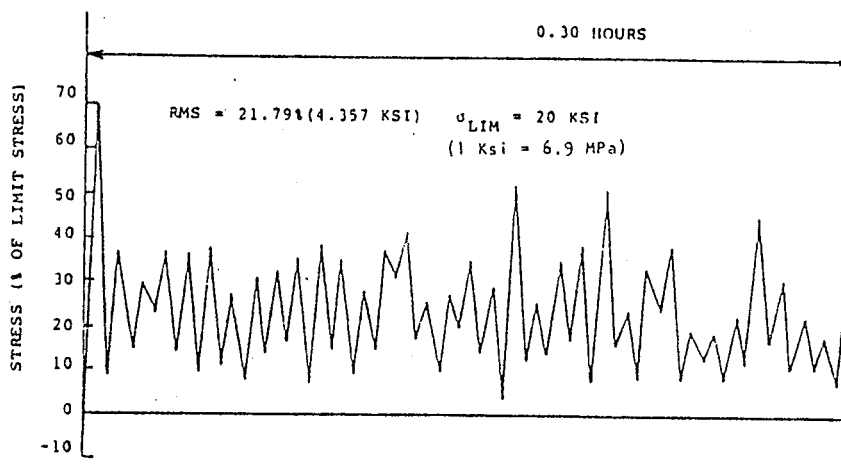


FIG. 9—Sample load history for a Fighter I-N mission.

TABLE 1—Mission profile and stress data of a transport.

Mission Type	Flight Segment	No. of Cycles	1.0 g Stress, ksi ^a	Ground Stress, ksi ^a
Assault	climb	65	10.783	...
	cruise	15	9.075	...
	gust	25	9.000	-6.4
	descent	45	10.622	...
Logistics	climb	10	9.339	...
	cruise	5	7.458	...
	gust	45	9.000	-11.5
	descent	10	10.272	...
Training	climb	40	6.559	...
	cruise	10	6.171	-8.9
	gust	45	9.000	...
	descent	20	8.648	...

^a1 ksi = 6.9 MPa.

PREDICTING FATIGUE CRACK GROWTH UNDER RANDOM LOADING

TABLE 2—ASTM Task Group E24.06.01 random spectrum round-robin analysis summary.

Test No.	Mission Type	Test Life, cycles; (c_i to c_f , in. ^a)	Analytical Predictions, cycles; (N_{pred}/N_{test})					
			JC(1)	CMH	JN	WSJ	JR	JC(2)
M-81	Fighter (A-A) ^b DLS ^c = 20 ksi ^d	115 700 (0.16 to 0.501)	140 720 (1.21)	246 000 (2.13)	115 800 (1.01)	137 000 (1.18)	213 110 (1.84)	168 720 (1.46)
M-82	Fighter (A-A) DLS = 30 ksi	58 585 (0.15 to failure)	44 525 (0.76)	79 000 (1.35)	39 125 (0.67)	57 000 (0.97)	74 055 (1.26)	53 312 (0.91)
M-83	Fighter (A-A) DLS = 40 ksi	18 612 (0.15 to failure)	14 703 (0.79)	25 359 (1.36)	11 940 (0.64)	19 700 (1.06)	25 944 (1.39)	17 309 (0.93)
M-84	Fighter (A-G) ^e DLS = 20 ksi	268 908 (0.158 to failure)	302 816 (1.13)	395 292 (1.47)	396 230 (1.47)	342 000 (1.27)	496 284 (1.85)	368 662 (1.37)
M-85	Fighter (A-G) DLS = 30 ksi	95 642 (0.144 to failure)	73 644 (0.77)	99 368 (1.04)	84 850 (0.89)	90 020 (0.94)	131 868 (1.38)	91 816 (0.96)
M-86	Fighter (A-G) DLS = 40 ksi	36 367 (0.153 to failure)	23 275 (0.64)	29 789 (0.82)	23 820 (0.65)	30 000 (0.82)	45 034 (1.24)	29 093 (0.80)
M-88	Fighter (I-N) ^f DLS = 30 ksi	380 443 (0.150 to failure)	281 528 (0.74)	475 292 (1.25)	959 700 (2.52)	589 000 (1.55)	810 900 (2.13)	528 816 (1.39)
M-89	Fighter (I-N) DLS = 40 ksi	164 738 (0.150 to failure)	95 548 (0.58)	155 294 (0.94)	242 380 (1.47)	223 000 (1.35)	288 900 (1.75)	184 507 (1.12)
M-90	Fighter Composite DLS = 20 ksi	218 151 (0.153 to failure)	231 240 (1.06)	430 225 (1.97)	255 090 (1.17)	270 000 (1.24)	401 140 (1.84)	290 140 (1.33)
M-91	Fighter Composite DLS = 30 ksi	65 627 (0.15 to failure)	51 845 (0.79)	93 473 (1.42)	51 165 (0.78)	66 000 (1.01)	97 679 (1.49)	65 630 (1.01)
M-92	Fighter Composite DLS = 40 ksi	22 182 (0.15 to failure)	17 080 (0.77)	31 446 (1.42)	15 370 (0.69)	22 800 (1.03)	34 000 (1.53)	21 738 (0.98)
M-93	Transport Composite MSS ^g = 14 ksi	1 359 000 (0.25 to 0.54)	2 419 020 (1.78)	...	1 031 200 (0.76)	1 470 000 (1.08)	3 599 000 (2.65)	1 780 290 (1.31)
M-94	Transport Composite MSS = 19.6 ksi	279 000 (0.258 to 0.38)	426 870 (1.53)	...	348 550 (1.25)	257 000 (0.92)	628 074 (2.25)	318 060 (1.14)
Average (N_{pred}/N_{test}) ratio			(0.96)	(1.38)	(1.07)	(1.11)	(1.74)	(1.13)
Standard deviation			(0.36)	(0.42)	(0.33)	(0.20)	(0.42)	(0.22)

^a1 in. = 25.4 mm.
^bA-A = Air-to-Air.
^cDLS = Design limit stress.
^d1 ksi = 6.9 MPa.
^eA-G = Air-to-Ground.
^fJN = Instrumentation and Navigation.
^gMSS = Maximum spectrum stress.

TABLE 3—Analytical methods and computer codes used in the round-robin predictions.

Analytical Predictions	Prediction Method	Computer Code
JC(1)	Walker crack growth rate equation; compressive loads set to zero; tensile load retardation not accounted for	EFFGRO
CMH	root-mean-square	CYCLIF
JN	modified Elber's equation; load interaction effects accounted for by analytical closure model	FAST
WSJ	modified Forman's equation; load interaction effects accounted for by multiple-parameter yield zone model	CGR-LaRC
JR	Walker's crack growth rate equation; compressive loads set to zero; tensile load retardation effect accounted for by generalized Willenborg model	CRACKS
JC(2)	Walker's crack growth rate equation; load interaction effects accounted for by Willenborg/Chang model	EFFGRO

TABLE 4—Summary of prediction ratios of each test case.

Test No.	Mission Type	Test Life, cycles	N_{pred}/N_{test}
M-81	Fighter (A-A) ^a DLS ^b = 20 ksi ^c	115 700	1.47 ± 0.43
M-82	Fighter (A-A) DLS = 30 ksi	58 585	0.99 ± 0.27
M-83	Fighter (A-A) DLS = 40 ksi	18 612	1.03 ± 0.3
M-84	Fighter (A-G) ^d DLS = 20 ksi	268 908	1.43 ± 0.24
M-85	Fighter (A-G) DLS = 30 ksi	95 642	0.99 ± 0.21
M-86	Fighter (A-G) DLS = 40 ksi	36 367	0.83 ± 0.22
M-88	Fighter (I-N) ^e DLS = 30 ksi	380 443	1.60 ± 0.64
M-89	Fighter (I-N) DLS = 40 ksi	164 738	1.20 ± 0.41
M-90	Fighter Composite DLS = 20 ksi	218 151	1.44 ± 0.38
M-91	Fighter Composite DLS = 30 ksi	65 627	1.08 ± 0.31
M-92	Fighter Composite DLS = 40 ksi	22 182	1.07 ± 0.34
M-93	Transport Composite MSS ^f = 14 ksi	1 359 000	1.52 ± 0.73
M-94	Transport Composite MSS = 19.6 ksi	279 000	1.42 ± 0.51

^a A-A = Air-to-Air.

^b DLS = Design limit stress.

^c 1 ksi = 6.9 MPa.

^d A-G = Air-to-Ground.

^e I-N = Instrumentation and Navigation.

^f MSS = Maximum spectrum stress.

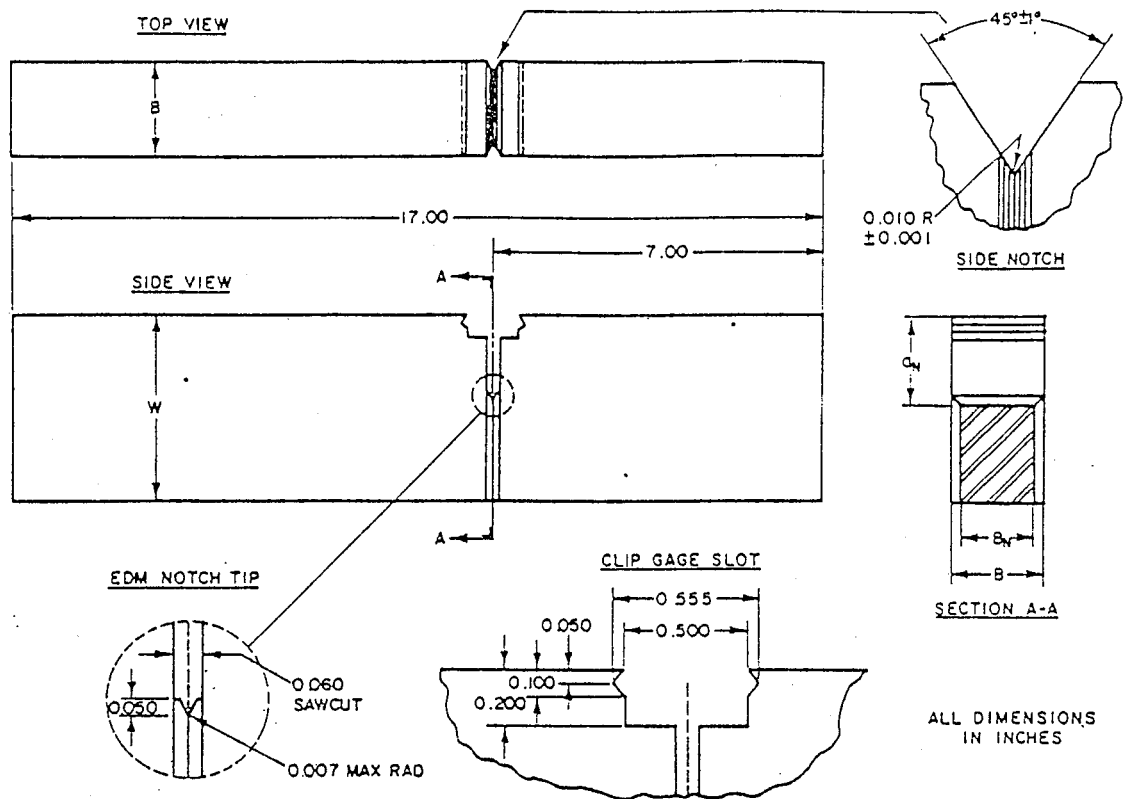


FIG. 10.1. Fatigue-cracked cantilever-beam test specimen.

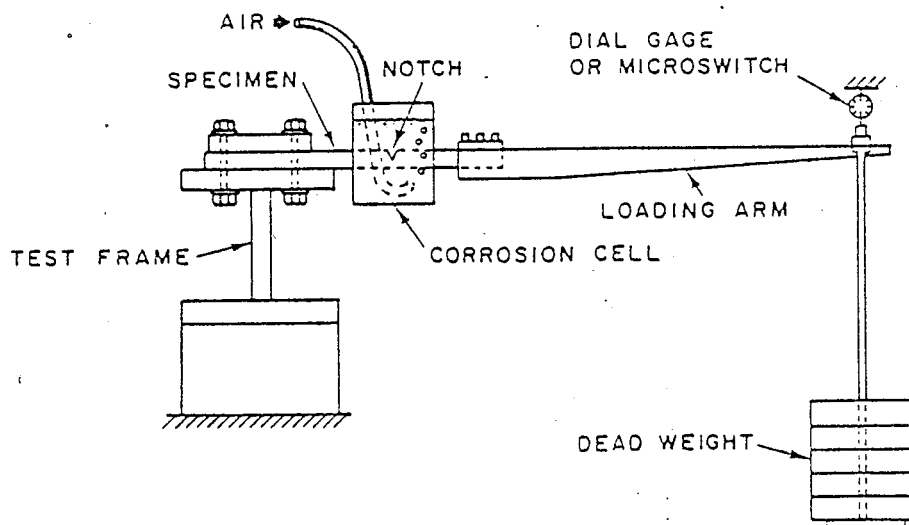


FIG. 10.2. Schematic drawing of fatigue-cracked cantilever-beam test specimen and fixtures.

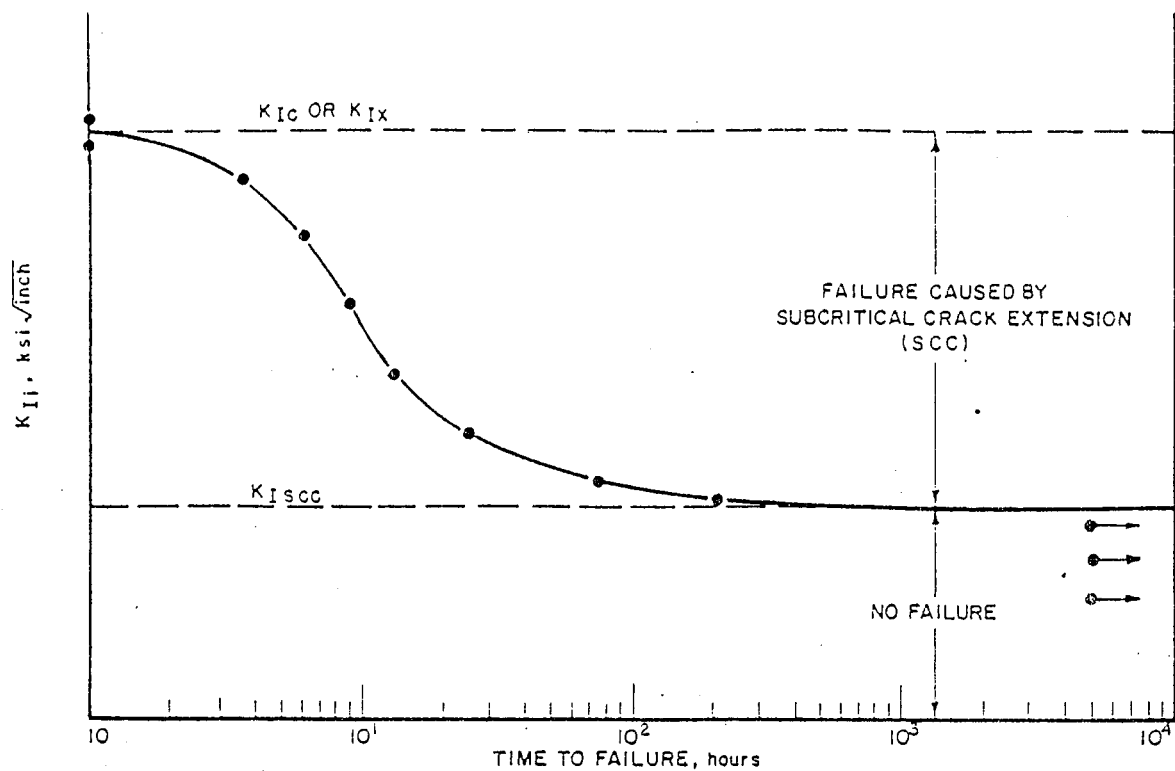


FIG. 10.3. Procedure to obtain K_{Isc} with precracked cantilever-beam specimens.

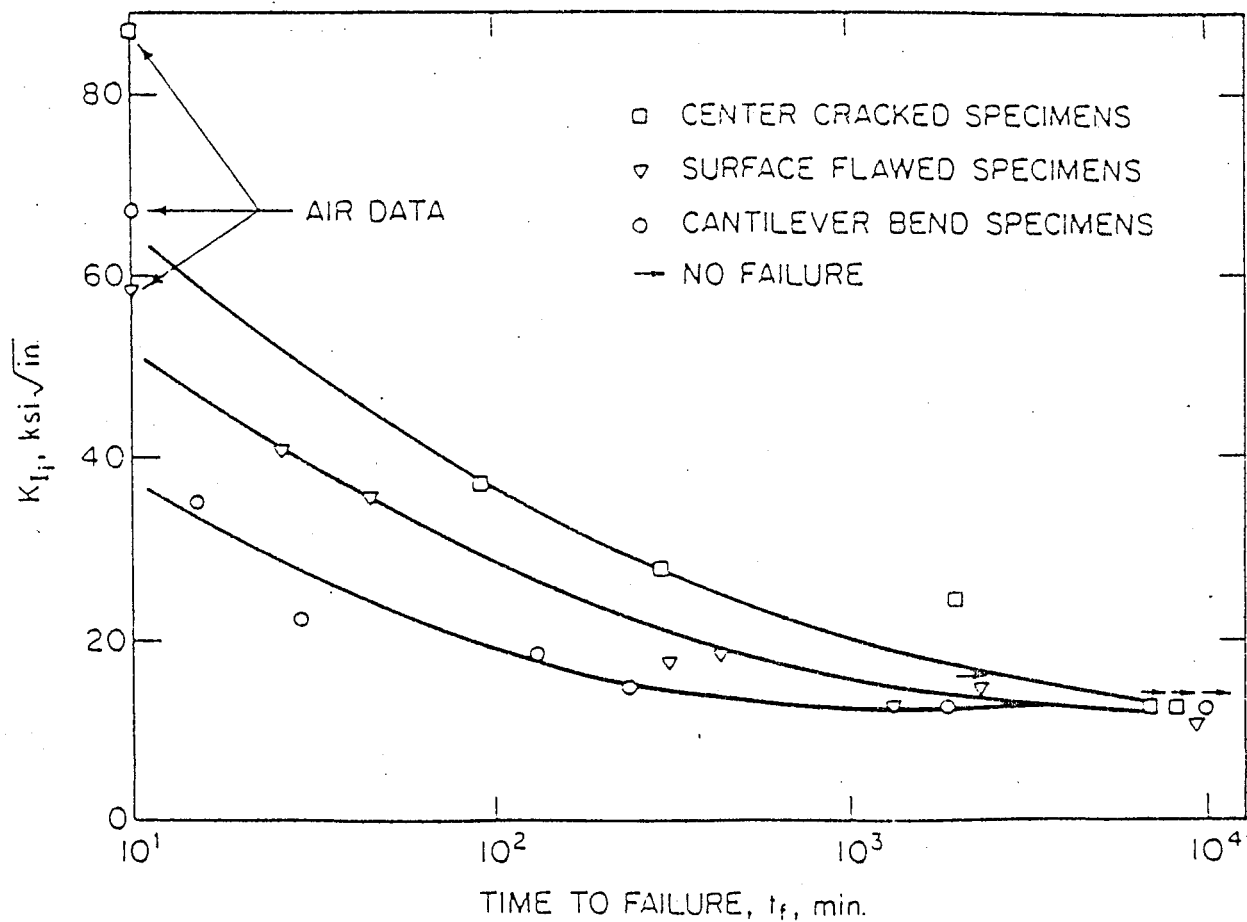


FIG. 10.8. Influence of specimen geometry on the time to failure (AISI).

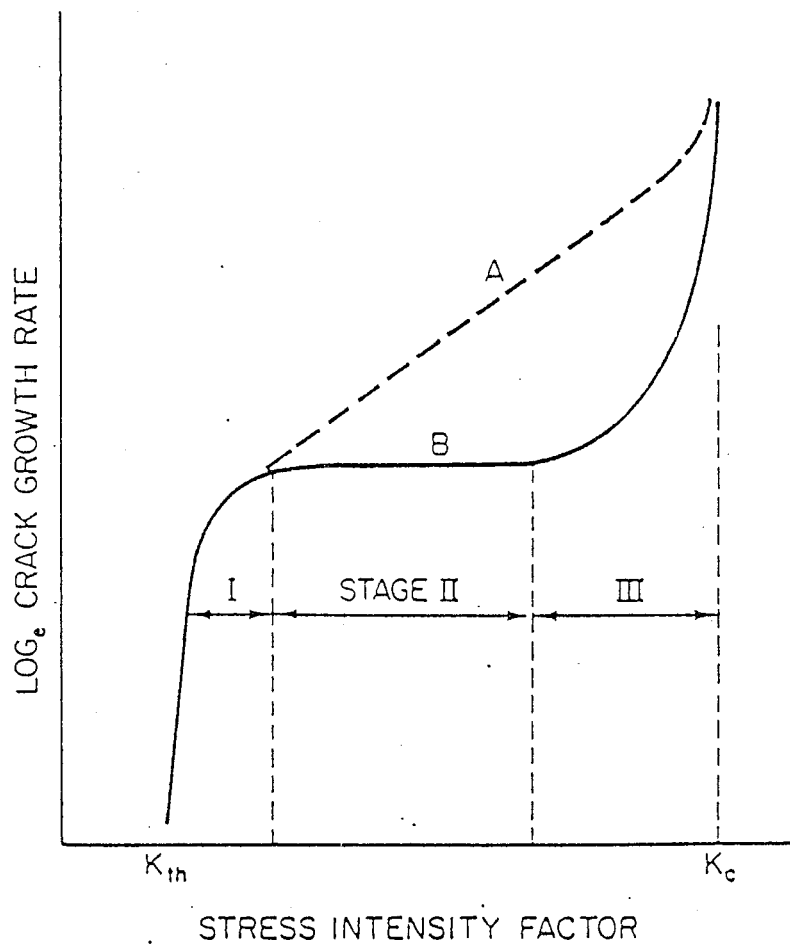


FIG. 10.17. Schematic illustration of the functional relationship between stress-intensity factor (K) and subcritical crack growth rate (da/dt).

K_{ISCC}/K_{IC} for Various Materials - Environment Systems

Material	Temp [°F]	σ_y [ksi]	Environment	K_{ISCC}/K_{IC}
6Al-4V-T _i	RT	160	Methanol	0.24
	RT	160	Freon	0.58
	RT	160	H ₂ O ₂ (30%)	0.74
	RT	160	H ₂ O ₂ (60%)	0.83
	RT	160	NaCl + H ₂ O	0.82
	RT	160	H ₂ O	0.80
	RT	160	He	0.90
	RT	160	Aerozine 50	0.82
	90	160	H ₂ O ₂ (30%)	0.71
	90	160	H ₂ O ₂ (60%)	0.75
	105	160	Mono-Hydrazine	0.75
	110	160	Aerozene 50	0.75
2219 T87 Alumina	RT	58	Air	0.96
	370	66	Liquid Hydrogen	0.82
	423	72	Liquid Hydrogen	0.85
4330	RT	205	H ₂ O	0.24
4340	RT	> 200	NaCl + H ₂ O	0.20
6Al-4V-T _i Weldments	RT	200	NaCl + H ₂ O (spray)	> 0.70
	RT	235	NaCl + H ₂ O	> 0.70
	RT	170	NaCl + H ₂ O	> 0.70

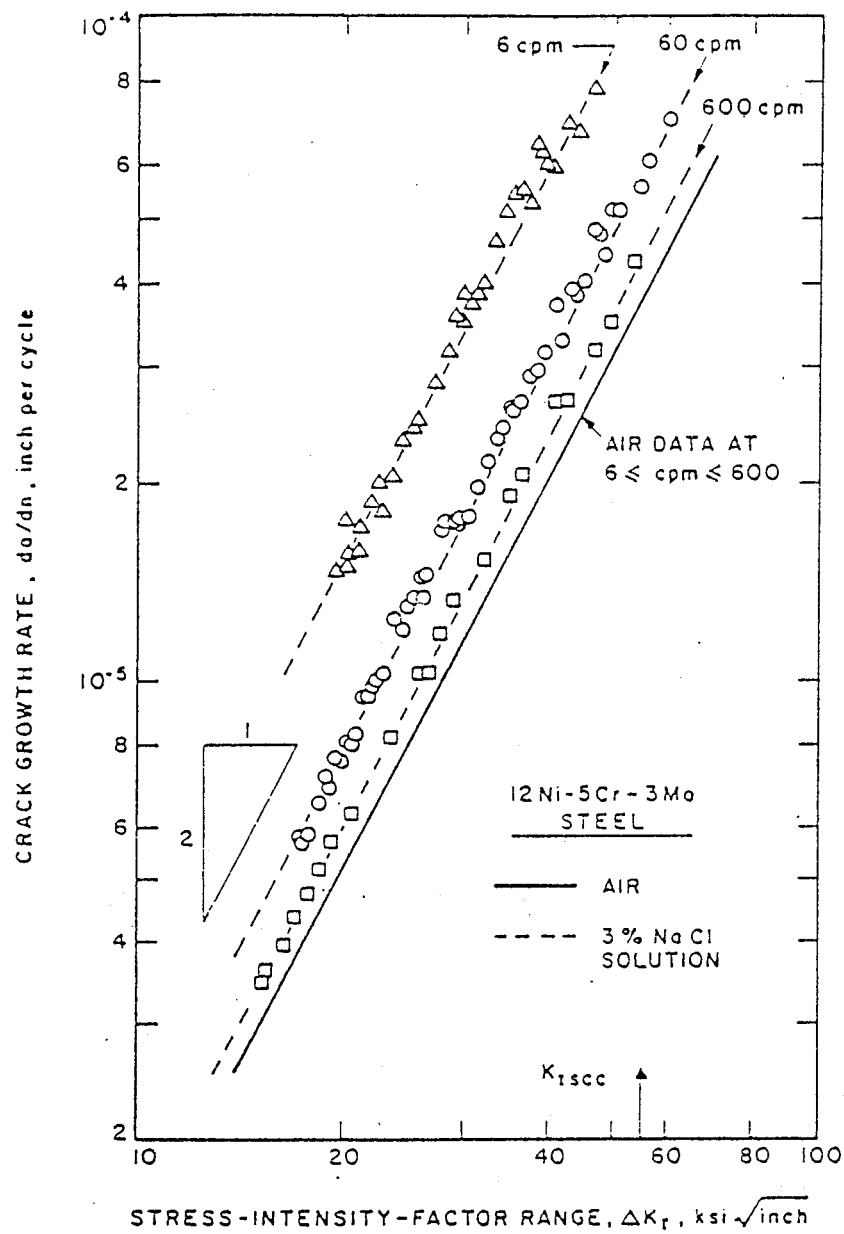


FIG. 11.2. Corrosion-fatigue-crack growth data as a function of test frequency.

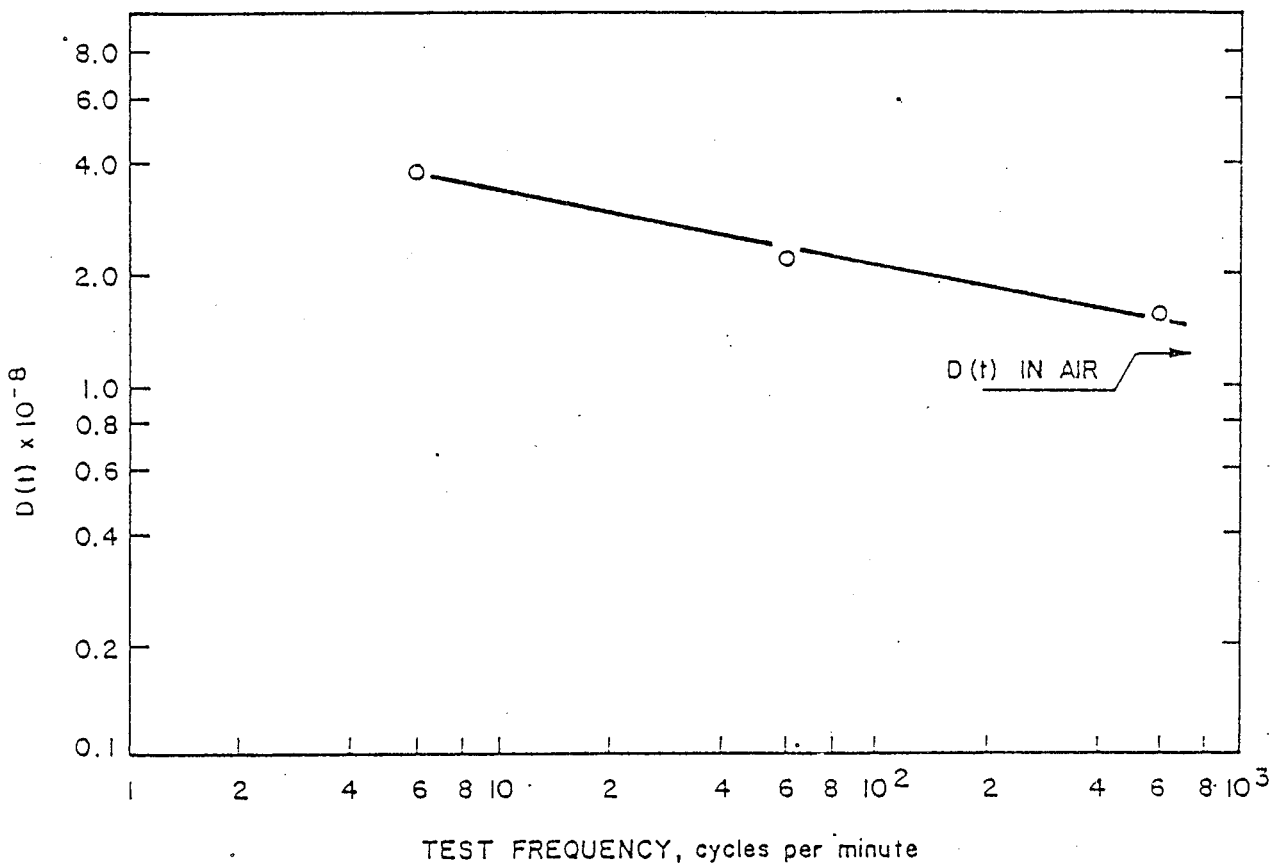


FIG. 11.3. Correlation between time-dependent function $D(t)$ and test frequency for 12Ni-5Cr-3Mo steel tested in sodium chloride solution.

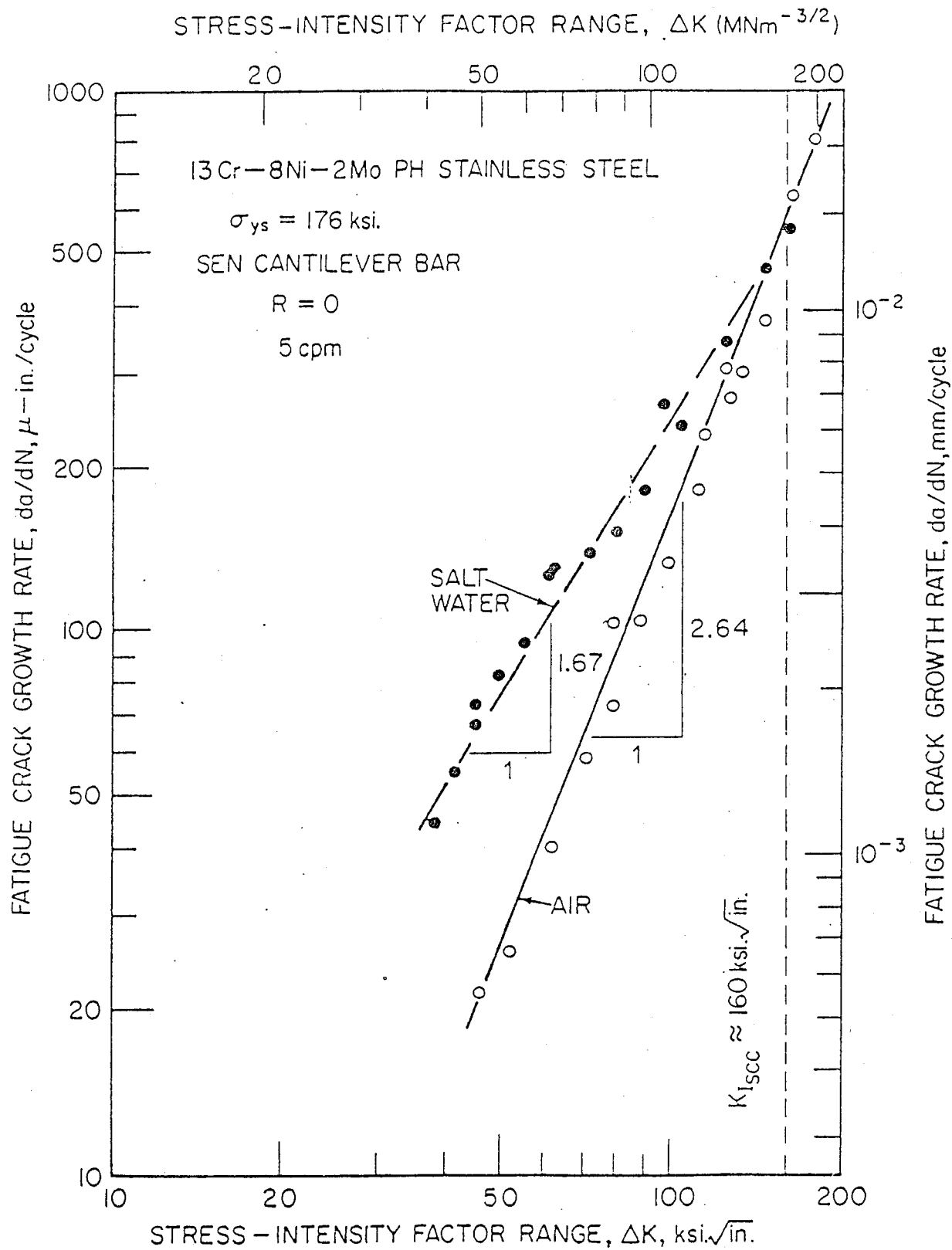


FIG. 11.4. Air and salt water fatigue crack growth rate behavior of 13Cr-8 Ni-2 Mo PH stainless steel.

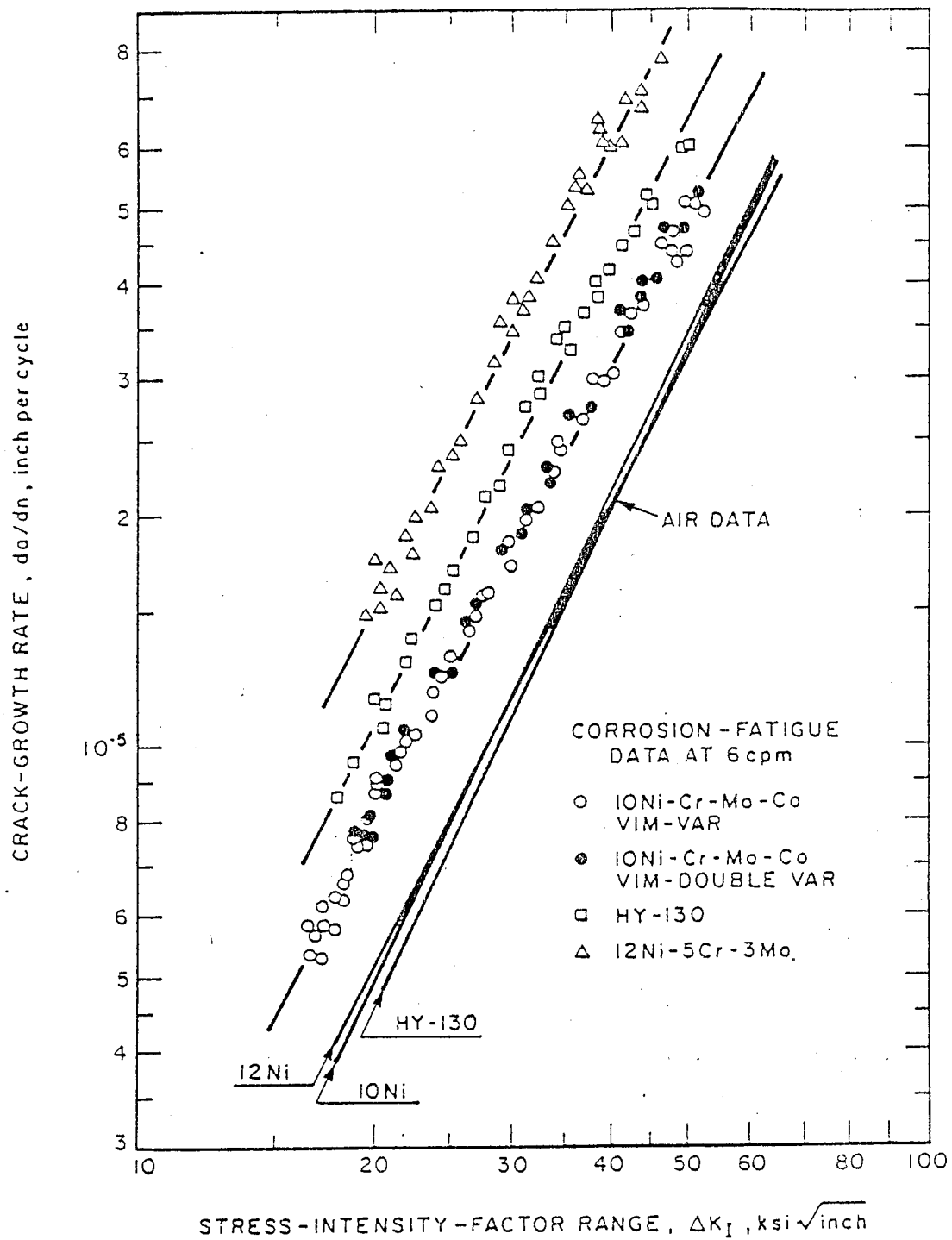


FIG. 11.5. Fatigue-crack-growth rates in air and in 3% solution of sodium chloride below K_{Isc} for various high-yield-strength steel.

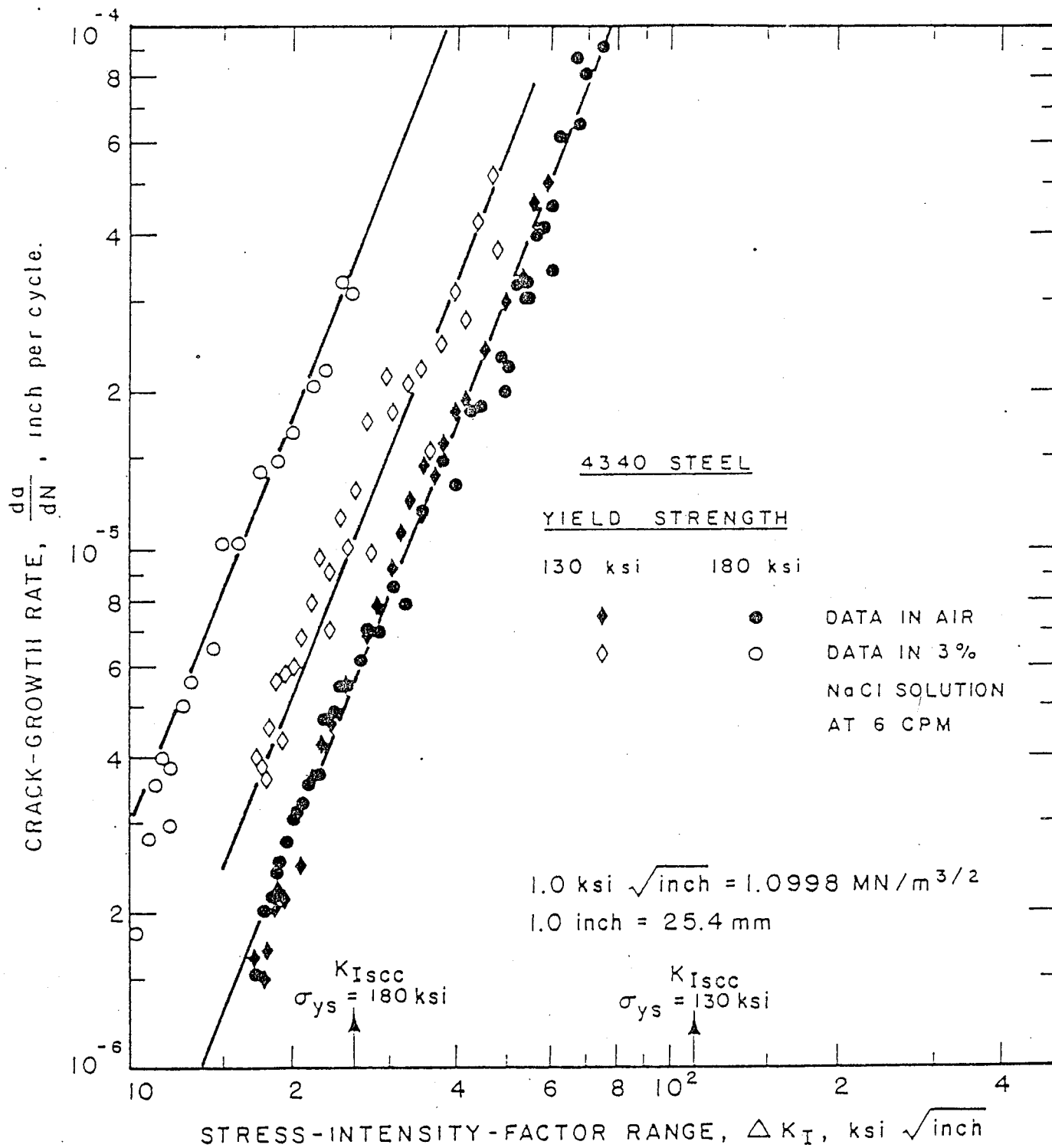


FIG. 11.6. Corrosion-fatigue-crack-growth data.

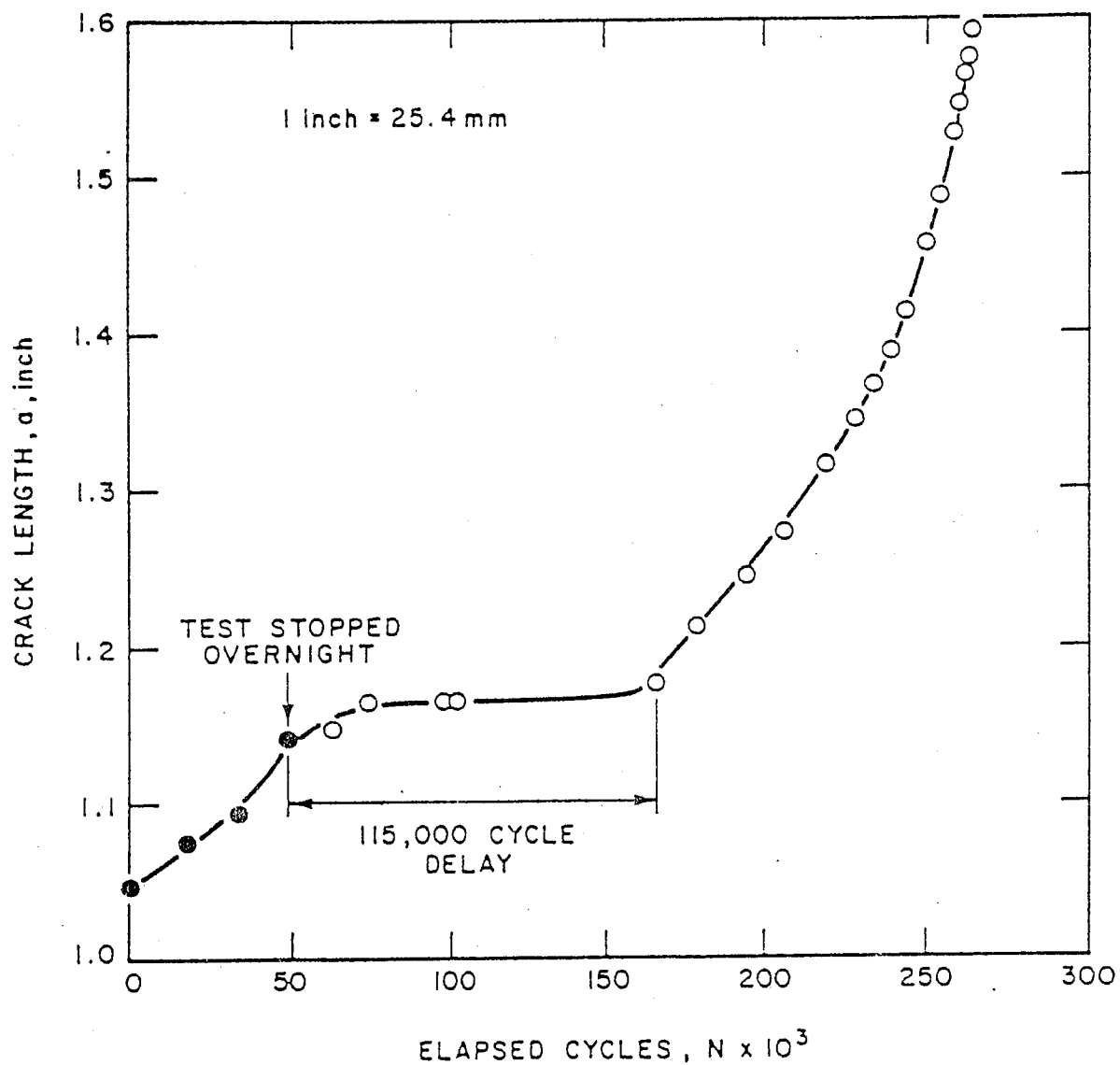


FIG. 11.21. Retardation of corrosion-fatigue-crack-growth rate under wet and dry environmental conditions for A514 Grade F steel.

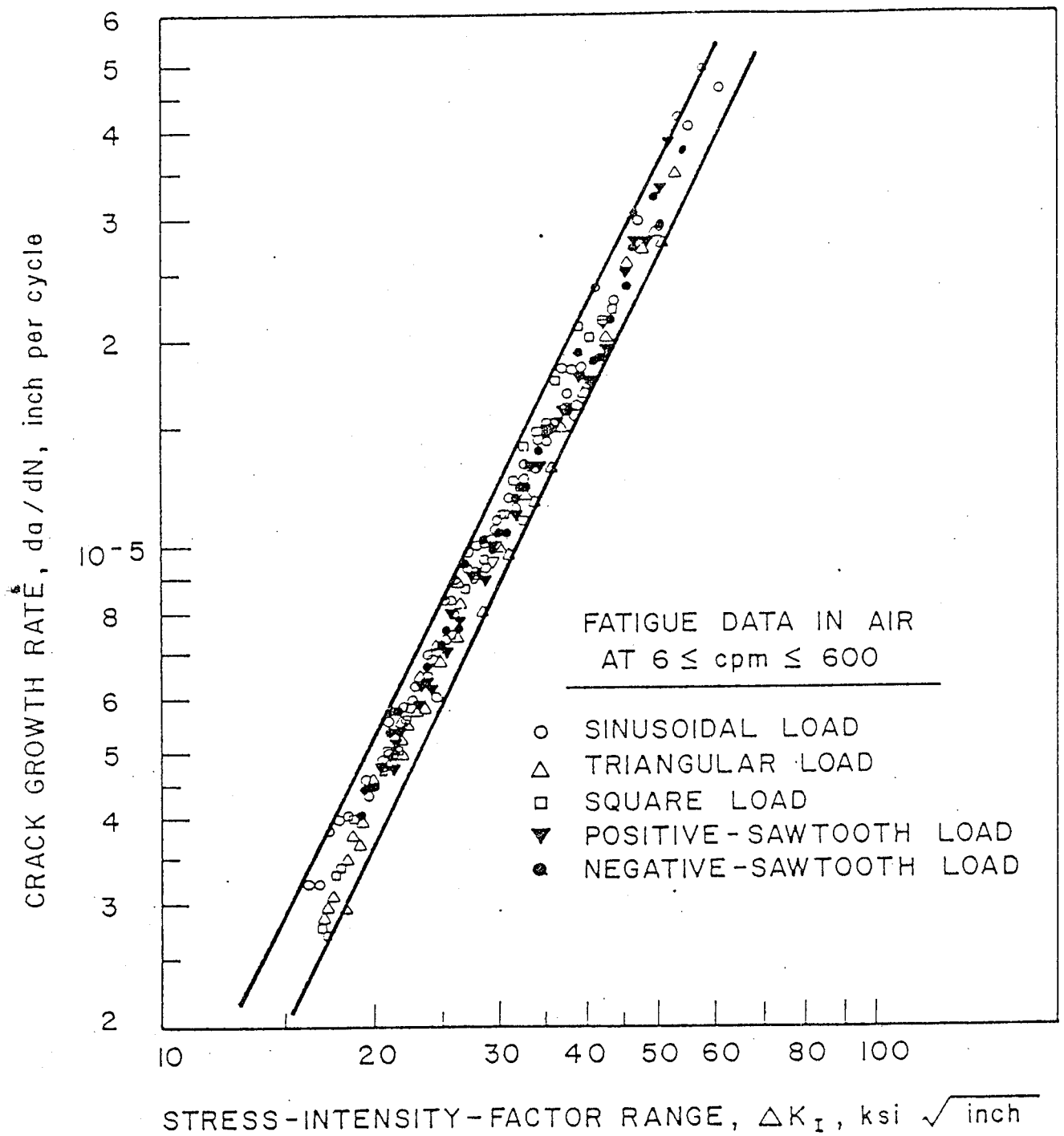


FIG. 11.22. Fatigue-crack-growth rates in 12Ni-5Cr-3Mo steel under various cyclic-stress fluctuations with different stress-time profiles.

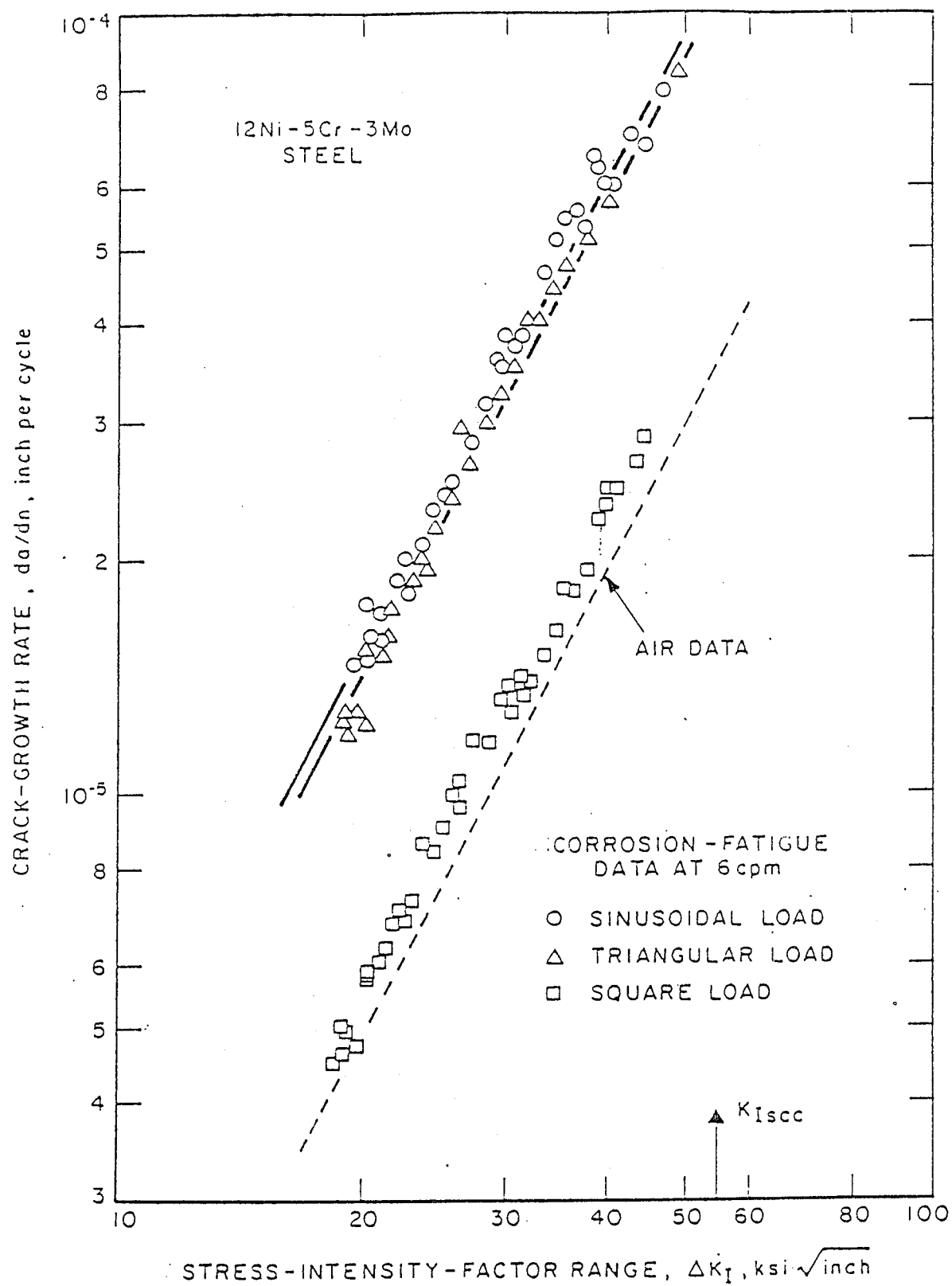


FIG. 11.23. Corrosion-fatigue-crack-growth rates below K_{Isc} under sinusoidal, triangular, and square loads.

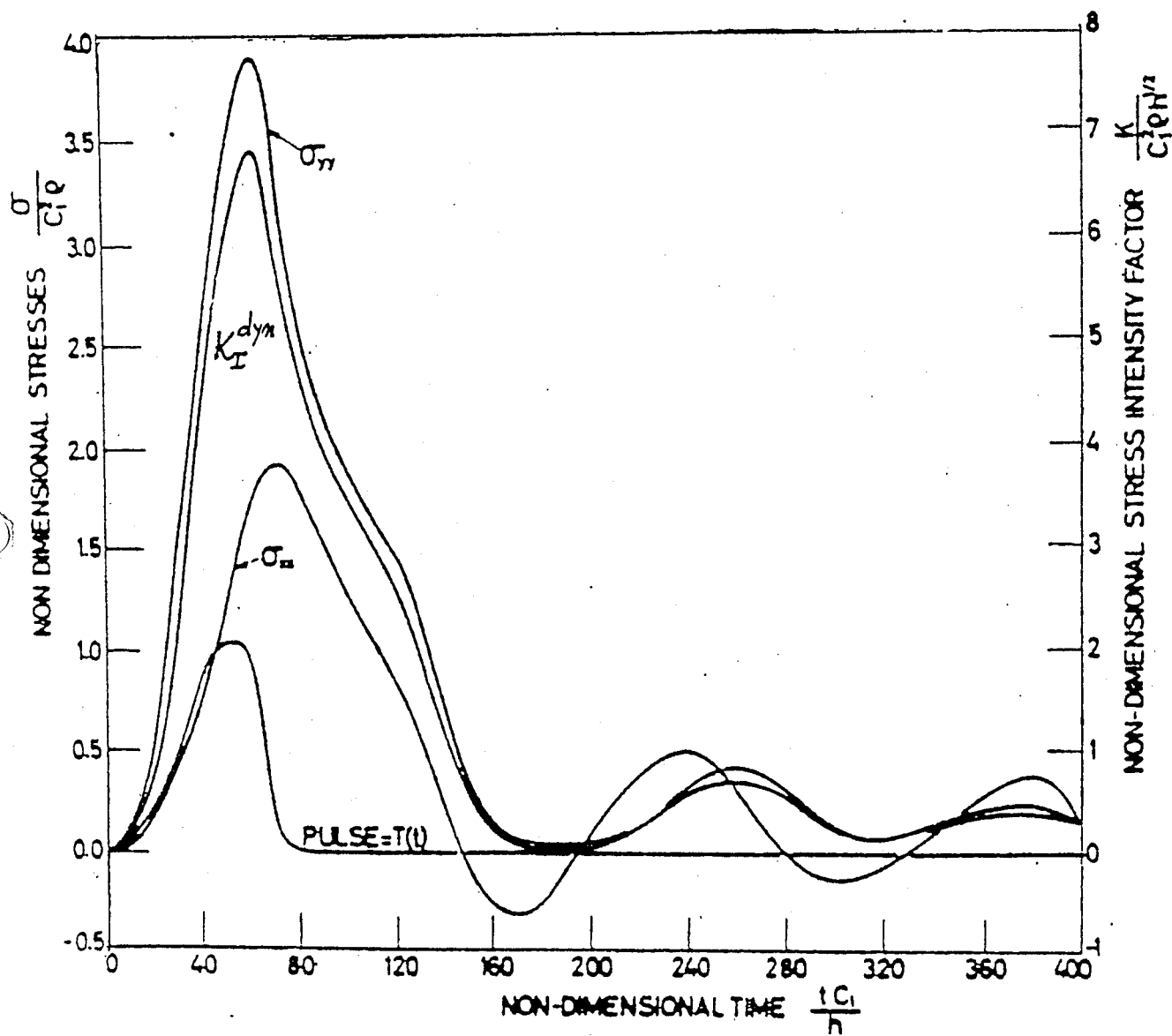


Fig. 7 Variation of Stresses Ahead of a Short Pulse Loaded Edge Crack Tip. $a = 20h$, $L = 60h$, $H = 120h$ (see Fig. 1). Stresses are related to the point $(x = a+0.5h, y=0)$; maximum $K_{Istat}/C_1^2 \rho h^{1/2} = 8.88$.

DYNAMICALLY LOADED CENTRAL CRACK

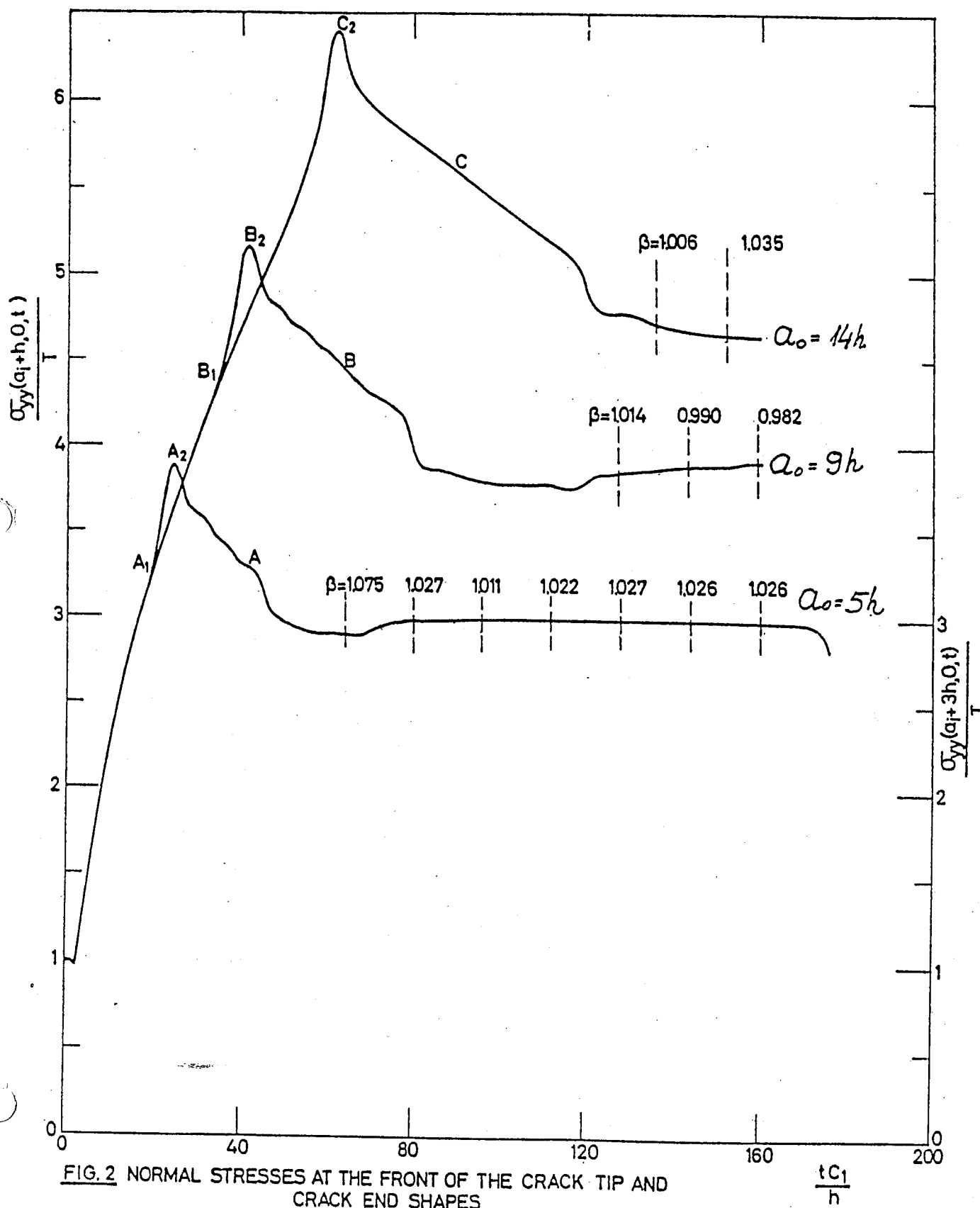


FIG. 2 NORMAL STRESSES AT THE FRONT OF THE CRACK TIP AND CRACK END SHAPES

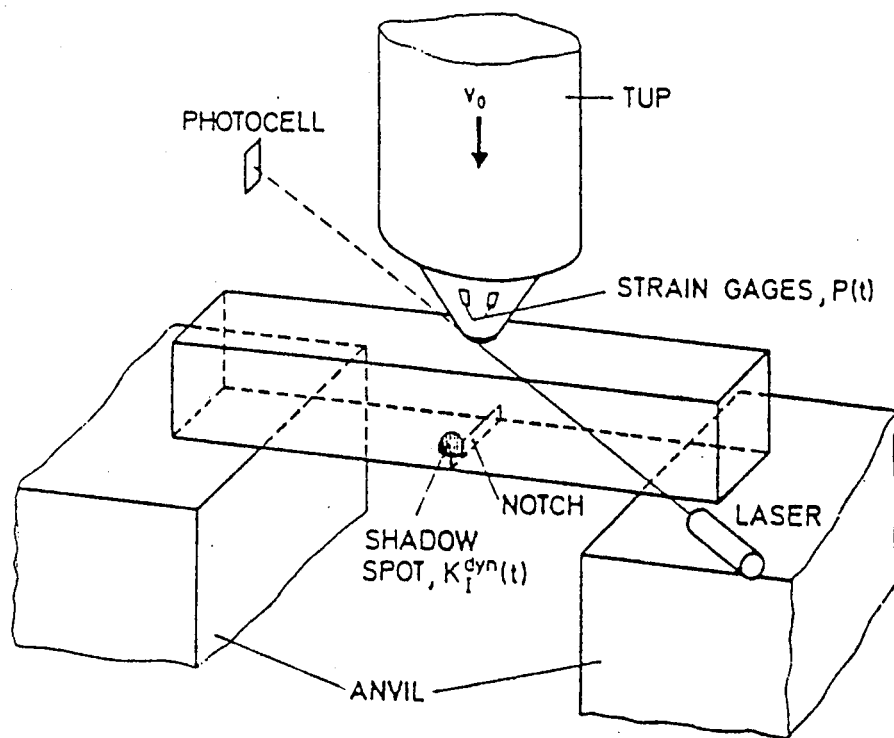


Figure 1. Experimental set up (schematically)

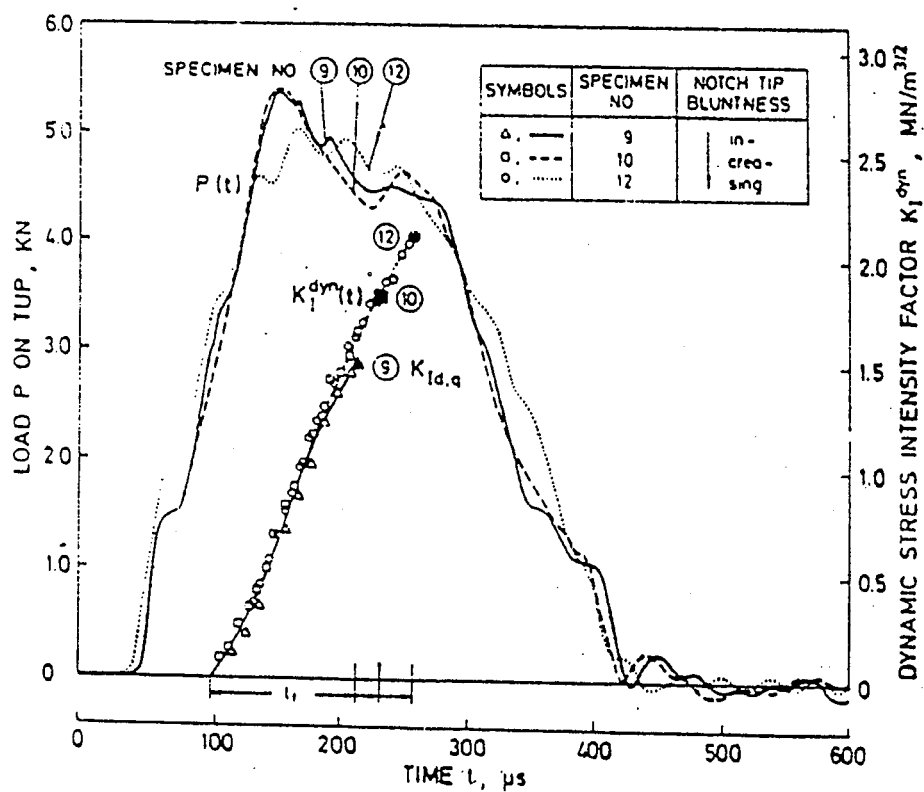


Figure 2. Comparison of the load and the stress intensity factor curves

The Spatial Distribution of the Stress Field
Near the Tip of a Moving Crack

$$\sigma_{ij} = \frac{K_I^{\text{dyn}}(t)}{\sqrt{2\pi}} \cdot B(v) \cdot f_{ij}^{\text{dyn}}(r, \theta, v, c_1, c_s)$$

where:

$$B(v) = \frac{1 + \alpha_s^2}{4\alpha_1\alpha_s - (1 + \alpha_s^2)^2}$$

$$f_{I_{xx}}^{\text{dyn}} = (1 + 2\alpha_1^2 - \alpha_s^2) \frac{\cos(\theta_{1/2})}{r_1^{1/2}} - \frac{4\alpha_1\alpha_s}{(1 + \alpha_s^2)} \cdot \frac{\cos(\theta_{s/2})}{r_s^{1/2}}$$

$$f_{I_{xy}}^{\text{dyn}} = \frac{\sin(\theta_{1/2})}{r_1^{1/2}} - \frac{\sin(\theta_{s/2})}{r_s^{1/2}}$$

$$f_{I_{yy}}^{\text{dyn}} = -(1 + \alpha_s^2) \frac{\cos(\theta_{1/2})}{r_1^{1/2}} + \frac{4\alpha_1\alpha_s}{(1 + \alpha_s^2)} \cdot \frac{\cos(\theta_{s/2})}{r_s^{1/2}}$$

$$\alpha_1 = \left(1 - \frac{v^2}{c_1^2}\right)^{1/2} \quad \alpha_s = \left(1 - \frac{v^2}{c_s^2}\right)^{1/2}$$

$$r_1 l^{i\theta_1} = \varepsilon + i\alpha_1 \eta$$

$$r_s l^{i\theta_s} = \varepsilon + i\alpha_s \eta$$

$$K_I^{dyn} = k(v) K_I^{stat}$$

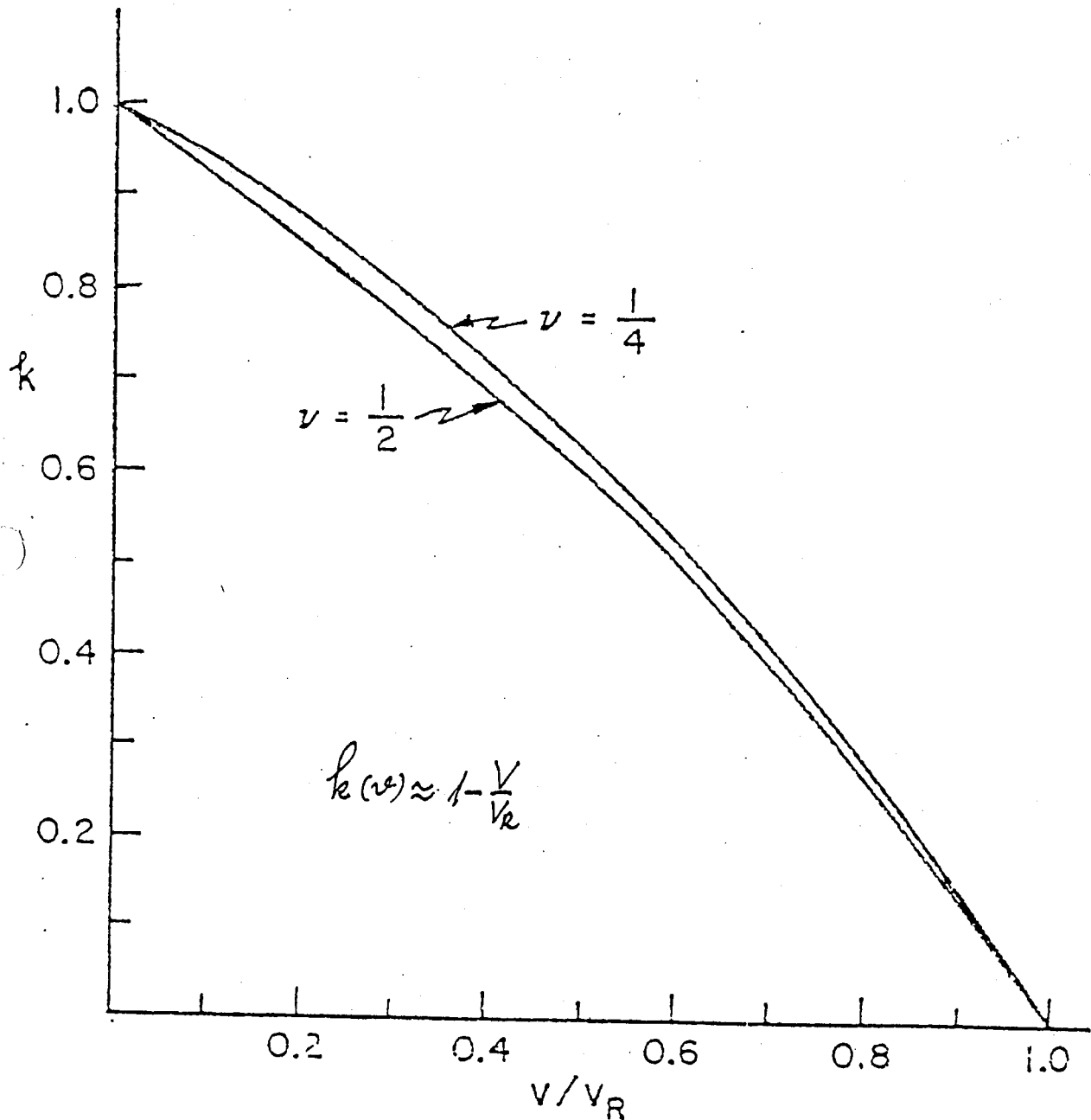
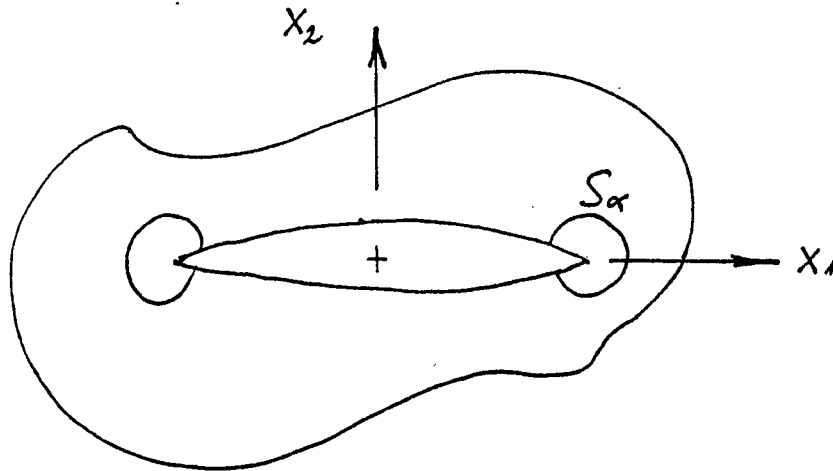


FIG. 2. The ratio of dynamic to static stress intensity factors vs. dimensionless crack speed for $\nu = 1/4, 1/2$.

The Energy Flux into a Moving Crack



$$F = \int_{S_\alpha} \left[\sigma_{ij} n_j \dot{u}_i + \frac{1}{2} (\sigma_{ij} u_{i,j} + \rho \dot{u}_i \dot{u}_i) V_x \right] dS$$

for $r \rightarrow 0$

$$F = \frac{1-v^2}{E} \frac{v^3 \alpha_1 (K_I^{\text{dyn}})^2}{(1-v) c_s^2 [4\alpha_1 \alpha_s - (1+\alpha_s)^2]}$$

$$G_{ID} = \frac{F}{v}$$

$$G_I^{dyn} = g(v) G_I^{stat}$$

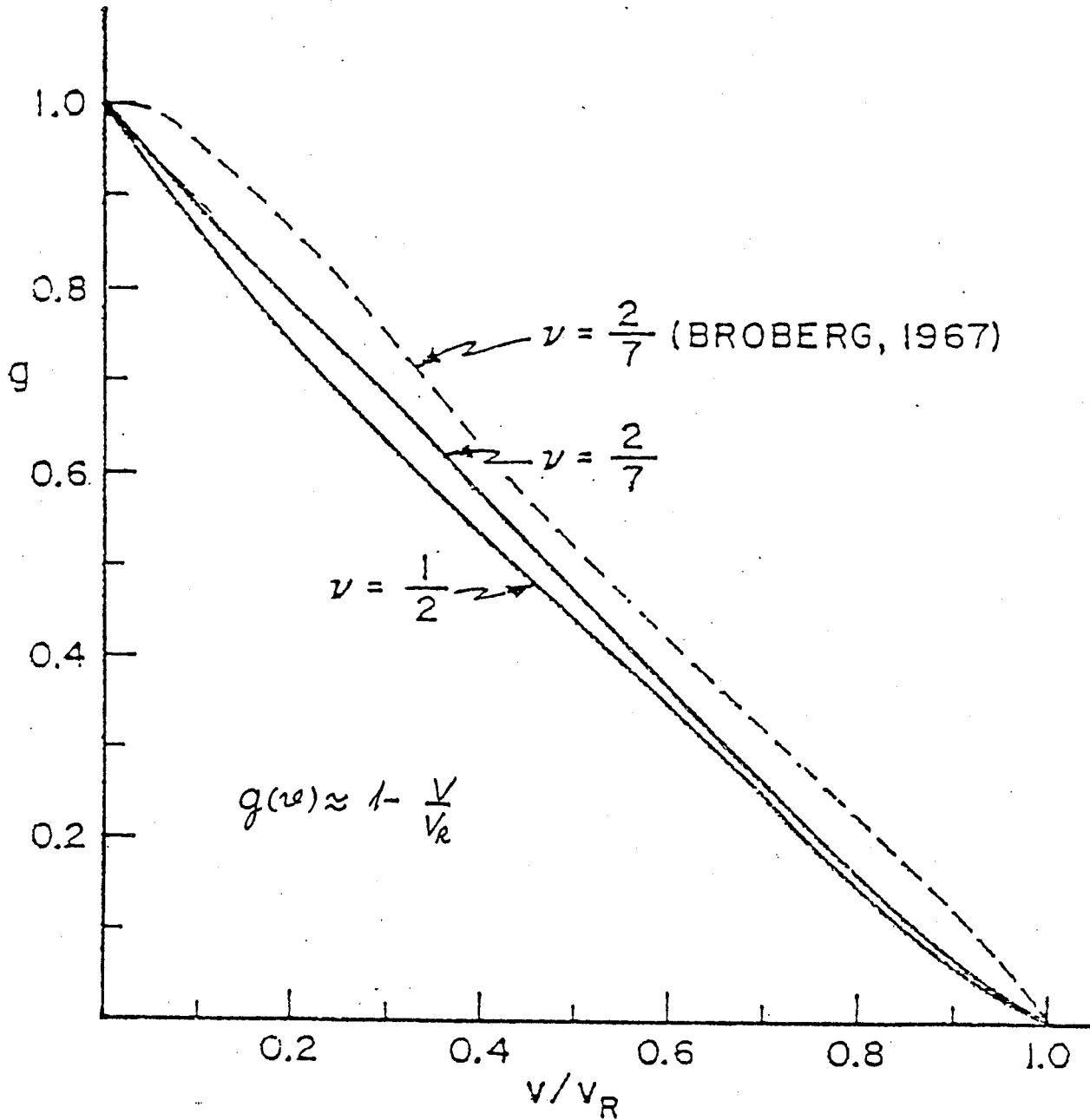


FIG. 4. The ratio of dynamic to static energy-release rates vs. dimensionless crack speed for $\nu = 2/7, 1/2$.



Standard Test Method for Plane-Strain Fracture Toughness of Metallic Materials¹

This standard is issued under the fixed designation E 399; the number immediately following the designation indicates the year of original adoption or, in the case of revision, the year of last revision. A number in parentheses indicates the year of last reapproval. A superscript epsilon (ϵ) indicates an editorial change since the last revision or reapproval.

This method has been approved for use by agencies of the Department of Defense and for listing in the DoD Index of Specifications and Standards.

1. Scope

1.1 This test method covers the determination of the plane-strain fracture toughness (K_{Ic}) of metallic materials by tests using a variety of fatigue-cracked specimens having a thickness of 0.063 in. (1.6 mm) or greater.² The details of the various specimen and test configurations are shown in Annexes A1 through A7.

NOTE 1—Plane-strain fracture toughness tests of thinner materials that are sufficiently brittle (see 7.1) can be made with other types of specimens (1).³ There is no standard test method for testing such thin materials.

1.2 This test method also covers the determination of the specimen strength ratio R_{xx} where x refers to the specific specimen configuration being tested. This strength ratio is a function of the maximum load the specimen can sustain, its initial dimensions and the yield strength of the material.

1.3 Measured values of plane-strain fracture toughness stated in inch-pound units are to be regarded as standard.

1.4 This test method is divided into two main parts. The first part gives general information concerning the recommendations and requirements for K_{Ic} testing. The second part is composed of annexes that give the displacement gage design, fatigue cracking procedures, and special requirements for the various specimen configurations covered by this method. In addition, an annex is provided for the specific procedures to be followed in rapid-load plane-strain fracture toughness tests. General information and requirements common to all specimen types are listed as follows:

	Sections
Referenced Documents	2
Summary of Test Method	3
Significance and Use	4
Precautions	4.1.1 to 4.1.3
Practical Applications	4.2
Definitions	5
Stress-Intensity Factor	5.1.1
Plane-Strain Fracture Toughness	5.1.2
Apparatus	6
Loading Fixtures	6.2
Displacement Gage Design	Annex A1
Displacement Measurements	6.3

¹ This test method is under the jurisdiction of ASTM Committee E-24 on Fracture Testing and is the direct responsibility of Subcommittee E24.01 on Fracture Mechanics Test Methods.

Current edition approved April 24, 1983. Published July 1983. Originally published as E 399 - 70 T. Last previous edition E 399 - 81.

² For additional information relating to the fracture toughness testing of aluminum alloys, see Method B 645.

³ The boldface numbers in parentheses refer to the list of references at the end of this method.

	Sections
Specimen Size, Configurations, and Preparation	7
Specimen Size Estimates	7.1
Standard and Alternative Specimen Configurations	7.2
Forms of Fatigue Crack Starter Notch	7.3.1
Fatigue Cracking	Annex A2
Crack Extension Beyond Starter	7.3.2.2
Measurements before Testing	
Thickness	8.2.1
Width	8.2.3
Starter Notch Root Radius	7.3.1
Specimen Testing	
Loading Rate	8.3
Test Record	8.4
Measurements after Testing	
Crack Length	8.2.2
Crack Plane Angle	8.2.4
Calculation and Interpretation of Results	9
Analysis of Test Record	9.1
Validity Requirements on P_{max}/P_Q	9.1.2
Validity Requirements on Specimen Size	9.1.3
Crack Plane Orientation Designations	9.2
Fracture Appearance Descriptions	9.3
Reporting	10
Precision and Bias	11
Special Requirements for Rapid-Load K_{Ic} (t) Tests	Annex A7

1.5 Special requirements for the various specimen configurations appear in the following order:

Bend Specimen $SE(B)$	Annex A3
Compact Specimen $C(T)$	Annex A4
Arc-Shaped Specimen $A(T)$	Annex A5
Disk-Shaped Compact Specimen $DC(T)$	Annex A6
Rapid Load K_{Ic} (t) Tests	Annex A7

2. Referenced Documents

2.1 ASTM Standards:

- B 645 Practice for Plane Strain Fracture Toughness Testing of Aluminum Alloys⁴
- E 8 Test Methods of Tension Testing of Metallic Materials⁵
- E 21 Practice for Elevated Temperature Tension Tests of Metallic Materials⁶
- E 337 Test Method for Measuring Humidity with a Psychrometer (the Measurement of Wet- and Dry-Bulb Temperatures)⁷
- E 338 Method of Sharp-Notch Tension Testing of High-Strength Sheet Materials⁶
- E 616 Terminology Relating to Fracture Testing⁶

3. Summary of Test Method

3.1 This test method involves testing of notched speci-

⁴ Annual Book of ASTM Standards, Vol 02.02.

⁵ Annual Book of ASTM Standards, Vols 02.02 and 03.01.

⁶ Annual Book of ASTM Standards, Vol 03.01.

⁷ Annual Book of ASTM Standards, Vols 07.01, 11.03, and 15.09.

mens that have been precracked in fatigue by loading either in tension or three-point bending. Load versus displacement across the notch at the specimen edge is recorded autographically. The load corresponding to a 2 % apparent increment of crack extension is established by a specified deviation from the linear portion of the record. The K_{Ic} value is calculated from this load by equations that have been established on the basis of elastic stress analysis of specimens of the types described in this method. The validity of the determination of the K_{Ic} value by this test method depends upon the establishment of a *sharp-crack* condition at the tip of the fatigue crack, in a specimen of adequate size. To establish a suitable crack-tip condition, the stress intensity level at which the fatigue precracking of the specimen is conducted is limited to a relatively low value.

3.2 The specimen size required for testing purposes increases as the square of the ratio of toughness to yield strength of the material; therefore a range of proportional specimens is provided.

4. Significance and Use

4.1 The property K_{Ic} determined by this test method characterizes the resistance of a material to fracture in a neutral environment in the presence of a sharp crack under severe tensile constraint, such that the state of stress near the crack front approaches triaxial plane strain, and the crack-tip plastic region is small compared with the crack size and specimen dimensions in the constraint direction. A K_{Ic} value is believed to represent a lower limiting value of fracture toughness. This value may be used to estimate the relation between failure stress and defect size for a material in service wherein the conditions of high constraint described above would be expected. Background information concerning the basis for development of this test method in terms of linear elastic fracture mechanics may be found in Refs (1) and (2).

4.1.1 The K_{Ic} value of a given material is a function of testing speed and temperature. Furthermore, cyclic loads can cause crack extension at K_I values less than the K_{Ic} value. Crack extension under cyclic or sustained load will be increased by the presence of an aggressive environment. Therefore, application of K_{Ic} in the design of service components should be made with awareness to the difference that may exist between the laboratory tests and field conditions.

4.1.2 Plane-strain crack toughness testing is unusual in that there can be no advance assurance that a valid K_{Ic} will be determined in a particular test. Therefore it is essential that all of the criteria concerning validity of results be carefully considered as described herein.

4.1.3 Clearly it will not be possible to determine K_{Ic} if any dimension of the available stock of a material is insufficient to provide a specimen of the required size. In such a case the specimen strength ratio determined by this method will often have useful significance. However, this ratio, unlike K_{Ic} , is not a concept of linear elastic fracture mechanics, but can be a useful comparative measure of the toughness of materials when the specimens are of the same form and size, and that size is insufficient to provide a valid K_{Ic} determination, but sufficient that the maximum load results from pronounced crack propagation rather than plastic instability.

4.1.3.1 The strength ratio for center-cracked plate specimens tested in uniaxial tension may be determined by Method E 338.

4.2 This method can serve the following purposes:

4.2.1 In research and development to establish, in quantitative terms, significant to service performance, the effects of metallurgical variables such as composition or heat treatment, or of fabricating operations such as welding or forming, on the fracture toughness of new or existing materials.

4.2.2 In service evaluation, to establish the suitability of a material for a specific application for which the stress conditions are prescribed and for which maximum flaw sizes can be established with confidence.

4.2.3 For specifications of acceptance and manufacturing quality control, but only when there is a sound basis for specification of minimum K_{Ic} values, and then only if the dimensions of the product are sufficient to provide specimens of the size required for valid K_{Ic} determination. The specification of K_{Ic} values in relation to a particular application should signify that a fracture control study has been conducted on the component in relation to the expected history of loading and environment, and in relation to the sensitivity and reliability of the crack detection procedures that are to be applied prior to service and subsequently during the anticipated life.

5. Definitions

5.1 Terminology E 616 is applicable to this method.

5.1.1 *stress-intensity factor*, K , K_I , K_2 , K_3 [$FL^{-3/2}$]*—*the magnitude of the ideal-crack-tip stress field (a stress-field singularity) for a particular mode in a homogeneous, linear-elastic body.

NOTE—Values of K for modes 1, 2, and 3 are given by:

$$K_I = \lim_{r \rightarrow 0} [\sigma_y(2\pi r)^{1/2}],$$

$$K_2 = \lim_{r \rightarrow 0} [\tau_{xy}(2\pi r)^{1/2}], \text{ and}$$

$$K_3 = \lim_{r \rightarrow 0} [\tau_{yz}(\pi_{yz}(2\pi r)^{1/2})],$$

where r = a distance directly forward from the crack tip to a location where the significant stress is calculated.

Discussion—In this test method, mode 1 is assumed.

5.1.2 *plane-strain fracture toughness*—the crack-extension resistance under conditions of crack-tip plane strain.

NOTE 1—For example, in mode 1 for slow rates of loading and negligible plastic-zone adjustment, plane-strain fracture toughness is the value of stress-intensity factor designated K_{Ic} [$FL^{-3/2}$] as measured using the operational procedure (and satisfying all of the validity requirements) specified in this test method, which provides for the measurement of crack-extension resistance at the start of crack extension and provides operational definitions of crack-tip sharpness, start of crack extension, and crack-tip plane strain.

NOTE 2—See also definitions of crack-extension resistance, crack-tip plane strain, and mode.

Discussion—In this test method, mode 1 is assumed.

5.1.3 *crack plane orientation*—an identification of the plane and direction of a fracture in relation to product geometry. This identification is designated by a hyphenated code with the first letter(s) representing the direction normal to the crack plane and the second letter(s) designating the expected direction of crack propagation.

5.1.3.1 The fracture toughness of a material usually depends on the orientation and direction of propagation of the

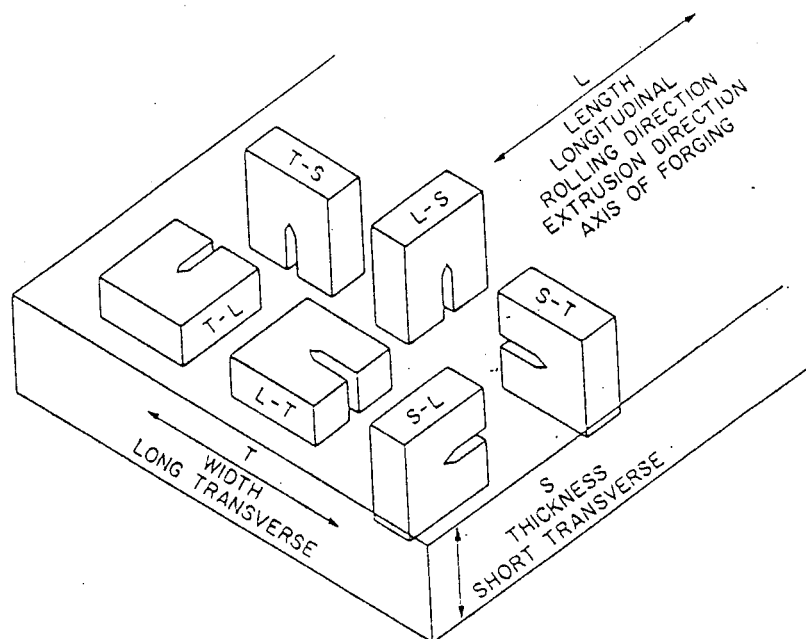


FIG. 1 Crack Plane Orientation Code for Rectangular Sections

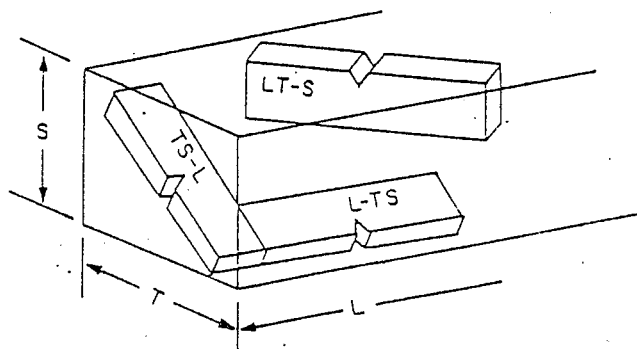


FIG. 2 Crack Plane Orientation Code for Rectangular Sections Where Specimens are Tilted with Respect to the Reference Directions

crack in relation to the anisotropy of the material, which depends, in turn, on the principal directions of mechanical working or grain flow. The orientation of the crack plane should be identified wherever possible in accordance with the following systems (11). In addition, the product form should be identified (for example, straight-rolled plate, cross-rolled plate, pancake forging, etc.).

5.1.3.2 For rectangular sections, the reference directions are identified as in Figs. 1 and 2, which give examples for a rolled plate. The same system would be useful for sheet, extrusions, and forgings with nonsymmetrical grain flow.

L = direction of principal deformation (maximum grain flow),
 T = direction of least deformation, and
 S = third orthogonal direction.

5.1.3.3 Using a two letter code, the first letter designates the *direction normal* to the crack plane, and the second letter the *expected direction of crack propagation*. For example, in Fig. 1 the $T-L$ specimen has a fracture plane whose normal is in the width direction of a plate and an expected direction

of crack propagation coincident with the direction of maximum grain flow or longitudinal direction of the plate.

5.1.3.4 For specimens that are tilted in respect to two of the reference axes, Fig. 2, the orientation is identified by a three-letter code. The code $L-TS$, for example, means that the crack plane is perpendicular to the direction of principal deformation (L direction), and the expected fracture direction is intermediate between T and S . The code $TS-L$ means the crack plane is perpendicular to a direction intermediate between T and S , and the expected fracture direction is in the L direction.

5.1.3.5 For certain cylindrical sections where the direction of principal deformation is parallel to the longitudinal axis of the cylinder, the reference directions are identified as in Fig. 3, which gives examples for a drawn bar. The same system would be useful for extrusions or forged parts having circular cross section.

L = direction of maximum grain flow,
 R = radial direction, and
 C = circumferential or tangential direction.

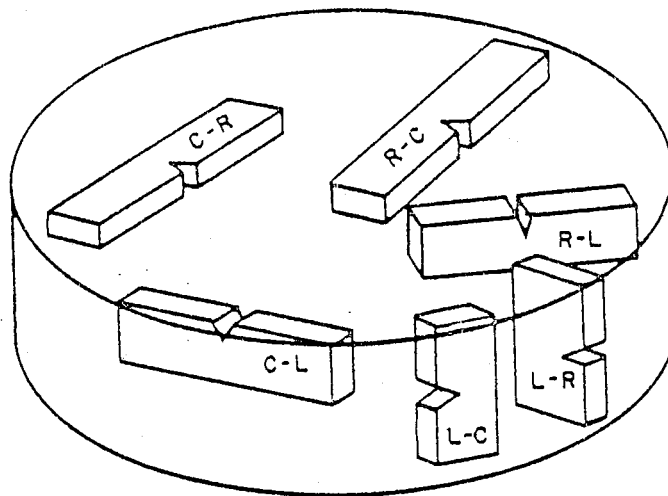
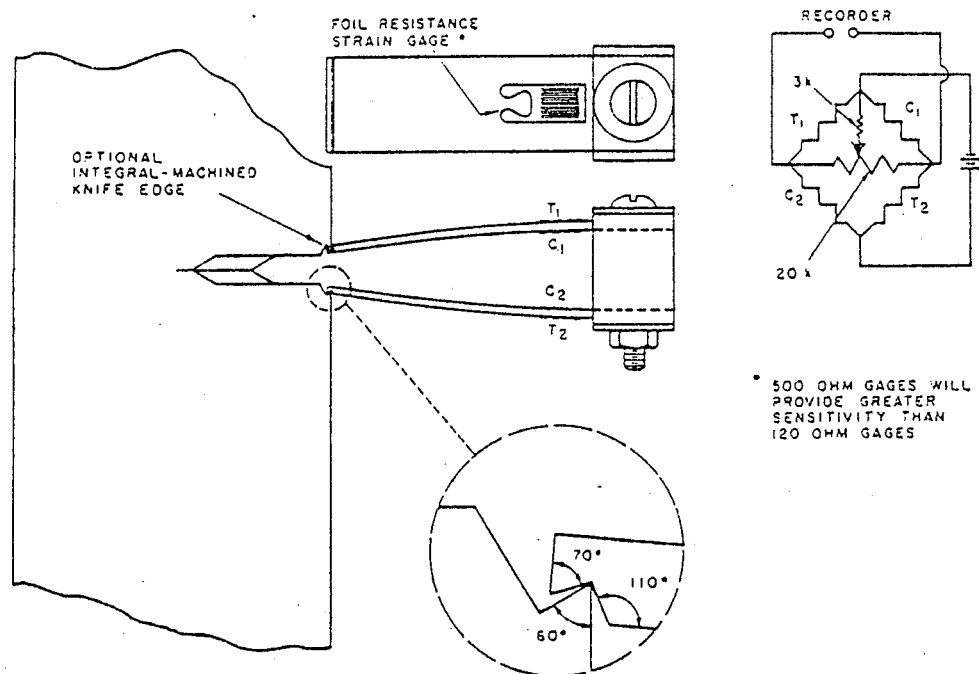


FIG. 3 Crack Plane Orientation Code for Bar and Hollow Cylinder

FIG. 4 Double-Cantilever Clip-in Displacement Gage Showing Mounting by Means of Integral Knife Edges
(Gage Design Details are Given in Annex A1)

6. Apparatus

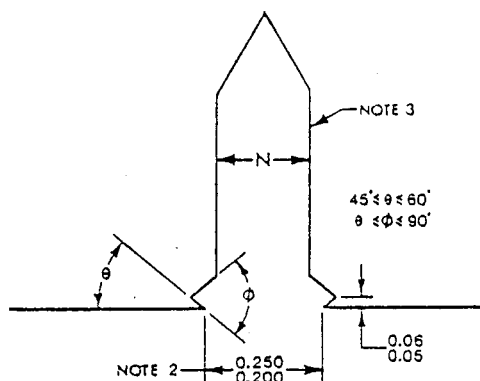
6.1 *Loading*—Specimens should be loaded in a testing machine that has provision for autographic recording of the load applied to the specimen.

6.2 *Fixtures*—Fixtures suitable for loading the specimen configurations covered by this method are shown in the appropriate annex. These fixtures are so designed as to minimize the frictional contributions to the measured load.

6.3 *Displacement Gage*—The displacement gage output shall indicate the relative displacement of two precisely located gage positions spanning the crack starter notch mouth. Exact and positive positioning of the gage on the specimen is essential, yet the gage must be released without

damage when the specimen breaks. A recommended design for a self-supporting, releasable gage is shown in Fig. 4 and described in Annex A1. The strain gage bridge arrangement is also shown in Fig. 4.

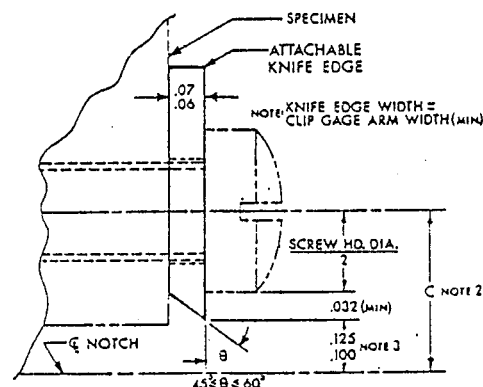
6.3.1 The specimen must be provided with a pair of accurately machined knife edges that support the gage arms and serve as the displacement reference points. These knife edges can be machined integral with the specimen as shown in Fig. 4 and Fig. 5 or they may be separate pieces fixed to the specimen. A suggested design for such attachable knife edges is shown in Fig. 6. This design is based on a knife edge spacing of 0.2 in. (5.1 mm). The effective gage length is established by the points of contact between the screw and



NOTE 1—Dimensions in inches.
NOTE 2—Gage length shown corresponds to clip gage spacer block dimensions shown in Annex A1, but other gage lengths may be used provided they are appropriate to the specimen (see 6.3.3).
NOTE 3—For starter notch configurations see Fig. 7.

Metric Equivalents				
in.	0.050	0.060	0.200	0.250
mm	1.3	1.5	5.1	6.4

FIG. 5 Example of Integral Knife Edge Design



NOTE 1—Dimensions are in inches.
NOTE 2—Effective gage length = $2C + \text{Screw Thread Diameter} \leq W/2$. (This will always be greater than the gage length specified in A1.1.)
NOTE 3—Dimension shown corresponds to clip gage spacer block dimension in Annex A1.

Metric Equivalents				
in.	0.032	0.06	0.07	0.100
mm	0.81	1.5	1.8	2.54

FIG. 6 Example of Attachable Knife Edge Design

the hole threads. For the design shown, the major diameter of the screw has been used in setting this gage length. A No. 2 screw will permit the use of attachable knife edges for specimens having $W > 1$ in. (25 mm).

6.3.2 Each gage shall be checked for linearity using an extensometer calibrator or other suitable device; the resettability of the calibrator at each displacement interval should be within $+0.000020$ in. (0.00050 mm). Readings shall be taken at ten equally spaced intervals over the working range of the gage (see Annex A1). This calibration procedure should be performed three times, removing and reinstalling the gage in the calibration fixture between each run. The required linearity shall correspond to a maximum deviation of $+0.0001$ in. (0.0025 mm) of the individual

displacement readings from a least-squares-best-fit straight line through the data. The absolute accuracy, as such, is not important in this application, since the method is concerned with relative changes in displacement rather than absolute values (see 9.1).

6.3.3 It is not the intent of this method to exclude the use of other types of gages or gage-fixing devices provided the gage used meets the requirements listed below and provided the gage length does not exceed those limits given in the annex appropriate to the specimen being tested.

7. Specimen Size, Configurations, and Preparation

7.1 Specimen Size:

7.1.1 In order for a result to be considered valid according to this method it is required that both the specimen thickness, B , and the crack length, a , exceed $2.5 (K_{Ic}/\sigma_{YS})^2$, where σ_{YS} is the 0.2 % offset yield strength of the material for the temperature and loading rate of the test (1, 5, 6).

7.1.2 The initial selection of a size of specimen from which valid values of K_{Ic} will be obtained may be based on an estimated value of K_{Ic} for the material. It is recommended that the value of K_{Ic} be overestimated, so that a conservatively large specimen will be employed for the initial tests. After a valid K_{Ic} result is obtained with the conservative-size initial specimen, the specimen size may be reduced to an appropriate size [a and $B \geq 2.5 (K_{Ic}/\sigma_{YS})^2$] for subsequent testing.

7.1.3 Alternatively, the ratio of yield strength to Young's modulus can be used for selecting a specimen size that will be adequate for all but the toughest materials:

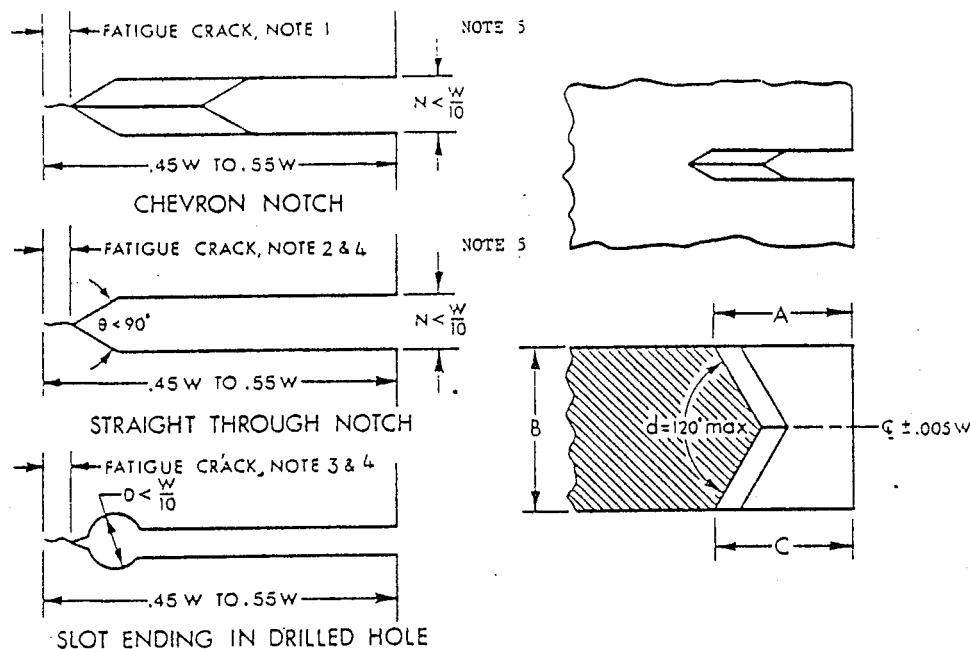
σ_{YS}/E	Minimum Recommended Thickness and Crack Length	
	in.	mm
0.0050 to 0.0057	3	75
0.0057 to 0.0062	2½	63
0.0062 to 0.0065	2	50
0.0065 to 0.0068	1¾	44
0.0068 to 0.0071	1½	38
0.0071 to 0.0075	1¼	32
0.0075 to 0.0080	1	25
0.0080 to 0.0085	¾	20
0.0085 to 0.0100	½	12½
0.0100 or greater	¼	6½

When it has been established that $2.5 (K_{Ic}/\sigma_{YS})^2$ is substantially less than the minimum recommended thickness given in the preceding table, then a correspondingly smaller specimen can be used. On the other hand, if the form of the available material is such that it is not possible to obtain a specimen with both crack length and thickness greater than $2.5 (K_{Ic}/\sigma_{YS})^2$, then it is not possible to make a valid K_{Ic} measurement according to this method.

7.2 Specimen Configurations—The configurations of the various specimens are shown in the following annexes: Annex A3, Bend Specimen SE (B), Annex A4, Compact Specimen C (T), Annex A5, Arc-Shaped Specimen A (T), and Annex A6, Disk-Shaped Compact Specimen DC (T).

7.2.1 Standard Specimens—The crack length, a (crack starter notch plus fatigue crack) is nominally equal to the thickness, B , and is between 0.45 and 0.55 times the width, W . The ratio W/B is nominally equal to two.

7.2.2 Alternative Specimens—In certain cases it may be desirable to use specimens having W/B ratios other than two.



(a) Starter Notches and Fatigue Cracks

NOTE 1—For a chevron crack starter notch the fatigue crack shall emerge on both surfaces of the specimen.

NOTE 2—Fatigue crack extension on each surface of the specimen containing a straight-through notch shall be at least 0.025 W or 0.050 in. (1.3 mm), whichever is larger.

NOTE 3—Fatigue crack extension on each surface of the specimen from the stress raiser tipping the hole shall be at least 0.5 D or 0.050 in. (1.3 mm), whichever is larger.

NOTE 4—Crack starter notch shall be perpendicular to the specimen surfaces and to the intended direction of crack propagation within $\pm 2^\circ$.

NOTE 5—Notch width N need not be less than $\frac{1}{16}$ in. (1.6 mm).

(b) Detail of Chevron Notch

NOTE 1— $A = C$ within 0.010 W

NOTE 2—Cutter tip angle 90° max

NOTE 3—Radius at chevron notch bottom 0.010 in. (0.25 mm) max

FIG. 7 Crack Starter Notch and Fatigue Crack Configurations

Alternative proportions for bend specimens are $1 \leq W/B \leq 4$. For the other specimen configurations alternative specimens may have $2 \leq W/B \leq 4$. These alternative specimens shall have the same crack length-to-width ratio as the standard specimens. It should be appreciated that K_{Ic} values obtained using alternative specimen proportions may not agree with those obtained using the standard specimens (15).

7.3 Specimen Preparation—The dimensional tolerances and surface finishes shown on the specimen drawings given in Annexes A3 to A6 shall be followed in specimen preparation.

7.3.1 Fatigue Crack Starter Notch—Three forms of fatigue crack starter notches are shown in Fig. 7. To facilitate fatigue cracking at low stress intensity levels, the root radius for a straight-through slot terminating in a V-notch should be 0.003 in. (0.08 mm) or less. If a chevron form of notch is used, the root radius may be 0.010 in. (0.25 mm) or less. In the case of a slot tipped with a hole it will be necessary to provide a sharp stress raiser at the end of the hole. Care should be taken to ensure that this stress raiser is so located that the crack plane orientation requirements (8.2.4) can be met.

7.3.2 Fatigue Cracking—Fatigue cracking shall be conducted in accordance with the procedures outlined in Annex A2. Fatigue cycling shall be continued until the fatigue crack

will satisfy the requirements stated in the following two sections.

7.3.2.1 The crack length (total length of the crack starter configuration plus the fatigue crack) shall be between 0.45 and 0.55 W .

7.3.2.2 For a straight-through crack starter terminating in a V-notch (see Fig. 7), the length of the fatigue crack on each surface of the specimen shall not be less than 2.5 % of W or 0.050 in. (1.3 mm) min, and for a crack starter tipped with a drilled hole (see Fig. 7), the fatigue crack extension from the stress raiser tipping the hole shall not be less than 0.5 D or 0.050 in. on both surfaces of the specimen, where D is the diameter of the hole (1.3 mm), min. For a chevron notch crack starter (see Fig. 7), the fatigue crack shall emerge from the chevron on both surfaces of the specimen.

8. General Procedure

8.1 Number of Tests—It is recommended that at least three replicate tests be made for each material condition.

8.2 Specimen Measurement—Specimen dimensions shall conform to the tolerances shown in the appropriate annex. Three fundamental measurements are necessary for the calculation of K_{Ic} , namely, the thickness, B , the crack length, a , and the width, W .

8.2.1 Measure the thickness, B , to the nearest 0.001 in. (0.025 mm) or to 0.1 %, whichever is larger, at not less than

three equally spaced positions along the line of intended crack extension from the fatigue crack tip to the unnotched side of the specimen. The average of these three measurements should be recorded as B .

8.2.2 Measure the crack length, a , after fracture to the nearest 0.5 % at the following three positions: at the center of the crack front, and midway between the center of the crack front, and the end of the crack front on each surface of the specimen. Use the average of these three measurements as the crack length to calculate K_Q . The following requirements shall apply to the fatigue crack front: (1) The difference between any two of the three crack length measurements shall not exceed 10 % of the average. (2) For a chevron notch starter (see Fig. 7), the fatigue crack shall emerge from the chevron on both surfaces of the specimen, neither surface crack length shall differ from the average length by more than 10 %, and the difference between these two surface measurements shall not exceed 10 % of the average crack length. (3) For a straight-through starter notch (see Fig. 7) no part of the crack front shall be closer to the machined starter notch than 2.5 % W or 0.050 in. (1.3 mm) minimum, nor shall the surface crack length measurements differ from the average crack length by more than 15 %, and the differences between these two measurements shall not exceed 10 % of the average crack length.

8.2.3 Measure the width, W , as described in the annex appropriate to the specimen type being tested.

8.2.4 The plane of the crack shall be parallel to both the specimen width and thickness direction within $\pm 10^\circ$ (7).

8.3 *Loading Rate*—For conventional (static) testing load the specimen at a rate such that the rate of increase of stress intensity is within the range from 30 000 to 150 000 psi·in.^{1/2}/min (0.55 to 2.75 MPa·m^{1/2}/s). The loading rates corresponding to these stress intensity rates are given in the appropriate annex for the specimen being tested. For rapid-load testing the loading rates are given in Annex A7.

8.4 *Test Record*—Make a test record consisting of an autographic plot of the output of the load-sensing transducer versus the output of the displacement gage. The initial slope of the linear portion shall be between 0.7 and 1.5. It is conventional to plot the load along the vertical axis, as in an ordinary tension test record. Select a combination of load-sensing transducer and autographic recorder so that the load, P_Q (see 9.1), can be determined from the test record with an accuracy of ± 1 %. With any given equipment, the accuracy of readout will be greater than the larger the scale of the test record.

8.4.1 Continue the test until the specimen can sustain no further increase in load. In some cases the range of the chart will not be sufficient to include all of the test record up to maximum load, P_{max} . In any case, read the maximum load from the dial of the testing machine (or other accurate indicator) and record it on the chart.

9. Calculation and Interpretation of Results

9.1 *Interpretation of Test Record and Calculation of K_{Ic}* —In order to establish that a valid K_{Ic} has been determined, it is necessary first to calculate a conditional result, K_Q , which involves a construction on the test record, and then to determine whether this result is consistent with the size and

yield strength of the specimen according to 7.1. The procedure is as follows:

9.1.1 Draw the secant line OP_s , shown in Fig. 7 through the origin of the test record with slope $(P/v)_s = 0.95 (P/v)_0$, where $(P/v)_0$ is the slope of the tangent OA to the initial linear part of the record (Note 6). The load P_Q is then defined as follows: if the load at every point on the record which precedes P_s is lower than P_s , then P_s is P_Q (Fig. 8 Type I); if, however, there is a maximum load preceding P_s which exceeds it, then this maximum load is P_Q (Fig. 8 Types II and III).

NOTE 6—Slight nonlinearity often occurs at the very beginning of a record and should be ignored. However, it is important to establish the initial slope of the record with high precision and therefore it is advisable to minimize this nonlinearity by a preliminary loading and unloading with the maximum load not producing a stress intensity level exceeding that used in the final stage of fatigue cracking.

9.1.2 Calculate the ratio P_{max}/P_Q , where P_{max} is the maximum load the specimen was able to sustain (see 8.4). If this ratio does not exceed 1.10, proceed to calculate K_Q as described in the annex appropriate to the specimen being tested. If P_{max}/P_Q does exceed 1.10, then the test is not a valid K_{Ic} test because it is then possible that K_Q bears no relation to K_{Ic} . In this case proceed to calculate the specimen strength ratio.

9.1.3 Calculate $2.5 (K_Q/\sigma_{YS})^2$ where σ_{YS} is the 0.2 % offset yield strength in tension (see Methods E 8). If this quantity is less than both the specimen thickness and the crack length, then K_Q is equal to K_{Ic} . Otherwise, the test is not a valid K_{Ic} test. Expressions for calculations of K_Q are given in the annex appropriate to the specimen being tested.

9.1.4 If the test result fails to meet the requirements in 9.1.2 or in 9.1.3, or both, it will be necessary to use a larger specimen to determine K_{Ic} . The dimensions of the larger specimen can be estimated on the basis of K_Q but generally will be at least 1.5 times those of the specimen that failed to yield a valid K_{Ic} value.

9.1.5 Calculate the specimen-strength ratio R_{sx} according to the annex appropriate to the specimen being tested.

9.2 *Fracture Appearance*—The appearance of the fracture is valuable supplementary information and shall be noted for each specimen. Common types of fracture appearance are shown in Fig. 9. For fractures of Types (a) or (b), measure the average width, f , of the central flat fracture area, and note and record the proportion of oblique fracture per unit thickness $(B-f)/B$. Make this measurement at a location midway between the crack tip and the unnotched edge of the specimen. Report fractures of Type (c) as full oblique fractures.

10. Report

10.1 The specimen configuration code as shown with the specimen drawing in the appropriate annex shall be reported. In addition, this code shall be followed with loading code (T for tension and B for bending) and the code for crack plane orientation (see Section 5). These latter two codes should appear in separate parentheses. For example, a test result obtained using the compact specimen (see Annex A4) might be designated as follows: C(T)(S-T). The first letter indicates compact specimen. The second letter indicates the loading was tension and the first of the last two letters indicates that

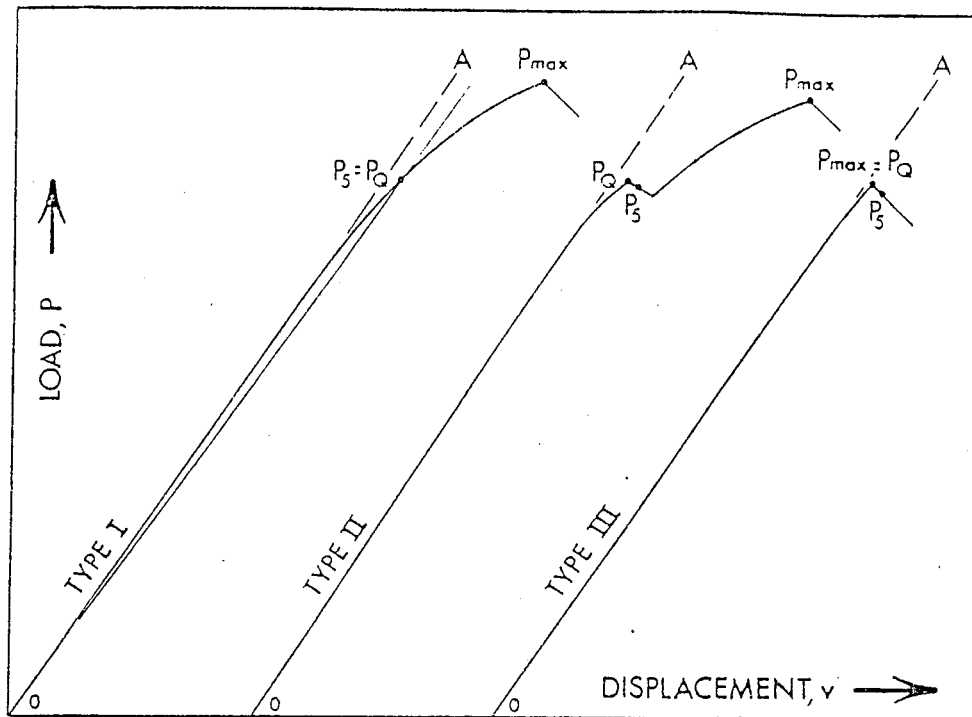


FIG. 8 Principal Types of Load-Displacement Records

the normal to the crack plane is in the direction of principal deformation and the second of these letters indicates the intended direction of crack propagation is in the direction of least deformation.

10.2 In addition, the following information should be reported for each specimen tested.

10.2.1 The form of the product tested, that is, forging, plate, casting etc.

10.2.2 Thickness, B .

10.2.3 Width (depth), W .

10.2.3.1 Offset of the loading holes, X , for the arc-shaped specimen.

10.2.3.2 Outer and inner radii, r_2 and r_1 for the arc-shaped specimen.

10.2.4 Fatigue precracking conditions in terms of:

10.2.4.1 Maximum stress intensity, $K(\max)$ and number of cycles for terminal fatigue crack extension over a length at least 2.5 % of the overall length of notch plus crack, and

10.2.4.2 The stress intensity range for terminal crack extension.

10.2.5 Crack length measurements.

10.2.5.1 At center of crack front,

10.2.5.2 Midway between the center and the end of the crack front on each side, and

10.2.5.3 At each surface,

10.2.6 Test temperature.

10.2.7 Relative humidity as determined by Method E 337.

10.2.8 Loading rate in terms of K_I (change in stress intensity factor per unit time) (2).

10.2.9 Load-displacement record and associated calculations.

10.2.10 Fracture appearance,

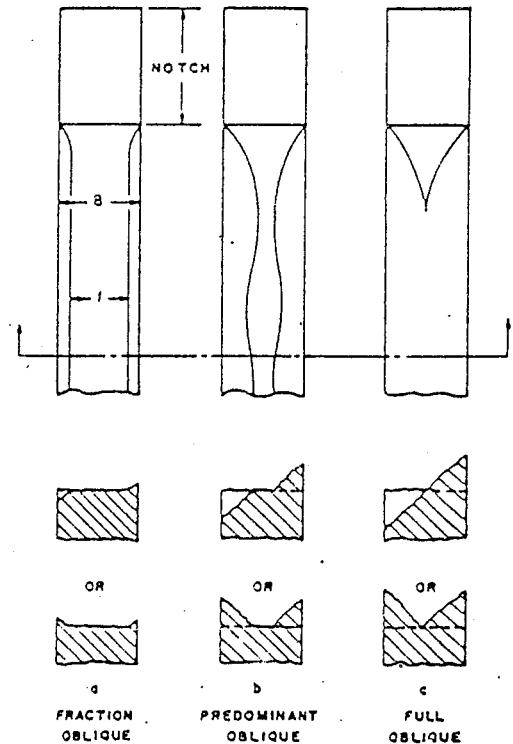


FIG. 9 Common Types of Fracture Appearance

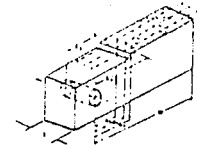
10.2.11 Yield strength (offset = 0.2 %) as determined by Methods E 8,

10.2.12 K_{Ic} or K_{Qc} followed by the parenthetical statement: "invalid according to section(s) of ASTM Test Method E 399," and

ASTM DATA SHEET 1^a
(SAMPLE)

MATERIAL/FORM _____ HEAT TREAT _____
SPECIMEN I.D. _____ SPECIMEN TYPE _____

DATE ____/____/____ DATE REPORT _____



PARTICULARS	DATA	REF. PARAGRAPH	FRACTURE TEST	DATA	REF. PARAGRAPH
• Crack Plane Orientation		3.2	• Crack Lengths -		
• Material 0.2% Offset Yield Strength, σ_{ys} , per IS		3.2.2	- At Center of Crack Front (a_c)		3.2.2
• Thickness, B		3.2.2	- At Right of Center (a_r)		3.2.2
• Depth (Width), W		3.2.2	- At Left of Center (a_l)		3.2.2
for - SE(B)		3.4.1 (Annex 3)	- At Right of Surface (a_s)		3.2.2
for - C(T)		3.4.1 (Annex 3)	- At Left Surface (a_l)		3.2.2
for - DC(T)		3.4.1.2 (Annex 3)	• Crack Plane Symmetry		3.2.4
• Arc Shaped Specimen -			- Loading Rate (ksi./min.)		3.3
- Width, W		3.4.1 (Annex 3)	- Test Temperature		3.3.4
- Loading hole Offset, X		3.4.1 (Annex 3)	- Relative Humidity		3.3.7
- Outer and Inner Radii, r_1 & r_2		3.4.1 (Annex 3)	- Load-Displacement Record		3.4 & 3.1
FATIGUE PRECRACKING	DATA	REF. PARAGRAPH	CALCULATION OF K_{Ic} & R_{Ic}	DATA	REF. PARAGRAPH
• $\frac{K_{Ic}}{B} < 0.001a^{-3/2}$ (0.00032a ^{-3/2})		A2.3.2	• $P_{max}/P_Q < 1.1$		3.1.2
• $K_{Ic} < 0.6 K_Q$		A2.3.2	- K_Q SE(B)		3.5.3 (Annex 3)
• $K_{Ic} < 0.8 K_{Ic}$		A2.3.1 and A2.4.2	- K_Q C(T)		3.5.3 (Annex 3)
• at Temperature T_{max} (°F) & K_Q (ksi)		A2.4.4	- K_Q A(T)		3.5.3 (Annex 3)
• Crack Length - SENAR Slot plus Fatigue			- K_Q DC(T)		3.5.3 (Annex 3)
- $a = 0.10W$		A2.3.2 and Figure 4	• Valid K_{Ic}		3.1.3
- P_{max} 1K			- R_{Ic}		3.1.3
- Cycles for last 1.32 of "a"					

FIG. 10 Suggested Form of Table for Reporting Information Listed in 10.1 and 10.2

10.2.13 R_{yx} where x refers to the specimen configuration as given in the appropriate annex.

10.2.14 P_{max}/P_Q .

10.3 It is desirable to list the information required in 10.1 and 10.2 in the form of a table. A suggested form for such a table is given in Fig. 10.

11. Precision and Bias

11.1 *Bias*—There is no accepted "standard" value for the plane strain fracture toughness of any material. In the absence of such a true value, any statement concerning bias is not meaningful.

11.2 *Precision*—The precision of a K_{Ic} determination is a function of the precision and bias of the various measurements of linear dimensions of the specimen and testing fixtures, the precision of the displacement measurement, and the bias of the load measurement as well as the bias of the recording devices used to produce the load displacement record and the precision of the constructions made on this record. It is not possible to make meaningful statements concerning precision and bias for all these measurements. However, it is possible to derive useful information concerning the precision of a K_{Ic} measurement in a global sense from three interlaboratory test programs (17) (18). The results of these programs are summarized in Table 1 which gives the standard deviation of K_{Ic} for the bend specimen, the compact specimen, and the arc-shaped specimen as derived from tests on several high-strength alloys which were all very uniform in composition and structure. It should be appreciated that

TABLE 1 Grand Means and Standard Deviations for K_{Ic} as Obtained from Three Interlaboratory Test Programs^a

	Bend Specimens			
	2219T851 σ_{ys} = 51.0 ksi (353 MPa)	4340 σ_{ys} = 238 ksi (1640 MPa)	18 Ni Marage σ_{ys} = 276 ksi (1902 MPa)	4340 σ_{ys} = 206 ksi (1419 MPa)
Grand mean \bar{X} , ksi-in. ^{1/2}	32.7	44.2	51.8	79.8
Standard deviation, S	1.87	1.85	2.04	2.87
	Compact Specimens			
	2219T851 σ_{ys} = 51.0 ksi (353 MPa)	4340 σ_{ys} = 238 ksi (1640 MPa)	18 Ni Marage σ_{ys} = 276 ksi (1902 MPa)	4340 σ_{ys} = 206 ksi (1419 MPa)
Grand mean \bar{X} , ksi-in. ^{1/2}	32.4	45.5	53.9	79.4
Standard deviation, S	1.15	1.27	1.64	1.79
	Arc-Shaped Specimens (4335V, σ_{ys} = 192 ksi (1320 MPa))			
	$X/W = 0$	$X/W = 0.5$	$X/W = 0$	$X/W = 0.5$
Grand mean \bar{X} , ksi-in. ^{1/2}	102.3	101.7	102.3	101.7
Standard deviation, S	3.50	2.36	3.50	2.36

^a The standard deviation has been pooled for all laboratories testing a given alloy. Data for the bend and compact specimen can be found in Ref (17) and for the arc-shaped specimen in Ref (18).

the measures of precision shown in Table 1 apply to tests on high-strength alloys that do not exhibit strong transitional behavior in terms of temperature or strain rate. If temperature and rate effects have a large influence on the toughness, increased scatter in K_{Ic} measurements may be noted. For example, within or below the transition range of a structural steel the initial advance of the fatigue crack will be controlled

by abrupt fracture of local elements at the crack tip accompanied by rapid transfer of load to adjacent regions which then exhibit cleavage fracture. Under these circumstances, a

statistical size effect may be noticed as the specimen size is changed, and tests on small specimens will be characterized by larger scatter than will tests on larger specimens.

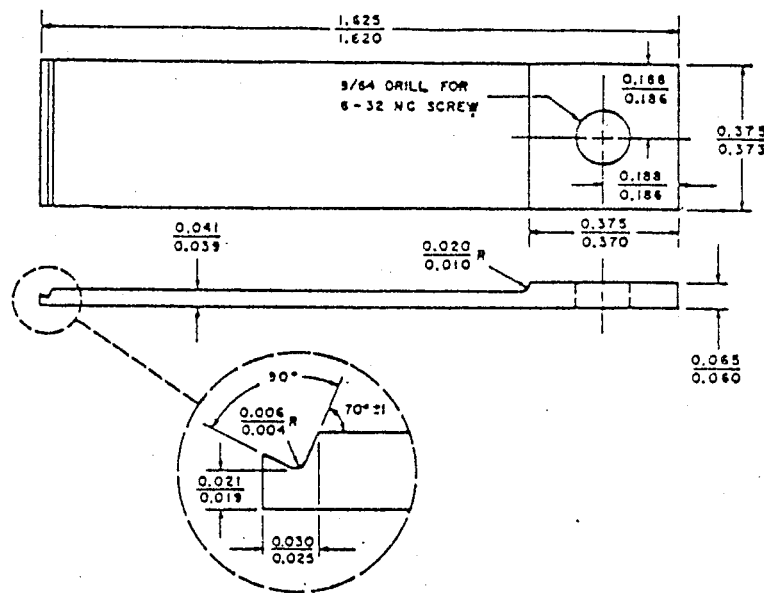
ANNEXES

(Mandatory Information)

A1. DESIGN FOR DOUBLE-CANTILEVER DISPLACEMENT GAGE

A1.1 The gage consists of two cantilever beams and a spacer block which are clamped together with a single nut and bolt, as shown in Fig. 4. Electrical-resistance strain gages are cemented to the tension and compression surfaces of each beam, and are connected as a Wheatstone bridge incorporating a suitable balancing resistor. The material for the gage beams should have a high ratio of yield strength to elastic modulus, and titanium alloy 13V-11Cr-3Al in the solution treated condition has been found very satisfactory for this purpose. If a material of different modulus is substituted, the spring constant of the assembly will change correspondingly, but the other characteristics will not be

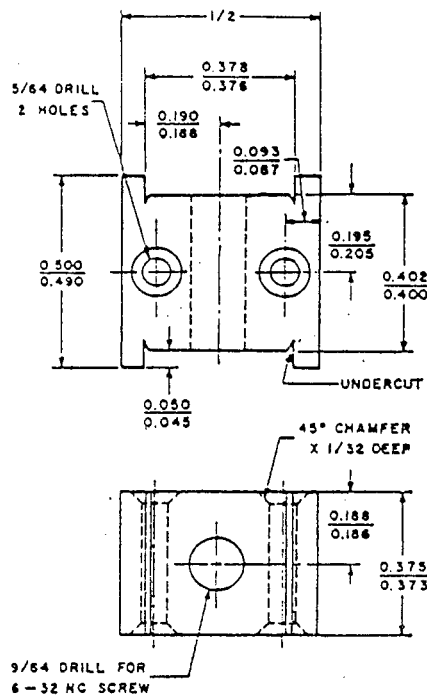
affected. Detailed dimensions for the beams and spacer block are given in Figs. A1.1 and A1.2. For these particular dimensions the linear range (working range) is from 0.15 to 0.30 in. (3.8 to 7.6 mm) and the recommended gage length is from 0.20 to 0.25 in. (5.1 to 6.3 mm). The clip gage can be altered to adapt it to a different gage length by substituting a spacer block of appropriate height. As discussed in 6.3.2 the required precision of the gage corresponds to a maximum deviation of ± 0.0001 in. (0.0025 mm) of the displacement readings from a least-squares-best-fit straight line through the data. Further details concerning design, construction and use of these gages are given in Ref (10).



NOTE—Dimensions are in inches.

in.	mm	in.	mm
0.004	0.10	0.060	1.52
0.006	0.15	0.065	1.65
0.010	0.25	$\frac{1}{16}$	3.6
0.019	0.48	0.186	4.72
0.020	0.51	0.188	4.78
0.021	0.53	0.370	9.40
0.025	0.64	0.373	9.47
0.030	0.76	0.375	9.52
0.039	0.99	1.620	41.15
0.041	1.04	1.625	41.28

FIG. A1.1 Beams for Double-Cantilever Displacement Gage



NOTE 1— $\frac{5}{64}$ -in. diameter holes are for strain gage leads.
NOTE 2—Dimensions are in inches.

Metric Equivalents			
in.	mm	in.	mm
$\frac{1}{32}$	0.80	0.195	4.95
0.045	1.14	0.205	5.21
0.050	1.27	0.373	9.47
$\frac{5}{64}$	2.00	0.375	9.52
0.087	2.21	0.376	9.55
0.093	2.36	0.378	9.60
0.125	3.18	0.400	10.16
$\frac{9}{64}$	3.60	0.402	10.21
0.186	4.72	0.490	12.45
0.188	4.78	$\frac{1}{2}$	12.70
0.190	4.83	0.500	12.70

FIG. A1.2 Aluminum-Alloy Spacer Block for Double-Cantilever Displacement Gage

A2. FATIGUE PRECRACKING OF K_{Ic} FRACTURE TOUGHNESS SPECIMENS

A2.1 Introduction

A2.1.1 Experience has shown that it is impractical to obtain a reproducibly sharp, narrow machined notch that will simulate a natural crack well enough to provide a satisfactory K_{Ic} test result. The most effective artifice for this purpose is a narrow notch from which extends a comparatively short fatigue crack, called the precrack. The dimensions of the notch and the precrack, and the sharpness of the precrack, must meet certain conditions which can be readily met with most engineering materials since the fatigue cracking process can be closely controlled when careful attention is given to the known contributory factors. However, there are some materials that are too brittle to be fatigue cracked since they fracture as soon as the fatigue crack initiates; these are outside the scope of the present test method. The purpose of this annex is to provide guidance on the production of satisfactory

fatigue precracks, and to state the associated requirements for a valid K_{Ic} test.

A2.1.2 A fatigue precrack is produced by cyclically loading the notched specimen with a ratio of minimum to maximum stress between -1 and $+0.1$ for a number of cycles usually between about 10^4 and 10^6 , depending on specimen size, notch preparation, and stress intensity level. The maximum stress intensity in the terminal (2.5 %) stage of fatigue crack growth must not exceed 60 % of the K_{Ic} value of the material. Some fraction of the total number of cycles required to produce the fatigue precrack is consumed in initiation of the crack at the notch root; the remainder accounts for growth of the crack to the required length. If the total number of cycles is excessive, the reason is usually that the number of cycles required for initiation is excessive rather than that the subsequent rate of crack growth is low.

There are several ways of promoting early crack initiation: (1) by providing a very sharp notch tip; (2) by using a chevron notch (Fig. 7); (3) by statically preloading the specimen in such a way that the notch tip is compressed in a direction normal to the intended crack plane but without allowing the specimen strength ratio (see 9.1.5) to be less than -1 ; (4) by using a negative fatigue load ratio; for a given maximum fatigue load, the more negative the load ratio, the earlier crack initiation is likely to occur.

A2.2 Equipment

A2.2.1 The equipment for fatigue cracking shall be such that the stress distribution is uniform through the specimen thickness; otherwise the crack will not grow uniformly. The stress distribution shall also be symmetrical about the plane of the prospective crack; otherwise the crack will deviate unduly from that plane and the test result will be significantly affected (7).

A2.2.2 The K calibration for the specimen, as loaded by the equipment, shall be known with an error of not more than 5 %. The K calibration is the relation of the stress intensity factor K to either the load or to some prescribed displacement and the specimen dimensions (1). The fixtures recommended in the test method (see appropriate annex) are also suitable for fatigue cracking, and K calibrations for specimens loaded through these fixtures are given in the annexes of this test method. If different fixtures are used, the appropriate K calibration should be determined experimentally with these fixtures (7). The advantage of experimental K calibration, as compared with numerical methods of analysis, is that accurate modeling of the boundary conditions with the actual fixtures is assured. It is important to bear in mind that if the fatigue cycle involves reversal of load, the K calibration can be very sensitive to the distribution of clamping forces necessary to grip the specimen.

A2.3 Specimen Requirements

A2.3.1 The fatigue precracking shall be conducted with the specimen fully heat treated to the condition in which it is to be tested.

A2.3.2 The combination of starter notch and fatigue precrack must conform to the requirements shown in Fig. 7. The nominal crack length is equal to $0.50W$ and is the total length of the starter notch slot plus fatigue crack. To facilitate fatigue precracking at a low level of stress intensity, the notch root radius of a straight-across notch should be no more than 0.003 in. (0.08 mm). If a chevron notch is used (Fig. 7), the notch root radius can be as much as 0.01 in. (0.25 mm) because of the compound stress intensification at the point of the chevron. Early crack initiation can also be promoted by precompression of the notch tip region, as stated in A2.1.2.

A2.3.3 It is advisable to mark two pencil lines on each side of the specimen normal to the anticipated paths of the surface traces of the fatigue crack. The line most distant from the notch tip should indicate the minimum required length of fatigue crack, and the other the terminal part of that length equal to not less than 2.5 % of the overall length of

notch plus fatigue crack, that is $0.0125W$. During the final stage of fatigue crack extension, for at least this distance, the ratio of maximum stress intensity of the fatigue cycle to the Young's modulus of the material, K_{\max}/E shall not exceed $0.002\text{in.}^{1/2}$ ($0.0032\text{ m}^{1/2}$). Furthermore, K_{\max} must not exceed 60 % of the K_Q value determined in the subsequent test if K_Q is to qualify as a valid K_{Ic} result.

A2.4 Precracking Procedure

A2.4.1 Fatigue precracking can be conducted under either load control or displacement control provided that the appropriate K calibration is known with requisite accuracy for the specimen and fixture (A2.2.1). If the load cycle is maintained constant, the maximum K and the K range will increase with crack length; if the displacement cycle is maintained constant, the reverse will happen. The initial value of the maximum fatigue load or displacement should be calculated from the K calibration and the specimen and notch dimensions. It is suggested that this load be selected so that the maximum stress intensity factor in the initial portion of the fatigue cycle does not exceed 80 % of the estimated K_{Ic} value of the material. Higher K values may result in undesirably high crack growth rates. The minimum is then selected so that the stress ratio is between -1 and $+0.1$. The more negative the stress ratio, the faster the fatigue precrack will be completed, but this advantage is offset by the need for more elaborate fixtures than are required when the stress ratio is positive.

A2.4.2 The specimen shall be accurately located in the loading fixture and secured as required so that the boundary conditions correspond to the applicable K calibration. Fatigue cycling is then begun, usually with a sinusoidal waveform and near to the highest practical frequency. There is no known marked frequency effect on fatigue precrack formation up to at least 100 Hz in the absence of adverse environments. The specimen should be carefully monitored until crack initiation is observed on one side. If crack initiation is not observed on the other side before appreciable growth is observed on the first, then fatigue cycling should be stopped to try to determine the cause and remedy for the unsymmetrical behavior. Sometimes, simply turning the specimen around in relation to the fixture will solve the problem. When the most advanced crack trace has almost reached the first scribed line corresponding to 97.5 % of the final crack length, the maximum load or displacement, as appropriate, shall be reduced so that the terminal value of K_{\max} is unlikely to exceed 60 % of the estimated minimum value of K_{Ic} of the material, and also the terminal value of K_{\max}/E will not exceed $0.002\text{ in.}^{1/2}$ ($0.0032\text{ m}^{1/2}$). The minimum setting is then adjusted so that the stress ratio is between -1 and $+0.1$. Fatigue cycling is then continued until the surface traces on both sides of the specimen indicate that the overall length of notch plus crack will meet the requirements of 7.3.2.1, 7.3.2.2, and Fig. 7 of this test method.

A2.4.4 When fatigue cracking is conducted at a temperature T_1 and testing at a different temperature T_2 , K_{\max} must not exceed $0.6(\sigma_{YS1}/\sigma_{YS2})K_Q$, where σ_{YS1} and σ_{YS2} are the yield strengths at the respective temperatures T_1 and T_2 .

A3. SPECIAL REQUIREMENTS FOR THE TESTING OF BEND SPECIMENS

A3.1 Specimen

A3.1.1 The standard bend specimen is a single edge-notched and fatigue cracked beam loaded in three-point bending with a support span, S , nominally equal to four times the width, W . The general proportions of this specimen configuration are shown in Fig. A3.1.

A3.1.2 Alternative specimens may have $1 \leq W/B \leq 4$. These specimens shall also have a nominal support span equal to $4W$.

A3.2 Specimen Preparation

A3.2.1 For generally applicable specifications concerning specimen size and preparation see Section 7.

A3.2.2 It is desirable to fatigue crack the bend specimen in the same fixtures in which it will be tested so that the K calibration is accurately known. However, bend specimens are sometimes cracked in cantilever bending because this method permits ease of reversed loading. If the K calibration for three-point bending is used in cantilever bending, the bending moments for a given K value will be underestimated (7). While fatigue cracking in cantilever bending can yield satisfactory results, it should be emphasized that the crack tip stress field can be distorted and the fatigue crack orientation changed by excessive clamping forces.

A3.3 Apparatus

A3.3.1 *Bend Test Fixture*—The general principles of the bend test fixture are illustrated in Fig. A3.2. This fixture is designed to minimize frictional effects by allowing the support rollers to rotate and move apart slightly as the specimen is loaded, thus permitting rolling contact. Thus, the support rollers are allowed limited motion along plane surfaces parallel to the notched side of the specimen, but are initially positively positioned against stops that set the span length and are held in place by low-tension springs (such as rubber bands).

A3.3.2 *Displacement Gage*—For generally applicable details concerning the displacement gage see 6.3. For the bend specimen the displacements will be essentially independent of the gage length up to a gage length of $W/2$.

A3.4 Procedure

A3.4.1 *Measurement*—For a bend specimen measure the

width (depth), W , and the crack length, a , from the notched side of the specimen to the opposite side and to the crack front, respectively.

A3.4.1.1 For general requirements concerning specimen measurement see 8.2.

A3.4.2 *Bend Specimen Testing*—Set up the test fixture so that the line of action of the applied load shall pass midway between the support roll centers within 1 % of the distance between these centers (for example, within 0.04 in. (1.0 mm) for a 4-in. (100-mm) span). Measure the span to within 0.5 % of nominal length. Locate the specimen with the crack tip midway between the rolls to within 1 % of the span, and square to the roll axes within 2°. Seat the displacement gage on the knife edges to maintain registry between knife edges and gage grooves. In the case of attachable knife edges, seat the gage before the knife edge positioning screws are tightened.

A3.4.2.1 Load the specimen at a rate such that the rate of increase of stress intensity is within the range 30 to 150 ksi·in.^{1/2}/min (0.55 to 2.75 MPa·m^{1/2}/s), corresponding to a loading rate for the standard ($B = 0.5W$) 1-in. (25.4-mm) thick specimen between 4000 and 20 000 lbf/min (0.30 to 1.5 kN/s).

A3.4.3 For details concerning recording of the test record see 8.4.

A3.5 Calculations

A3.5.1 *Interpretation of Test Record*—For general requirements and procedures in interpretation of the test record see 9.1.

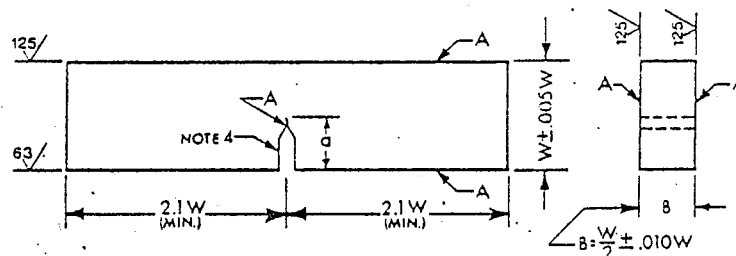
A3.5.2 *Validity Requirements*—For a description of the validity requirements in terms of limitations on P_{max}/P_Q and the specimen size requirements, see 9.1.2 through 9.1.3.

A3.5.3 *Calculation of K_Q* —For the bend specimen calculate K_Q in units of ksi·in.^{1/2} (MPa·m^{1/2}) as follows (Note A3.1):

$$K_Q = (P_Q S / BW^{3/2}) \cdot f(a/W)$$

where:

$$f(a/W) = \frac{3(a/W)^{1/2} [1.99 - (a/W)(1 - a/W) \times (2.15 - 3.93a/W + 2.7a^2/W^2)]}{2(1 + 2a/W)(1 - a/W)^{3/2}}$$



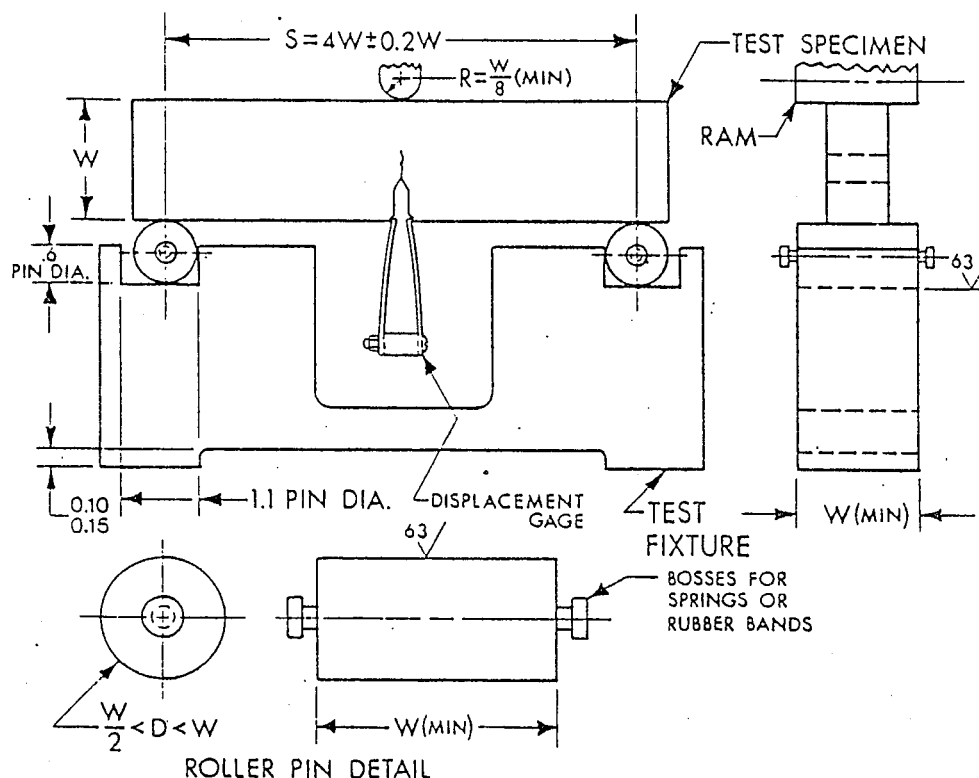
NOTE 1—A surfaces shall be perpendicular and parallel as applicable within 0.001 W TIR.

NOTE 2—Crack starter notch shall be perpendicular to specimen surfaces to within $\pm 2^\circ$.

NOTE 3—Integral or attachable knife edges for clip gage attachment may be used (see Figs. 5 and 6).

NOTE 4—For starter notch and fatigue crack configurations see Fig. 7.

FIG. A3.1 Bend Specimen SE (B)—Standard Proportions and Tolerances



NOTE 1—Roller pins and specimen contact surface of loading ram must be parallel to each other within 0.002 W .
NOTE 2—0.10 in. = 2.54 mm, 0.15 in. = 3.81 mm.

FIG. A3.2 Bend Test Fixture Design

where:

P_Q = load as determined in 9.1.1, klf (kN),
 B = specimen thickness as determined in 8.2.1, in. (cm),
 S = span as determined in A3.4.2, in. (cm),
 W = specimen depth (width) as determined in A3.4.1, in. (cm), and
 a = crack length as determined in 8.2.2, in. (cm).

To facilitate calculation of K_Q , values of $f(a/W)$ are tabulated in the following table for specific values of a/W .

Bend Specimens			
a/W	$f(a/W)$	a/W	$f(a/W)$
0.450	2.29	0.500	2.66
0.455	2.32	0.505	2.70
0.460	2.35	0.510	2.75
0.465	2.39	0.515	2.79
0.470	2.43	0.520	2.84
0.475	2.46	0.525	2.89
0.480	2.50	0.530	2.94
0.485	2.54	0.535	2.99
0.490	2.58	0.540	3.04
0.495	2.62	0.545	3.09
		0.550	3.14

NOTE A3.1—The expression in A3.5.3 is considered to be accurate within $\pm 0.5\%$ over the entire range of a/W from 0 to 1 for an $S/W = 4$ (12).

A3.5.4 Calculation of R_{sb} —For the bend specimen calculate the specimen strength ratio (which is dimensionless and has the same value in any consistent system of units):

$$R_{sb} = \frac{6P_{\max}W}{B(W-a)^2\sigma_{YS}}$$

where:

P_{\max} = maximum load that the specimen was able to sustain,
 B = thickness of specimen as determined in 8.2.1,
 W = width (depth) of specimen, as determined in A3.4.1,
 a = crack length as determined in 8.2.2, and
 σ_{YS} = yield strength in tension (offset = 0.2 %) (see Methods E 8).

A4. SPECIAL REQUIREMENTS FOR THE TESTING OF COMPACT SPECIMENS

A4.1 Specimen

A4.1.1 The standard compact specimen is a single edge-notched and fatigue cracked plate loaded in tension. The general proportions of this specimen configuration are shown in Fig. A4.1.

A4.1.2 Alternative specimens may have $2 \leq W/B \leq 4$ but with no change in other proportions.

A4.2 Specimen Preparation

A4.2.1 For generally applicable specifications concerning



U

FIG. A4.1 Compact Specimen: C (T) Standard Proportions and Tolerances

specimen size and preparation see Section 7.

A4.3 Apparatus

A4.3.1 Tension Testing Clevis—A loading clevis suitable for testing compact specimens is shown in Fig. A4.2. Both ends of the specimen are held in such a clevis and loaded through pins, in order to allow rotation of the specimen during testing. In order to provide rolling contact between the loading pins and the clevis holes, these holes are provided with small flats on the loading surfaces (4). Other clevis designs may be used if it can be demonstrated that they will accomplish the same result as the design shown.

A4.3.1.1 The critical tolerances and suggested proportions of the clevis and pins are given in Fig. A4.2. These proportions are based on specimens having $W/B = 2$ for $B > 0.5$ in. (12.7 mm) and $W/B = 4$ for $B \leq 0.5$ in. (12.7 mm). If a 280 000-psi (1930-MPa) yield strength maraging steel is used for the clevis and pins, adequate strength will be obtained for testing the specimen sizes and σ_{YS}/E ratios given in 7.1.3. If lower-strength grip material is used, or if substantially larger specimens are required at a given σ_{YS}/E ratio than those shown in 7.1.3, then heavier grips will be required. As indicated in Fig. A4.2 the clevis corners may be cut off sufficiently to accommodate seating of the clip gage in specimens less than 0.375 in. (9.5 mm) thick.

A4.3.1.2 Careful attention should be given to achieving as good alignment as possible through careful machining of all auxiliary gripping fixtures.

A4.3.2 *Displacement Gage*—For generally applicable details concerning the displacement gage see 6.3. For the compact specimen the displacements will be essentially independent of the gage length up to 1.2 W .

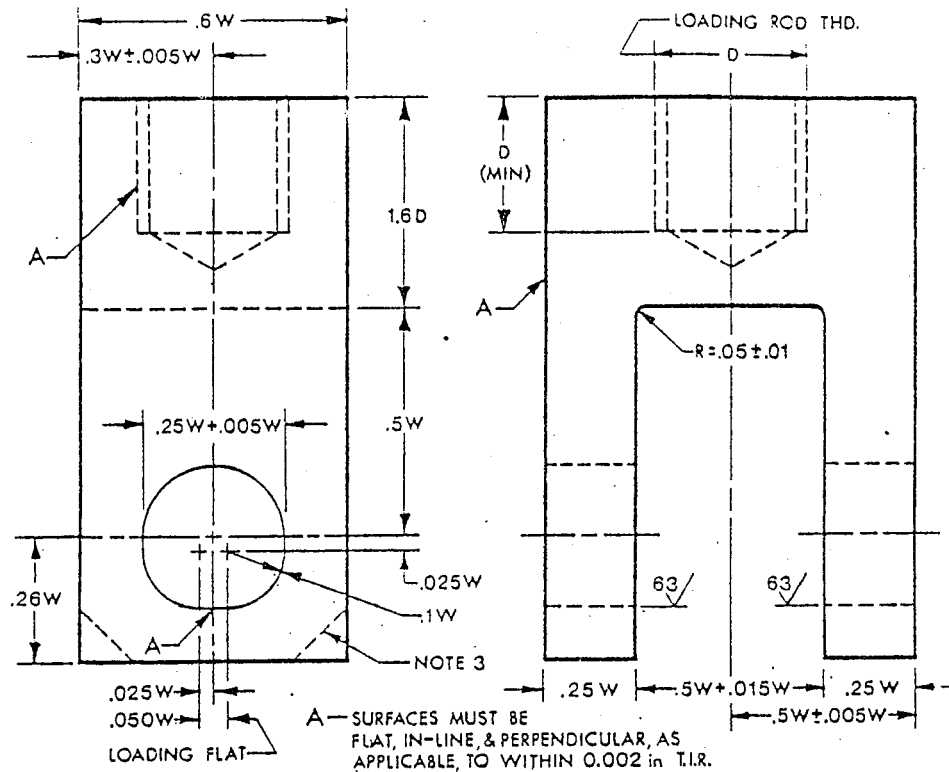
A4.4 Procedure

A4.4.1 *Measurement*—For a compact specimen measure the width, W , and the crack length, a , from the plane of the centerline of the loading holes (the notched edge is a convenient reference line but the distance from the centerline of the holes to the notched edge must be subtracted to determine W and a). Measure the width, W , to the nearest 0.001 in. (0.025 mm) or 0.1 %, whichever is larger, at not less than three positions near the notch location, and record the average value.

A4.4.1.1 For general requirements concerning specimen measurement see 8.2.

A4.4.2 Compact Specimen Testing—When assembling the loading train (clevises and their attachments to the tensile machine) care should be taken to minimize eccentricity of loading due to misalignments external to the clevises. To obtain satisfactory alignment keep the centerline of the upper and lower loading rods coincident within 0.03 in. (0.76 mm) during the test and center the specimen with respect to the clevis opening within 0.03 in. (0.76 mm).

A4.4.2.1 Load the compact specimen at such a rate that the rate of increase of stress intensity is within the range 30 to 150 ksi·in.^{1/2}/min (0.55 to 2.75 MPa·m^{1/2}/s) corresponding to a loading rate for a standard ($W/B = 2$) 1-in. thick



NOTE 1—Pin diameter = $0.24 W (+0.000 W/-0.005 W)$. For specimens with $\sigma_{YS} > 200$ ksi (1379 MPa) the holes in the specimen and in the clevis may be $0.3 W (+0.005 W/-0.000 W)$ and the pin diameter $0.288 W (+0.000 W/-0.005 W)$.

NOTE 2— 0.002 in. = 0.051 mm.

NOTE 3—Corners of the clevis may be removed if necessary to accommodate the clip gage.

FIG. A4.2 Tension Testing Clevis Design

specimen 4500 and 22 500 lbf/min (0.34 to 1.7 kN/s).

A4.4.2.2 For details concerning recording of the test record see 8.4.

A4.5 Calculations

A4.5.1 For general requirements and procedures in interpretation of the test record see 9.1.

A4.5.2 For a description of the validity requirements in terms of limitations on P_{max}/P_Q and the specimen size requirements see 9.1.2 through 9.1.3.

A4.5.3 Calculation of K_Q —For the compact specimen calculate K_Q in units of $\text{ksi} \cdot \text{in.}^{1/2}$ ($\text{MPa} \cdot \text{m}^{1/2}$) from the following expression (Note A4.1)

$$K_Q = (P_Q/BW^{1/2}) \cdot f(a/W)$$

where:

$$f(a/W) = \frac{(2 + a/W)(0.886 + 4.64a/W - 13.32a^2/W^2 + 14.762a^3/W^3 - 5.6a^4/W^4)}{(1 - a/W)^{3/2}}$$

where:

P_Q = load as determined in 9.1.1, klf (kN),
 B = specimen thickness as determined in 8.2.1, in. (cm),
 W = specimen width, as determined in A4.4.1, in. (cm), and
 a = crack length as determined in 8.2.2 and A4.4.1, in. (cm).

To facilitate calculation of K_Q , values of $f(a/W)$ are tabulated below for specific values of a/W .

Compact Specimens			
a/W	$f(a/W)$	a/W	$f(a/W)$
0.450	8.34	0.500	9.66
0.455	8.46	0.505	9.81
0.460	8.58	0.510	9.96
0.465	8.70	0.515	10.12
0.470	8.83	0.520	10.29
0.475	8.96	0.525	10.45
0.480	9.09	0.530	10.63
0.485	9.23	0.535	10.80
0.490	9.37	0.540	10.98
0.495	9.51	0.545	11.17
		0.550	11.36

NOTE A4.1—The expression in A4.5.3 is considered to be accurate within $\pm 0.5\%$ over the range of a/W from 0.2 to 1 (12) (13).

4.5.4 Calculation of R_{sc} —For the compact specimen calculate the specimen strength ratio (which is dimensionless and has the same value in any consistent system of units):

$$R_{sc} = \frac{2P_{max}(2W + a)}{B(W - a)^2 \sigma_{YS}}$$

where:

P_{max} = maximum load that the specimen was able to sustain,
 B = thickness of specimen as determined in 8.2.1,
 W = width of the specimen as determined in A4.4.1,
 a = crack length as determined in 8.2.2 and A4.4.1, and
 σ_{YS} = yield strength in tension (offset = 0.2 %) (see Methods E 8).

A5. SPECIAL REQUIREMENTS FOR THE TESTING OF THE ARC-SHAPED SPECIMEN

A5.1 Specimen

A5.1.1 The arc-shaped specimen is a single edge-notched and fatigue cracked ring segment loaded in tension. The general proportions of two designs of the standard arc-shaped specimen are shown in Fig. A5.1. The value of the radius ratio r_1/r_2 is not specified, so that specimens can be taken from any cylindrical geometry. However, it should be noted that specimens with $r_1/r_2 = 0$ (that is, from a solid cylinder) do not make the best possible use of the test material because the definition of W was chosen to accommodate hollow cylinders. The disk-shaped specimen should be used for tests on solid cylinders (see Annex A6).

A5.1.2 The arc-shaped specimen is intended to measure the fracture toughness so that the normal to the crack plane is in the circumferential direction and the direction of crack propagation is in the radial direction. This is the $C-R$ orientation as defined in 5.1.3. For other orientations, a bend (Annex A3) or a compact (Annex A4) specimen should be used.

A5.1.3 The arc-shaped specimen with $X/W = 0.5$ (Fig. A5.1a) represents a half ring segment. The specimen with $X/W = 0$ (Fig. A5.1b) represents the smallest specimen of this configuration that can be cut from a ring.

A5.1.4 Alternative specimens may have $2 \leq W/B \leq 4$ but with no change in other proportions. The use of alternative specimen proportions for the arc-shaped specimen can be advantageous because in many cases it is possible to test ring segments with no machining of the inner and outer radii, that is, with no change in W .

A5.2 Specimen Preparation

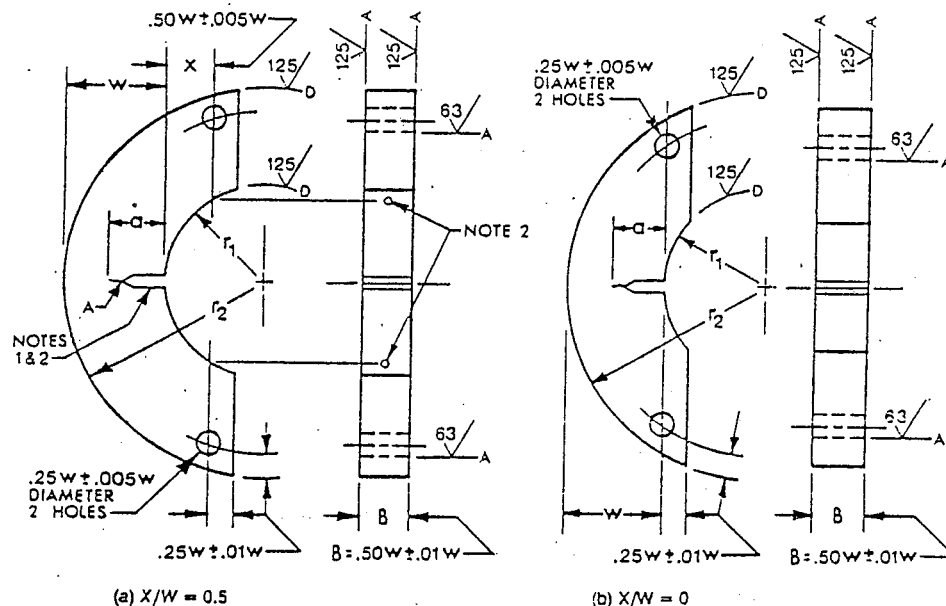
A5.2.1 For generally applicable specifications concerning specimen size and preparation see Section 7.

A5.3 Apparatus

A5.3.1 *Tension Testing Clevis*—A loading clevis suitable for testing arc-shaped specimens is shown in Fig. A5.2. Both ends of the specimen are held in such a clevis and loaded through pins, in order to allow rotation of the specimen during testing. In order to provide rolling contact between the loading pins and the clevis holes, these holes are provided with small flats on the loading surface (4). Other clevis designs may be used if it can be demonstrated that they will accomplish the same result as the design shown.

A5.3.1.1 The critical tolerances and suggested proportions of the clevis and pins are given in A5.2. These proportions are based on specimens having $W/B = 2$ for $B > 0.5$ in. (12.7 mm) and $W/B = 4$ for $B \leq 0.5$ in. (12.7 mm). If a 280 000-psi (1930-MPa) yield strength maraging steel is used for the clevis and pins, adequate strength will be obtained for testing the specimen sizes and σ_{YS}/E ratios given in 7.1.3. If lower-strength grip material is used, or if substantially larger specimens are required at a given σ_{YS}/E ratio than those shown in 7.1.3, then heavier grips will be required. As indicated in Fig. A5.2, the clevis corners may be cut off sufficiently to accommodate seating of the clip gage in specimens less than 0.375 in. (9.5 mm) thick.

A5.3.1.2 Careful attention should be given to achieving as



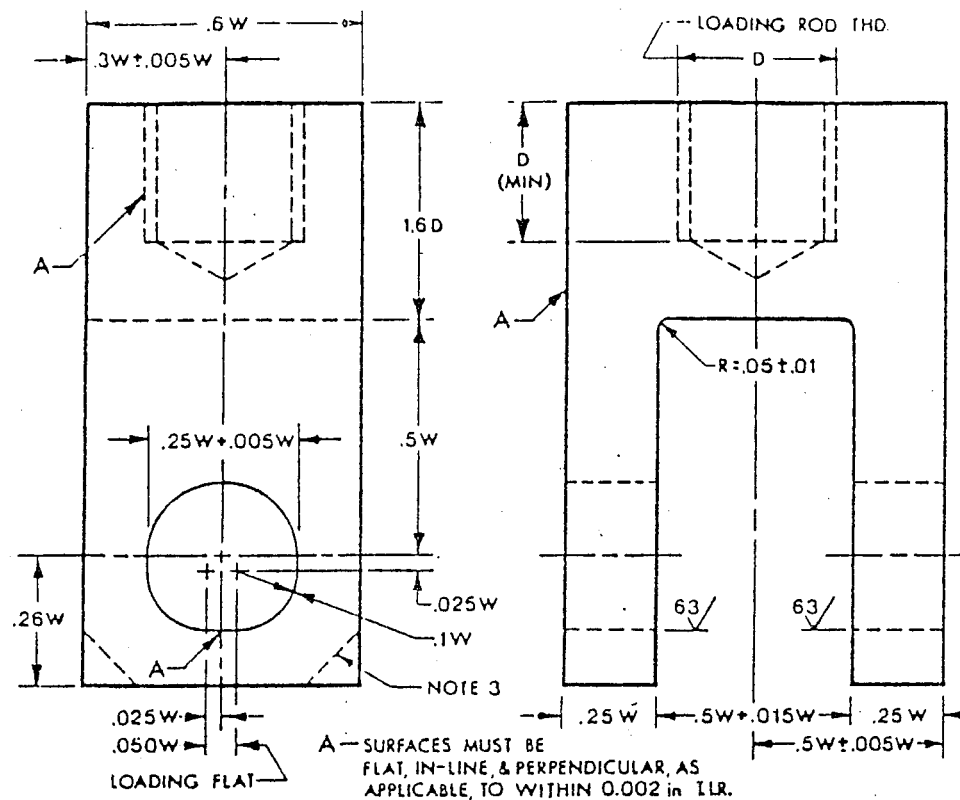
NOTE 1—For starter notch and fatigue crack configurations see Fig. 7.

NOTE 2—Alternative displacement gage reference points (see A5.4.1.1 for calculation of (a)).

NOTE 3—Axis of holes to be tangent to inner radius within 0.005W.

NOTE 4—A surfaces to be perpendicular and parallel as applicable to within 0.002 W TIR; D surfaces to be perpendicular or parallel as applicable to A surfaces to within 0.02 W TIR (see A5.4.1).

FIG. A5.1 Arc-Shaped Specimen Designs A (T) Standard Proportions and Tolerances.



NOTE 1—Pin diameter = $0.24 W (+0.000 W/-0.005 W)$. For specimens with $\sigma_{YS} > 200$ ksi (1379 MPa) the holes in the specimen and in the clevis may be $0.3 W (+0.005 W/-0.000 W)$ and the pin diameter $0.288 W (+0.000 W/-0.005 W)$.

NOTE 2— 0.002 in. = 0.051 mm.

NOTE 3—Corners of the clevis may be removed if necessary to accommodate the clip gage.

FIG. A5.2 Tension Testing Clevis Design

good alignment as possible through careful machining of all auxiliary gripping fixtures.

A5.3.2 *Displacement Gage*—For generally applicable details concerning the displacement gage see 6.3.

A5.3.2.1 An alternative means of measuring the displacement is allowed for the arc-shaped specimen with $X/W = 0.5$. Conical center-punch-type indentations are provided on the inner surface of the C-shaped specimen at mid-thickness and in the plane of the center line of the loading holes as shown in Fig. A5.1a. The load-point displacement of the specimen is measured at these points using a displacement gage fitted with points and meeting the requirements described in 6.4.1.

A5.3.2.2 The displacements will be essentially independent of the gage length for the arc-shaped specimen provided the gage length is equal to or less than $W/2$.

A5.4 Procedure

A5.4.1 *Measurement*—Before testing an arc-shaped specimen, measure $(r_1 - r_2)$ to the nearest 0.001 in. (0.025 mm) or to 0.1% , whichever is greater at mid-thickness positions on both sides of and immediately adjacent to the crack starter notch mouth. Record the average of these two readings as W . Also measure $(r_1 - r_2)$ at four positions, two as close as possible to the loading holes and two at approximately one-half the circumferential distance between the

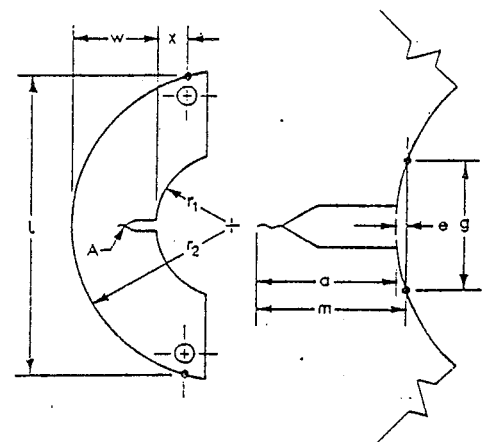


FIG. A5.3 Measurement of Outer Radius (r_2) and Crack Length for the Arc-Shaped Specimen (see A5.4.1)

loading holes and the crack plane. If any of these four measurements differ from W by more than 10% , the specimen should be discarded or reworked. Next, measure to the nearest 0.001 in. (0.025 mm) or to 0.1% , whichever is greater, the distance between the loading hole centers and the outside surface of the specimen at the notch plane. This

measurement should be made on both sides of the specimen by referencing the loading holes. Subtract W from the average of these two measurements and record the result as X . Measure within 5 % the outer radius, r_2 ; if this is not possible, determine the average value of r_2 as follows (see Note A5.1): Measure within 5 % the length, L , of the cord of the outer surface, which cord passes through the loading hole centers (see Fig. A5.3). Using this measurement, calculate:

$$r_2 = \frac{L^2}{8(W+X)} + \frac{(W+X)}{2}$$

Then $r_1/r_2 = 1 - W/r_2$.

NOTE A5.1—A 10 % variation of the ratio r_1/r_2 will affect the value of the stress intensity factor by 1 % or less, providing that the relative crack length a/W is not less than 0.3. However, the stress analysis is based on the assumption that the specimens are to be cut from stock of uniform, axisymmetric cross section. If inspection shows that the stock deviates from axisymmetry by more than 10 %, it should be reworked to within this tolerance.

A5.4.1.1 After fracture, measure the crack length in accordance with 8.2.2, but a special procedure is necessary for the arc-shaped specimen due to its curvature. Thus, a length measurement, m , made from a reference point adjacent to the crack mouth to a point on the crack front will be greater than the corresponding distance from the virtual point of intersection between the crack plane and the inside circumference of the specimen (see Fig. A5.3). The error, e , may be computed from the following expression:

$$e = r_1 - \left[r_1^2 - \frac{g^2}{4} \right]^{1/2}$$

where g is the distance across the crack mouth at the reference points for measurement of the crack length. It should be noted that g may be equal to N (Fig. 7) or larger than N if machined knife edges are used to hold the clip gage (for example, $g = 0.25$ in. (2.5 mm) as in Fig. 5). If the relative error $e/m < 0.01$, then record m as the crack length; otherwise e should be subtracted from m and the result recorded as the crack length.

A5.4.2 *Arc-Shaped Specimen Testing*—When assembling the loading train (clevises and their attachments to the tension machine) care should be taken to minimize eccentricity of loading due to misalignments external to the clevises. To obtain satisfactory alignment keep the centerline of the upper and lower loading rods coincident within 0.03 in. (0.76 mm) during the test and center the specimen with respect to the clevis opening within 0.03 in. (0.76 mm).

A5.4.2.1 Load the arc-shaped specimen at such a rate that the rate of increase of stress intensity is within the range 30 to 150 ksi·in.^{1/2}/min (0.55 to 2.75 MPa·m^{1/2}/s). The corresponding loading rates for a standard ($W/B = 2$) 1-in. thick specimen are: (1) for the specimen with an $X/W = 0.5$ between 2800 and 14 000 lbf/min (0.2 to 1.0 kN/s) and (2) for the specimen with an $X/W = 0$ between 4500 and 22 500 lbf/min (0.34 to 1.7 kN/s).

A5.4.2.2 For details concerning recording of the test record see 8.4.

A5.5 Calculations

A5.5.1 For general requirements and procedures in interpretation of the test record see 9.1.

A5.5.2 For a description of the validity requirements in terms of limitations on P_{\max}/P_Q and the specimen size requirements see 9.1.2 through 9.1.3.

A5.5.3 *Calculation of K_Q* —For the arc-shaped specimen calculate K_Q in units of ksi·in.^{1/2} (MPa·m^{1/2}) from the following expression (Note A5.2):

$$K_Q = (P_Q/BW^{1/2})[3X/W + 1.9 + 1.1a/W] \times [1 + 0.25(1 - a/W)^2(1 - r_1/r_2)]f(a/W) \quad (11)$$

where:

$$f(a/W) = [(a/W)^{1/2}/(1 - a/W)^{3/2}] \times [3.74 - 6.30a/W + 6.32(a/W)^2 - 2.43(a/W)^3]$$

where:

P_Q = load as determined in 9.1.1, klf (kN),
 B = specimen thickness as determined in 8.2.1, in. (cm),
 X = loading hole offset as determined in A5.4.1, in. (cm),
 W = specimen width as determined in A5.4.1, in. (cm),
 a = crack length as determined in 8.2.2 and A5.4.1.1, in. (cm), and

r_1/r_2 = ratio of inner to outer radii as determined in A5.4.1.

To facilitate calculation of K_Q , values of $f(a/W)$ are tabulated in the following table for specific values of a/W :

a/W	$f(a/W)$	a/W	$f(a/W)$
0.450	3.23	0.500	3.73
0.455	3.27	0.505	3.79
0.460	3.32	0.510	3.85
0.465	3.37	0.515	3.91
0.470	3.42	0.520	3.97
0.475	3.47	0.525	4.03
0.480	3.52	0.530	4.10
0.485	3.57	0.535	4.17
0.490	3.62	0.540	4.24
0.495	3.68	0.545	4.31
...	...	0.550	4.38

NOTE A5.2—The accuracy of the expression in A5.5.3 for all values of r_1/r_2 is considered to be as follows: (1) ± 1 % for $0.45 \leq a/W \leq 0.55$ and X/W of 0 or 0.5, (2) ± 1.5 % for $0.2 \leq a/W \leq 1$ and X/W of 0 or 0.5, and (3) ± 3 % for $0.2 \leq a/W \leq 1$ and $0 \leq X/W \leq 1$ (14).

A5.5.4 *Calculation of R_{sa}* —For the arc-shaped specimen calculate the specimen strength ratio (which is dimensionless and has the same value in any consistent system of units) as follows:

$$R_{sa} = \frac{2P_{\max}(3X + 2W + a)}{B(W - a)2\sigma_{YS}}$$

where:

P_{\max} = maximum load that the specimen was able to sustain,
 B = thickness of the specimen as determined in 8.2.1,
 X = loading hole offset as determined in A5.4.1,
 W = width of the specimen as determined in A5.4.1,
 a = crack length as determined in 8.2.2 and A5.4.1.1, and
 σ_{YS} = yield strength in tension (offset = 0.2 %) (see Methods E 8).

A6. SPECIAL REQUIREMENTS FOR THE TESTING OF THE DISK-SHAPED COMPACT SPECIMEN

A6.1 Specimen

A6.1.1 The standard disk-shaped compact specimen is a single edge-notched and fatigue cracked disk segment loaded in tension (16). The general proportions of this specimen configuration are shown in Fig. A6.1.

A6.1.2 Alternative specimens may have $2 < W/B < 4$ but with no change in other proportions.

A6.2 Specimen Preparation

A6.2.1 For generally applicable specifications concerning specimen size and preparation see Section 7.

A6.3 Apparatus

A6.3.1 *Tension Testing Clevis*—A loading clevis suitable for testing disk-shaped compact specimens is shown in Fig. A6.2. Both ends of the specimen are held in such a clevis and loaded through pins in order to allow rotation of the specimen during testing. In order to provide rolling contact between the loading pins and clevis holes, these holes are provided with small flats on the loading surfaces (4). Other clevis designs may be used if it can be demonstrated that they will accomplish the same result as the design shown.

A6.3.1.1 The critical tolerances and suggested proportions of the clevis and pins are given in Fig. A6.2. These proportions are based on specimens having $W/B = 2$ for $B > 0.5$ in. (12.7 mm) and $W/B = 4$ for $B \leq 0.5$ in. (12.7 mm). If a 280 000-psi (1930-MPa) yield strength maraging steel is used for the clevis and pins, adequate strength will be

obtained for testing the specimen sizes and σ_{YS}/E ratios given in 7.1.3. If lower-strength grip material is used, or if substantially larger specimens are required at a given σ_{YS}/E ratio than those shown in 7.1.3, then heavier grips will be required. As indicated in Fig. A6.2 the clevis corners may be cut off sufficiently to accommodate seating of the clip gage in specimens less than 0.375 in. (9.5 mm) thick.

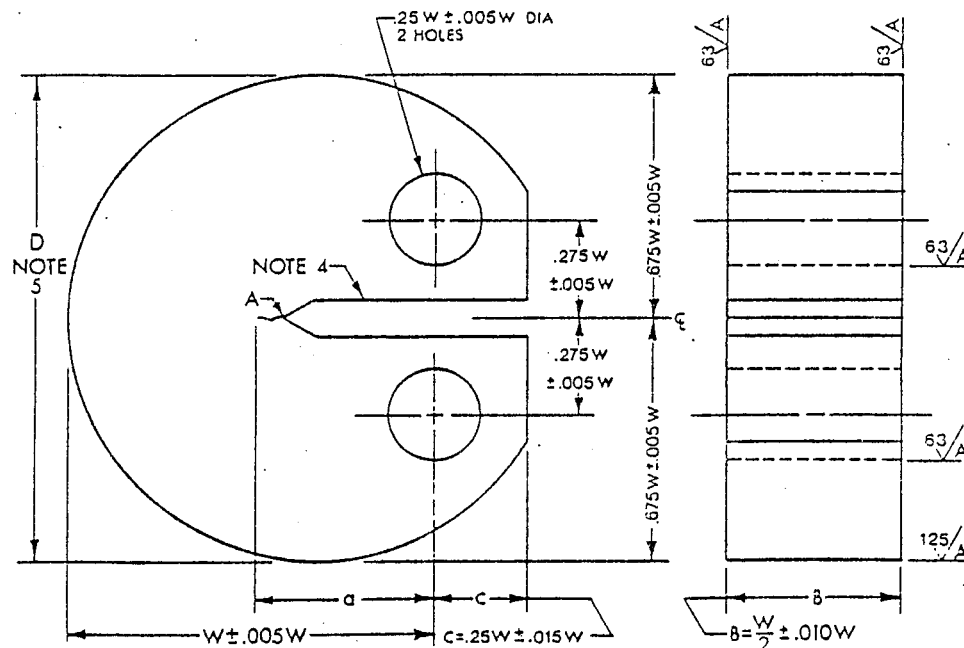
A6.3.1.2 Careful attention should be given to achieving as good alignment as possible through careful machining of all auxiliary gripping fixtures.

A6.3.2 *Displacement Gage*—For generally applicable details concerning the displacement gage see 6.3. For the disk-shaped compact specimen the displacements will be essentially independent of the gage length up to $0.55 W$.

A6.4 Procedure

A6.4.1 *Measurement*—The analysis assumes the specimen was machined from a circular blank and therefore measurements of circularity as well as width, W , and crack length, a , must be made for this specimen.

A6.4.1.1 The specimen blank should be checked for circularity before specimen machining. Measure the radius at eight equally spaced points around the circumference of the specimen blank. One of these points should lie in the intended notch plane. Average these readings to obtain the radius, r . If any measurement differs from r by more than 5 %, machine the blank to the required circularity. Otherwise, $D = 2r = 1.35 W$.



NOTE 1—A surfaces shall be perpendicular and parallel as applicable to within 0.002 W TIR.

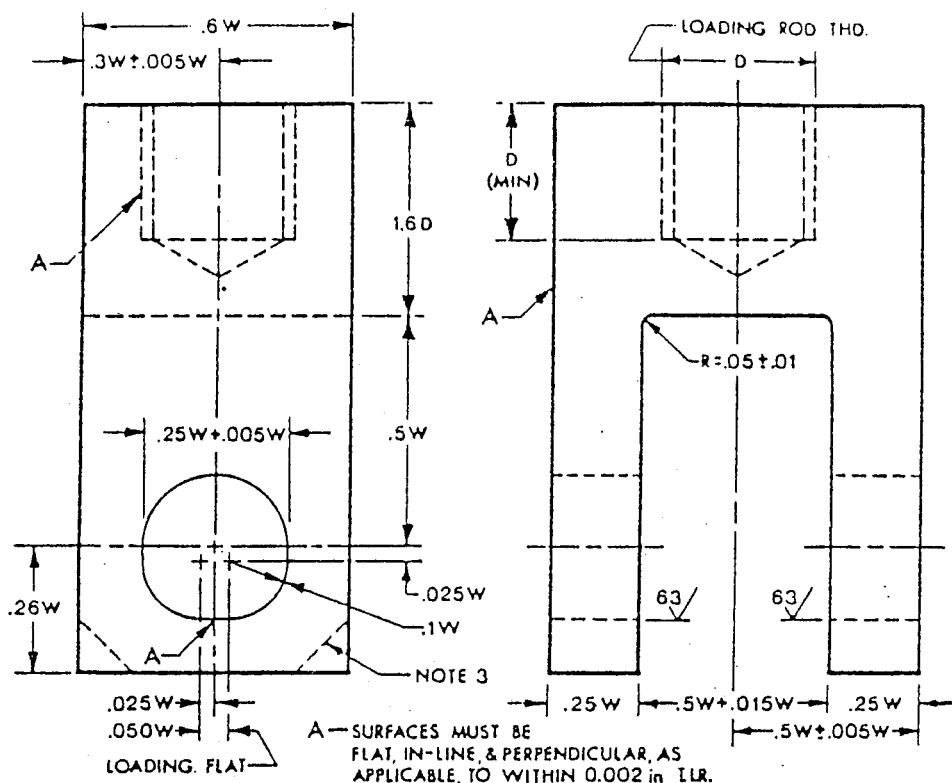
NOTE 2—The intersection of the crack starter notch tips on each surface of the specimen shall be equally distant within 0.005 W from the centerline of the loading holes.

NOTE 3—Integral or attachable knife edges for clip gage attachment to the crack mouth may be used (see Figs. 5 and 6).

NOTE 4—For starter notch and fatigue crack configuration see Fig. 7.

NOTE 5—For circularity requirements, see A6.4.1.1.

FIG. A6.1 Disk-Shaped Compact Specimen DC(T) Standard Proportions and Tolerances



NOTE 2—0.002 in. = 0.051 mm.

FIG. A6.2 Tension Testing Cl

FIG. A6.2 Tension Testing Clevis Design

A6.4.1.2 Measure the width, W , and the crack length, a , from the plane of the centerline of the loading holes (the notched edge is a convenient reference line but the distance from the centerline of the holes to the notched edge must be subtracted to determine W and a). Measure the depth, W , to the nearest 0.001 in. (0.025 mm) or 0.1 %, whichever is larger, at not less than three positions near the notch location, and record the average value.

A6.4.1.3 For general requirements concerning specimen measurement see 8.2.

A6.4.2 Disk-Shaped Compact Specimen Testing—When assembling the loading train (clevises and their attachments to the tension machine) care should be taken to minimize eccentricity of loading due to misalignments external to the clevises. To obtain satisfactory alignment keep the centerline of the upper and lower loading rods coincident within 0.03 in. (0.76 mm) during the test and center the specimen with respect to the clevis opening within 0.03 in. (0.76 mm).

A6.4.2.1 Load the disk-shaped compact specimen at such a rate that the rate of increase of stress intensity is within the range 30 to 150 ksi·in.^{1/2}/min (0.55 to 2.75 MPa·m^{1/2}/s), corresponding to a loading rate for a standard ($W/B = 2$) 1-in. thick specimen of 4500 and 22 500 lbf (0.34 to 1.7 kN/s), respectively.

A6.4.2.2 For details concerning recording of the test record see 8.4.

A6.5 Calculations

A6.5.1 For general requirements and procedures in interpretation of the test record see 9.1.

A6.5.2 For a description of validity requirements in terms of limitations on P_{\max}/P_Q and the specimen size requirements see 9.1.2 and 9.1.3.

A6.5.3 Calculation of K_Q —For the disk-shaped compact specimen calculate K_Q in units of ksi·in.^{1/2} (MPa·m^{1/2}) from the following expression (Note A6.1):

$$K_0 = (P_0/BW^{1/2})f(a/W)$$

where:

$$f(a/W) = \frac{(2 + a/W)(0.76 + 4.8a/W - 11.58(a/W)^2 + 11.43(a/W)^3 - 4.08(a/W)^4)}{(1 - a/W)^{3/2}}$$

where:

P_0 = load as determined in 9.1.1, klf (kN),

B = specimen thickness as determined in 8.2.1, in. (cm),

W = specimen width as determined in A6.4.1.2, in. (cm),
and

a = crack length as determined in 8.2.2 and A6.4.1.2, in.
(cm).

To facilitate calculation of K_Q , values of $f(a/W)$ are tabulated in the following table for specific values of a/W :

a/W	$f(a/W)$	a/W	$f(a/W)$
0.450	3.71	0.500	10.17
0.455	3.84	0.505	10.34
0.460	3.97	0.510	10.51
0.465	9.11	0.515	10.68
0.470	9.25	0.520	10.86
0.475	9.40	0.525	11.05
0.480	9.55	0.530	11.24
0.485	9.70	0.535	11.43
0.490	9.85	0.540	11.63
0.495	10.01	0.545	11.83
		0.550	12.04

NOTE A6.1—The expression in A6.5.3 is considered accurate to within $\pm 0.3\%$ over the range of a/W from 0.2 to 1.0 (19).

A6.5.4 Calculation of R_{sd} —For the disk-shaped compact

specimen calculate the specimen strength ratio (which is dimensionless and has the same value in any consistent set of units) as follows:

$$R_{sd} = \frac{2P_{\max}(2W + a)}{B(W - a)^2\sigma_{YS}}$$

where:

P_{\max} = maximum load that the specimen was able to sustain,
 B = thickness of the specimen as determined in 8.2.1,
 W = specimen width as determined in A6.4.1.2,
 a = crack length as determined in 8.2.2 and A6.4.1.2, and
 σ_{YS} = yield strength in tension (offset = 0.2 %) (see Methods E 8).

A7. SPECIAL REQUIREMENTS FOR RAPID-LOAD PLANE-STRAIN FRACTURE TOUGHNESS $K_{Ic}^{(r)}$ TESTING

A7.1 Scope

A7.1.1 This annex covers the determination of plane-strain fracture toughness (K_{Ic}) properties of metallic materials under conditions where the loading rates exceed those for conventional (static) testing [150 000 psi·in.^{1/2}/min (2.75 MPa·m^{1/2}/s)].

A7.2 Summary of Requirements

A7.2.1 Special requirements are necessary for plane-strain fracture toughness testing at loading rates exceeding those of conventional (static) plane-strain fracture toughness testing. This description of these requirements does not include impact or quasi-impact testing (free-falling or swinging masses). Conventional fracture toughness test specimens are prepared as described in this method, tested under rapid-load conditions, and a fracture toughness value is calculated. Load-deflection, load-time, and deflection-time curves are recorded for each test. The load-deflection curves resulting from these tests are analyzed to ensure that the initial linear portion of the load-displacement record is sufficiently well defined that P_Q can be determined unambiguously. In addition, a test time (t), restricted to not less than one ms is determined. This test time and an optionally calculated average stress intensity factor rate K characterize the rapid load test. The yield strength of the material must be determined or estimated for the loading time of the fracture test and is used in the analysis of the fracture test data. All of the criteria for static K_{Ic} determination apply to the rapid-load plane-strain fracture toughness test. The rapid-load plane-strain fracture toughness property is denoted by $K_{Ic}^{(r)}$ where the time to reach the load corresponding to K_Q in ms is indicated in the brackets ().

A7.3 Significance and Use

A7.3.1 The significance of the conventional (static) K_{Ic} properties applies also to the case of rapid loading. The plane-strain fracture toughness of certain materials is sensitive to the loading rate and substantial decreases in toughness may be noted as the loading rate increases. Generally, such materials also show a pronounced dependence of K_{Ic} on test temperature. For example, the loading rate sensitivity of structural grade steels has required the development of a lower bound K_{IR} curve, given in Appendix G of Division III of the ASME Boiler and Pressure Vessel Code, for the

fracture-safe design of heavy-wall nuclear pressure vessels. Additionally, K_{Ic} values for steels tested at various temperatures and loading rates are required for correlation with small-scale production control tests (such as the Charpy V-notch test) for setting material specifications and fracture-safe design procedures.

A7.4 Terminology

A7.4.1 Definitions:

A7.4.1.1 The definitions given in Terminology E 616 are applicable to this test method.

A7.4.1.2 *Stress-Intensity Factor*—See Section 5 of this test method.

A7.4.1.3 *Plane-Strain Fracture Toughness*—See Section 5 of this test method.

A7.4.1.4 *Rapid Load*—In fracture testing, any load that results in an average stress-intensity factor rate in excess of 150 000 psi·in.^{1/2}/min (2.75 MPa·m^{1/2}/s).

A7.4.1.5 *Stress-Intensity Factor Rate, K (FL^{-3/2} s⁻¹)*—In fracture testing, a change in stress-intensity factor, K , per unit time.

A7.4.1.6 *Crack-Plane Orientation*—See 5.1.3 of this test method.

A7.4.2 Description of Terms Specific to This Method:

A7.4.2.1 *Rapid-Load Plane-Strain Fracture Toughness: $K_{Ic}^{(r)}$ (FL^{-3/2})*—The crack extension resistance under conditions of crack-tip plane strain at average loading rates exceeding 150 000 psi·in.^{1/2}/min (2.75 MPa·m^{1/2}/s). The time, t , to reach P_Q in milliseconds is indicated in the brackets (t).

A7.5 Apparatus

A7.5.1 *Loading*—Generally, hydraulic machines with rapid-acting servo controlled valves are used. Depending on the compliance of the loading system and the pump capacity, an accumulator may be required.

A7.5.2 *Fixtures*—The fixtures used for static plane-strain fracture toughness tests are generally suitable for rapid-load tests. However, consideration should be given to the possibility that the toughness of the fixture material may be reduced by rapid loading.

A7.5.3 *Load and Displacement Transducers*—The transducers used for static plane-strain fracture toughness tests are generally suitable for rapid-load tests. However, these trans-

ducers must have response characteristics that will ensure that inertial effects will not contaminate the load and displacement signals.

NOTE A7.1—While not required, the resonant frequencies of these transducers may be determined by suitably exciting them and observing the wave characteristic on an oscilloscope. If ringing (high frequency oscillation) is observed within the time period required to reach the P_Q load, the stiffness of the transducers should be increased or their mass reduced. Load cells are quite stiff and should provide no problem at the minimum loading time of 1 ms. The displacement transducer might be cause for concern depending on its design. The cantilever beam displacement gage described in Annex A1 has been used successfully at loading times slightly lower than 1 ms (20). The resonant frequency of this gage when mounted in a specimen in a conventional manner and excited by tapping is about 3300 Hz. The free-arm resonant frequency is about 750 Hz. Other gages of the same type but having different dimensions should operate satisfactorily if their free arm resonance is at least 750 Hz. The following equation may be used to estimate the free-arm resonant frequency of such a gage:

$$f = 0.162 \left[\frac{b^3 E g}{\rho l^4} \right]^{1/2}$$

where:

f = resonant frequency in hertz,

b = arm thickness in inches,

E = elastic modulus of the arms in pound-force per square inch,

g = gravitational acceleration 386 in./s²,

ρ = density of the arm material in pounds per cubic inch, and

l = length of the uniform thickness section of the arms in inches.

The coefficient becomes 51.7 if SI units are used where b is in metres, E is in megapascals, g is 9.804 m/s², ρ is kilograms per cubic metres, and l is in metres.

A7.5.4 *Signal Conditioners*—Amplification or filtering of the transducer signals may be necessary. Such signal conditioning units should have a frequency response from dc to at least 20/ t (kHz) where t is the test time in milliseconds as defined in A7.7.3. As described in A7.6.2, conventional mechanical recording devices may not have sufficient frequency response to permit direct plotting of the load versus time and the displacement versus time signals.

A7.6 Procedure

A7.6.1 *Loading Rate*—The rate of loading is optional with the investigator but the time to reach the load corresponding to K_Q shall not be less than 1 ms. Use a preload to eliminate ringing in the load or displacement transducers associated with clearances in the load train being suddenly taken up by the start of rapid loading.

A7.6.2 For each test conducted, a load versus time, a displacement versus time, and a load versus displacement record shall be obtained. The time scale of these records shall be accurately determined since the time is used to characterize the test. Examine the time-dependent records for the presence of ringing before reaching the P_Q load. Such ringing can result from inertial effects as described in Note A7.1. The special record analysis procedure described in A7.7.3 may be helpful in assessing the magnitude of such effects.

NOTE A7.2—It should be recognized that some materials may exhibit a burst of crack extension at loads less than P_Q that is sufficiently abrupt to produce ringing in the displacement transducer signal. Such an abrupt advance of the crack may be associated with material inhomogeneities local to the fatigue crack tip. If the ringing is severe it may not be possible to unambiguously determine a value for P_Q . The presence of such bursts of crack extension should be recorded for those tests having analyzable load versus displacement records.

NOTE A7.3—The test data may be directly recorded if the recording devices have sufficient frequency response. Generally, it is advantageous to use a storage device that will capture the data and permit playing it out at a sufficiently slow speed that a pen recorder can be used in producing the required records. Such storage devices are commonly available in the form of digital storage oscilloscopes having pen recorder outputs. Separate storage instruments are also available. In general these digital storage devices have performance characteristics that are more than adequate to capture, store, and replay the transducer signals from a 1 ms test. For example, calculations show that for a typical fracture test such as described in (20) the crack mouth displacement resolution would be about 0.030 mils/sample (0.76 μ m/sample) and the load resolution would be about 160 lbf/sample (712 N/sample). It should be possible to obtain at least 1000 simultaneous samples of load and displacement during such a test. A digital storage scope capable of at least this performance would have the following characteristics: maximum digitizing rate 1 MHz, maximum sensitivity ± 100 mV, resolution 0.025 %, and memory of 4096 words by 12 bits. It may be necessary to amplify the output of the clip gage moderately and possibly that of the load cell depending on its capacity in terms of the range required. The above values of resolution are based on a total noise figure of about 50 μ V.

A7.7 Calculation and Interpretation of Results

A7.7.1 Special requirements are placed on the analysis of the load versus displacement record. These take into account the fact that experience (20) has shown load versus displacement records from rapid-load fracture toughness tests are not always as smooth in the linear range as those obtained from static tests. The special requirements of this annex are designed to ensure that an unambiguous value of P_Q can be determined.

A7.7.1.1 The test time must be determined from the load versus time record.

A7.7.2 The additional analysis of the load versus displacement record is illustrated in Fig. A7.1. The procedure is as follows: Construct the straight line OA best representing the initial portion of the test record which ideally should be linear but may not be smooth (also see Note 6). Then

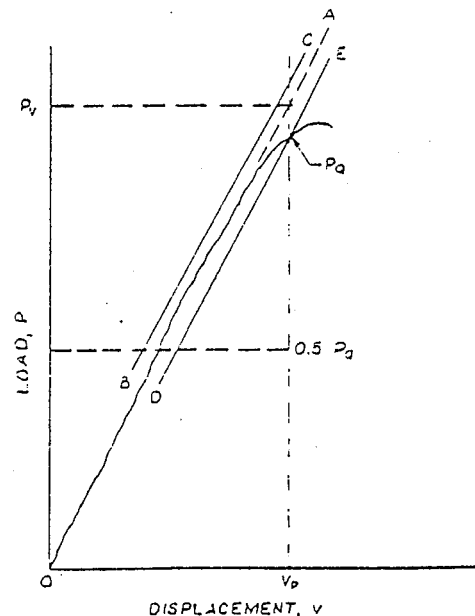


FIG. A7.1 Special Requirements for Analysis of Load Versus Displacement Records (5 % Secant Line Not Shown)

construct the line OP_0 as described in 9.1.1 (Fig. 8) and determine P_Q . Draw a vertical line at t_p passing through P_Q and define P_v at the point of intersection of this line with the line OA . Determine 5 % of P_v and construct two lines BC and DE parallel to OA with BC passing through $P_v + 0.05 P_v$ and DE passing through $P_v - 0.05 P_v$. Draw a horizontal line at $P = 0.5 P_Q$. For the test to be valid the recorded load versus displacement curve up to P_Q must lie within the envelope described by these parallel lines for the portion of the record with $P \geq 0.5 P_Q$.

A7.7.3 The test time t in milliseconds is determined from the record of load versus time as indicated in Fig. A7.2. Construct the best straight line OA through the most linear portion of the record. t is then determined from the point of intersection of this line with the time axis to the time corresponding to P_Q . This time t is shown in the brackets () following K_{Ic} . An average stress intensity rate K may be calculated by dividing K_Q or K_{Ic} by t with the result being expressed in $\text{ksi} \cdot \text{in.}^{1/2}/\text{s}$ or $\text{MPa} \cdot \text{m}^{1/2}/\text{s}$. It should be recognized that minor errors in determining the loading time are not significant because significant changes in the toughness require a change of several orders of magnitude in loading rate.

A7.7.4 The 0.2 % offset tensile yield strength σ_{YS} is used in determining the specimen size requirements for a valid test as described in 9.1.3. If the rapid load value of K_Q is valid using a static yield strength value determined at a temperature at or above that of the rapid-load test, no further yield strength considerations are necessary.

A7.7.5 If the test is invalid using such a yield strength, a tension test should be conducted on the test material at the

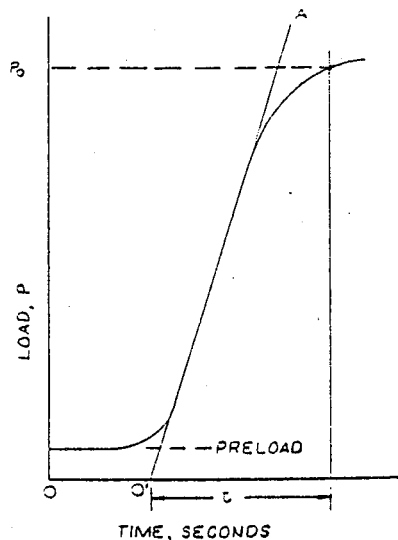


FIG. A7.2 Determination of Test Time From Load Versus Time Record

temperature and loading time of the rapid-load toughness test with the time to reach the yield load in the tension test approximately equal to the time t defined in A7.7.3.

A7.7.6 In the absence of σ_{YD} values as defined in A7.7.5 the dynamic yield strength σ_{YD} of certain steels may be estimated using the following equations (21) (22):

$$\sigma_{YD} = \sigma_{YS} + \frac{A}{T_x (\log_{10} (2 \times 10^7 t))} - B$$

where:

σ_{YS} = the 0.2 % offset room temperature static yield strength,
 t = the loading time in milliseconds (see A7.7.3), and
 T_x = the temperature of the rapid-load toughness test.

Units:

If σ_{YS} is in pound force per square inch, then $A = 174\,000 B = 27.2 \text{ ksi}$

If σ_{YS} is in megapascals, then $A = 1\,198\,860 B = 187.4 \text{ MPa}$

If the test temperature T is measured in $^{\circ}\text{F}$, then

$$T_x = (T + 460)$$

If the test temperature T is measured in K , then

$$T_x = 1.8 \times T$$

NOTE A7.4—The equation in A7.7.6 has been found useful only in estimating the low temperature dynamic yield strength of constructional steels having room temperature yield strengths below 70 ksi.

A7.8 Report

A7.8.1 The report must include the following additional information:

A7.8.1.1 The test time written in () after K_Q or K_{Ic} .

A7.8.1.2 The method by which the value of σ_{YD} used in A7.7.5 was obtained.

A7.8.1.3 Indications of ringing, that occur before P_Q is reached, in the load versus time or displacement versus time records.

A7.9 Precision and Bias

A7.9.1 *Bias*—There is no accepted "standard" value for the plane-strain fracture toughness of any material. In the absence of such a true value, any statement concerning bias is not meaningful.

A7.9.2 *Precision*—Eighteen valid values of $K_{Ic}(t)$ at -60°F (-51°C) were reported (20), with σ_{YD} being determined by extrapolation of dynamic tensile yield strength values obtained at strain rates from 0.01 to 1.0/s and temperatures from room to -40°F . No statistical analysis of the dynamic tensile yield strength data was made. The rapid-load plane-strain fracture toughness tests represented bend $SE(B)$ and compact $C(T)$ specimens tested in three thicknesses by seven laboratories. Not all laboratories tested all the thicknesses. Statistical tests for outliers and for the differences between means indicated that the data should be pooled. Considering all the valid data the grand mean $X = 55.64 \text{ ksi} \cdot \text{in.}^{1/2}$ ($61.20 \text{ MPa} \cdot \text{m}^{1/2}$), the standard deviation $S = 7.90 \text{ ksi} \cdot \text{in.}^{1/2}$ ($8.69 \text{ MPa} \cdot \text{m}^{1/2}$) and the coefficient of variation is 14 % of the average.

REFERENCES

- (1) Brown, W. F., Jr., and Srawley, J. E., "Plane Strain Crack Toughness Testing of High Strength Metallic Materials," *ASTM STP 410*, 1966.
- (2) Srawley, J. E., "Plane Strain Fracture Toughness," *Fracture*, Vol 4, Ch. 2, p. 45-68.
- (3) "Fracture Toughness Testing and Its Applications," *ASTM STP 381*, April 1965.
- (4) Jones, M. H., Bubsey, R. T., and Brown, W. F., Jr., "Clevis Design for Compact Tension Specimens Used in K_{Ic} Testing," *Materials Research and Standards*, ASTM, Vol 9, No. 5, May 1969.
- (5) Wessel, E. T., "State of the Art of the WOL Specimen for K_{Ic} Fracture Toughness Testing," *Engineering Fracture Mechanics*, Vol 1, No. 1, January 1968.
- (6) Srawley, J. E., Jones, M. H., and Brown, W. F., Jr., "Determination of Plane Strain Fracture Toughness," *Materials Research and Standards*, ASTM, Vol 7, No. 6, June 1967, p. 262.
- (7) Fisher, D. M., and Repko, A. J., "Note on Inclination of Fatigue Cracks in Plane Strain Fracture Toughness Test Specimens," *Materials Research and Standards*, ASTM, Vol 9, No. 4, April 1969.
- (8) Heyer, R. H., and McCabe, D. E., "Evaluation of a Test Method for Plane-Strain Fracture Toughness Using a Bend Specimen," *ASTM STP 463*, 1970, p. 22.
- (9) McCabe, D. E., "Evaluation of the Compact Tension Specimen for Determining Plane-Strain Fracture Toughness of High Strength Materials," *Journal of Materials*, Vol 7, No. 4, December 1972, p. 449.
- (10) Fisher, D. M., Bubsey, R. T., and Srawley, J. E., "Design and Use of a Displacement Gage for Crack Extension Measurements," *NASA T.V.D-3724*, Nat. Aeronautics and Space Administration, 1966.
- (11) Goode, R. J., "Identification of Fracture Plane Orientation," *Materials Research and Standards*, ASTM, Vol 12, No. 9, September 1972.
- (12) Srawley, J. E., "Wide Range Stress Intensity Factor Expressions for ASTM E 399 Standard Fracture Toughness Specimens," *International Journal of Fracture Mechanics*, Vol 12, June 1976, p. 475.
- (13) Newman, J. C., "Stress Analysis of Compact Specimens Including the Effects of Pin Loading," *ASTM STP 560*, 1974, p. 105.
- (14) Kapp, J. A., Newman, J. C., Jr., and Underwood, J. H., "A Wide Range Stress Intensity Factor Expression for the C-Shaped Specimen," *Journal of Testing and Evaluation*, Vol 8, No. 6, November 1980, pp. 314-317.
- (15) Jones, M. H., and Brown, W. F., Jr., "The Influence of Crack Length and Thickness in Plane Strain Fracture Toughness Tests," *ASTM STP 463*, 1970, p. 63.
- (16) Underwood, J. H., Newman, J. C., Jr., and Seeley, R. R., "A Proposed Standard Round Compact Specimen for Plane Strain Fracture Toughness Testing," *Journal of Testing and Evaluation*, Vol 8, No. 6, November 1980, p. 308-313.
- (17) McCabe, D. E., "Evaluation of the Compact Tension Specimen for Plane Strain Fracture Toughness of High Strength Materials," *Journal of Materials*, Vol 7, No. 4, December 1972, p. 449.
- (18) Underwood, J. H., and Kendall, D. P., "Cooperative Plane Strain Fracture Toughness Tests with C-Shaped Specimens," *Journal of Testing and Evaluation*, Vol 6, No. 5, September 1978, p. 296.
- (19) Newman, J. C., Jr., "Stress Intensity Factors and Crack Opening Displacements for Round Compact Specimens," *NASA TM 80174*, Langley Research Center, October 1979.
- (20) Shoemaker, A. K., and Seeley, R. R., "Summary Report of Round-Robin Testing by the ASTM Task Group E24.01.06 on Rapid Loading Plane-Strain Fracture Toughness K_{Ic} Testing," *Journal of Testing and Evaluation*, Vol 11, No. 4, July 1983 to be published.
- (21) Madison, R. B., and Irwin, G. R., "Dynamic K_{Ic} Testing of Structural Steel," *Journal of the Structural Division, ASCE*, Vol 100, No. ST 7, Proceedings paper 10653, July 1974, p. 1331.
- (22) Irwin, G. R., Krafft, J. M., Paris, P., and Wells, A. A., "Basic Aspects of Crack Growth and Fracture," *NRL Report 6598*, Naval Research Laboratory, November 1967.

The American Society for Testing and Materials takes no position respecting the validity of any patent rights asserted in connection with any item mentioned in this standard. Users of this standard are expressly advised that determination of the validity of any such patent rights, and the risk of infringement of such rights, are entirely their own responsibility.

This standard is subject to revision at any time by the responsible technical committee and must be reviewed every five years and if not revised, either reapproved or withdrawn. Your comments are invited either for revision of this standard or for additional standards and should be addressed to ASTM Headquarters. Your comments will receive careful consideration at a meeting of the responsible technical committee, which you may attend. If you feel that your comments have not received a fair hearing you should make your views known to the ASTM Committee on Standards, 1916 Race St., Philadelphia, PA 19103.